SOUTHERN PLAINS
TRANSPORTATION CENTER

INCORPORATION OF SPEED/TRAVEL-TIME DATA SETS IN TRAFFIC PERFORMANCE ANALYSIS

Hazem Refai, Ph.D.
Samir Ahmed, Ph.D.
Naim Bitar
Mohanad Kaleia
Nika Mostahinic
Tamer Alamiri
Varun Gupta

SPTC15.2-08-F

TECHNICAL REPORT DOCUMENTATION PAGE

1. REPORT NO. STPC 15.2 -08	2. GOVERNMENT ACCESSION NO.	3. RECIPIENT'S CATALOG NO.	
4. TITLE AND SUBTITLE Incorporation of Speed/Travel-Time Data Sets in Traffic Performance Analysis		5. REPORT DATE September 2019	
		6. PERFORMING ORGANIZATION CODE	
7. AUTHOR(S) Hazem Refai, Ph.D. Samir Ahmed, Ph.D. Naim Bitar, Graduate Student Mohanad Kaleia, Graduate Student Nika Mostahinic, Graduate Student Tamer Alamiri, Graduate Student Varun Gupta, Graduate Student		8. PERFORMING ORGANIZATION REPORT The University of Oklahoma 202 W. Boyd St., Room 104 Norman, OK. 73019-0631	
9. PERFORMING ORGANIZATION NAME AND ADDRESS School of Electrical and Computer Engineering, The University of Oklahoma		10. WORK UNIT NO.	
		11. CONTRACT OR GRANT NO. SPTC 15.2-08	
12. SPONSORING AGENCY NAME AND ADDRESS Oklahoma Department of Transportation Office of Research and Implementation 200 N.E. 21st Street, Room 3A7 Oklahoma City, OK 73105		13. TYPE OF REPORT AND PERIOD COVERED Final Report Jan 2016 - Jan 2019	
		14. SPONSORING AGENCY CODE	
15. SUPPLEMENTARY NOTES Click here to enter text.			
16. ABSTRACT An accurate Travel Time (TT) information is essential for traffic prediction and analysis. Correct TT measurements can be used to reduce congestions, improve safety and enhance traffic flow. The work detailed in this paper reports on the development and implementation of an inexpensive Bluetooth traffic monitoring system for reliable and real-time TT measurements. The Bluetooth system proved instant and accurate TT measurements 99.9% of the time. Furthermore, algorithms used for collecting traffic information from various ODOT platforms were fully developed, integrated, and evaluated. National Performance Management Research Dataset (NPRMDS) was chosen for developing TT models, and for identifying TT outliers and anomalies. Since incidents on highways increase TT, artificial neural network (ANN) model was designed for incident classification based on many features, such as vehicle count, weather condition and traffic flow. The ANN model reported accuracy of 91%. Moreover, a Bayesian model for detecting non-recurrent congestions was developed and evaluated.			
17. KEY WORDS Travel Time (TT), Travel Time Reliability (TTR), Bluetooth Traffic Monitoring System, Bayesian Model	18. DISTRIBUTION STATEMENT No restrictions. This publication is available from the Office of Research and Implementation, Oklahoma DOT.		
19. SECURITY CLASSIF. (OF THIS REPORT) Unclassified	20. SECURITY CLASSIF. (OF THIS PAGE) Unclassified	21. NO. OF PAGES 175	22. PRICE N/A

SI* (MODERN METRIC) CONVERSION FACTORS

APPROXIMATE CONVERSIONS TO SI UNITS

SYMBOL	WHEN YOU KNOW	MULTIPLY BY	TO FIND	SYMBOL
LENGTH				
in	inches	25.4	millimeters	mm
ft	feet	0.305	meters	m
yd	yards	0.914	meters	m
mi	miles	1.61	kilometers	km
AREA				
in^2	square inches	645.2	square millimeters	mm^2
ft^2	square feet	0.093	square meters	m^2
yd^2	square yard	0.836	square meters	m^2
ac	acres	0.405	hectares	ha
mi^2	square miles	2.59	square kilometers	km^2
VOLUME				
fl	fluid ounces	29.57	milliliters	mL
oz	gallons	3.785	liters	L
gal	cubic feet	0.028	cubic meters	m^3
ft^3	cubic yards	0.765	cubic	m^3
MASS				
oz	ounces	28.35	grams	g
lb	pounds	0.454	kilograms	kg
T	short tons (2000 lb)	0.907	megagrams (or "metric ton")	Mg (or "t")
TEMPERATURE (exact degrees)				
°F	Fahrenheit	5 (F-32)/9 Celsius or (F-32)/1.8		°C
ILLUMINATION				
fc	foot-candles	10.76	lux	lx
fl	foot-Lamberts	3.426	$candela/m^2$	cd/m^2
FORCE and PRESSURE or STRESS				
lbf	poundforce	4.45	newtons	N
lbf/in^2	poundforce per square inch	6.89	kilopascals	kPa

APPROXIMATE CONVERSIONS FROM SI UNITS

SYMBOL	WHEN YOU KNOW	MULTIPLY BY	TO FIND	SYMBOL
LENGTH				
mm	millimeters	0.039	inches	in
m	meters	3.28	feet	ft
m	meters	1.09	yards	yd
km	kilometers	0.621	miles	mi
AREA				
mm^2	square millimeters	0.0016	square inches	in^2
m^2	square meters	10.764	square feet	ft^2
m^2	square meters	1.195	square yards	yd^2
ha	hectares	2.47	acres	ac
km^2	square kilometers	0.386	square miles	mi^2
VOLUME				
mL	milliliters	0.034	fluid ounces	fl oz
L	liters	0.264	gallons	gal
m^3	cubic meters	35.314	cubic feet	ft^3
m^3	cubic meters	1.307	cubic yards	yd^3
MASS				
g	grams	0.035	ounces	oz
kg	kilograms	2.202	pounds	lb
Mg (or "t")	megagrams (or "metric ton")	1.103	short tons (2000 lb)	T
TEMPERATURE (exact degrees)				
°C	Celsius	1.8C+32	Fahrenheit	°F
ILLUMINATION				
lx	lux	0.0929	foot-candles	fc
cd/m^2	$candela/m^2$	0.2919	foot-Lamberts	fl
FORCE and PRESSURE or STRESS				
N	newtons	0.225	poundforce	lbf
kPa	kilopascals	0.145	poundforce per square	lbf/in^2

*SI is the symbol for the International System of Units. Appropriate rounding should be made to comply with Section 4 of ASTM E380.(Revised March 2003)

Acknowledgements

INCORPORATION OF SPEED/TRAVEL-TIME DATA SETS IN TRAFFIC PERFORMANCE ANALYSIS

FINAL REPORT ~ SPTC 15.2-08

Submitted by:
Hazem Refai[a], Ph.D.
Samir Ahmed[b], Ph.D.
Naim Bitar[a], Graduate Student
Mohanad Kaleia[a], Graduate Student
Nika Mostahinic[a], Graduate Student
Tamer Alamiri[a], Graduate Student
Varun Gupta[a], Graduate Student

School of Electrical and Computer Engineering (ECE)
[a]The University of Oklahoma
[b]Oklahoma State University

Table of Contents

List of Tables

List of Figures

Executive Summary

Travel time (TT) is a basic measure of traffic operation quality and level of service. This metric is considered a component of travel speed, thus an extremely valuable piece of information for travelers, shippers, and Traffic Management Center (TMC) personnel. TMC in particular use TT for traffic prediction and analyses, as its accuracy and reliability aids in reducing congestion, improving safety, and enhancing traffic flow (e.g., commuters avoiding congested roads; transportation agencies improving traffic management).

Measuring TT requires speed estimation, often including vehicle identification. Transportation agencies have leveraged a number of technologies for estimating TT (e.g., Bluetooth Wi-Fi identification detection, toll tag/automatic license plate reader, in-pavement magnetic detector, machine vision, radar equipment, inductive loop, crowdsourcing, and cell phone signal monitoring). A detailed description of these technologies and best practices for TT implementation and data collection can be found in [1] and [2]. A comprehensive, side-by-side study to evaluate various TT estimation technologies was reported in [3]. Each technology was characterized by advantages and disadvantages (e.g., accuracy, coverage, cost, portability, and other factors) for TMC to consider when designing a program for evaluating and/or improving TT reliability. Multi-sensor technologies proved the most efficient overall [3].

The PI and his research team developed, and then field tested, an inexpensive Bluetooth monitoring station for obtaining accurate, real-time TT measurements. This report details 1) system architecture information; 2) technical details for hardware/software, along with a discussion about algorithms used for estimating TT; and 3) results gathered during field testing and system evaluation.

The research group also developed a Bayesian model to detect infrequent, non-recurrent congestion at disjointed locations. Causes for these types of road conditions are plentiful, and identifying the source of each in a timely manner remains an open research problem. Understanding non-recurrent congestion is vital for alleviating its negative effects on traffic flow. Furthermore, gaining insight on such impacts aids motorists and TMC personnel in determining adequate trip planning time, estimating buffer time, and allocating resources for enhancing TT and improving traffic performance in an efficient, holistic manner. Sections below detail a Bayesian engine for identifying non-recurrent congestion using historic traffic speed (i.e., TT) probe data measurements obtained from the Department of Transportation Federal Highway Administration (FHWA) National Performance Management Research Dataset (NPMRDS). Likelihood models of several non-recurrent congestion sources are

estimated, and results demonstrating the approach employed are shown for highway I-35 across the state of Oklahoma. The proposed solution can promptly respond to changes in traffic patterns, proving that accurate TT (or "speed data") can be obtained in real-time. Developed model suitability is described in this report.

1. INTRODUCTION

1.1 Introduction

Speed, TT, and delay are related measures commonly used as performance metrics for traffic services. Combined, these metrics answer an important question posed by travelers and shippers, "How long does it take to get from point A (origin) to point B (destination)?" Motorists expect to complete their planned trip in a minimal amount of time, while taking safety into consideration. Travel performance is often described in terms of the ability to achieve the expected TT objective on a regular basis. For example, the Highway Capacity Manual [4] states that average travel speed is used as a measure of effectiveness for assessing the quality of traffic operations on arterials and two-lane rural highways. Control delay is the measure of effectiveness for signal- and stop-controlled street intersections, whereas level of service on basic, weaving, merge, and diverge freeway segments is directly related to density as a primary measure of effectiveness. Speed is an important component for evaluating freeway corridor and system operations.

Speed is defined as the rate of motion in distance per unit time. TT is the amount of time elapsed for a vehicle to traverse a defined section of roadway. Speed and TT are inversely related, as shown in the following formula:

$$S = \frac{d}{t} \qquad\qquad \textbf{Eq. 1-1}$$

where:

S = speed, mile/hour or feet/second

D = distance traversed, mile or feet

T = time to traverse distance d, measured in hours or seconds.

In a moving traffic stream, vehicles are likely to travel at various speeds, representing a frequency distribution. However, taken as a whole, the traffic stream can be characterized according to an average speed. Two methods can be used to determine average speed for a traffic stream:

• Time Mean Speed (TMS). This metric represents average speed of all vehicles passing a point on a highway or a lane with regard to a specified time period, making it a point measure of average speed. TMS is the simple average of a representative sample of vehicle speeds.

• Space Mean Speed (SMS). This metric represents average speed of all vehicles occupying a given section of a highway or a lane with regard to a specified time period, making it a space measure of average speed over a length. SMS is calculated by determining average TT for a vehicle to traverse the specified section, using average TT to compute speed.

As previously mentioned, speed is inversely related to TT. Reasons for and locations at which speeds (or TT) are measured can be, however, quite different. Speed measurements are typically recorded at a point (or on a short segment) of roadway under free-flow conditions (i.e., volumes less than 750 to 1,000 veh/h/ln on freeways or 500 veh/h/ln on other types of uninterrupted roadway flow). The aim is determining speeds at which drivers typically travel in the absence of congestion. This information can then be used to determine general speed trends, to set reasonable speed limits, and to assess safety. Such studies are referred to as "spot speed studies," because the focus is on a designated "spot" or location on a roadway.

TT must be measured over a distance. Although spot speeds can be measured in terms of TT over a short measured distance (generally less than 1,000 ft), most TT measurements are calculated using a significant length of roadway. Such studies are generally performed while the roadway is congested, specifically to measure or quantify the extent and/or cause(s) for the congestion. Information about TT between key points within a study area is used for many purposes, including the following:

• To identify problem locations on roadways by virtue of recurring lengthy TTs and/or delays.

• To determine arterial level of service based on average travel speeds and TTs.

• To provide necessary input for traffic assignment models utilizing link TT as a key determinant for route selection.

• To provide TT data for economic evaluation of transportation improvements.

• To develop time contour maps and other depictions of traffic congestion in a specified area or region.

• To compute measures of TT reliability.

The term TT delay describes the difference between actual TT to traverse a section of highway versus a traveler's expected or desired TT. Hence, travel delay is a component of total TT that travelers find particularly annoying. For example, a delay due to interrupted-flow on an arterial roadway might include stopped travel due to signals, midblock obstructions, or other causes. Hence, TT delay is more of a philosophical construct because there are no agreed-upon methodologies for determining a traveler's

2

expected TT for a given section of a roadway. TT delay is seldom used for assessing congestion along a specified segment.

Because speed is generally studied at specified points under free-flow roadway conditions and TT/TT delay are generally studied along sections of a roadway under congested conditions, techniques for studying each are quite different.

1.2 Field Measurement Techniques

Measuring TT has traditionally relied on monitoring instrumented probe vehicles traveling through a roadway section under study while an observer records elapsed times through the specified section, as well as at intermediate points within the section. To maintain result consistency, probe-vehicle drivers are instructed to use one of three techniques: 1) floating car; 2) maximum car; or 3) average car. A similar technique uses a GPS device to record vehicle trajectory along with time stamps. This method provides more frequent sampling along the route. However, both methods provide TT for only the probe vehicle, making it difficult to collect a large dataset for various routes and times of day.

Another traditional technique for collecting TT involves roadside observers and/or cameras for recording license plate numbers as vehicles pass designated points along a roadway. Time of passage is noted, along with the license plate number. Because it is virtually impossible to record every license plate align with an associated time of detection, sampling is difficult. For example, if a sample of 50% of all passing license plates is recorded at each study location, the probability that a license plate will be matched at two locations is 0.50 X 0.50, or 0.25 (or 25%). The probability that a license plate will be matched at three locations is 0.50 X 0.50 X 0.50 (or 12.5%). These sampling problems have been addressed by advances in license plate scanning technology that facilitates a high degree of identification accuracy for vehicles passing at designated points. Notably, the detail of delay information at intermediate points cannot be determined using this type of technology.

Automated Vehicle Identification (AVI) systems composed of an in-vehicle transponder and a roadside unit that receives the transponder signal have also been used to measure TT. This method is often integrated with a tolling infrastructure (e.g., PikePass /E-ZPass tag readers located overhead along tollways). Personal identification information is scrambled within the PikePass /E-ZPass controller prior to its use in TT calculations. This technique is limited PikePass /EZPass-equipped vehicles travelling on toll roads.

In recent years, Bluetooth and Wi-Fi signals have been used for measuring TT at a cost lower than traditional techniques mentioned above. Bluetooth is an open wireless technology standard for exchanging data from fixed and mobile devices over short

3

distances, creating personal area networks (PANs) with high levels of security. Bluetooth uses a radio technology (i.e., frequency-hopping spread spectrum) operating in the 2.4 GHz short-range radio frequency band. Many vehicle dashboard systems, cell phones, headsets, and other personal equipment are, or can be, Bluetooth-enabled to streamline the flow of information between devices. Interconnectedness between Bluetooth devices is achieved through transmission and acceptance of a 48-bit Media Access Control (or MAC) address between inquiring and receiving devices via a small transceiver that continuously transmits its device-specific MAC address in an effort to find other devices with which to communicate.

Once two Bluetooth devices are connected, transmission of the MAC address continues as long as the devices remain within range. Manufacturers typically assign unique MAC addresses to Bluetooth-equipped devices so that they cannot be tracked nor are the addresses readily available when a device is sold within the marketplace, making the device a personal, information-free identifier. Although the constant broadcast of MAC addresses is detectable and measurable, there is no relationship to personal or otherwise sensitive information, keeping the traveling public and their information anonymous.

Bluetooth readers mounted on the roadside at key locations can detect anonymous Bluetooth signals broadcast from mobile devices within vehicles passing along a roadway. Signal time stamps, along with the MAC address of the Bluetooth device, are used to determine TT and to accurately measure speed. The range of the reader is about 175 feet, which is sufficient to cover one direction of a multi-lane highway.
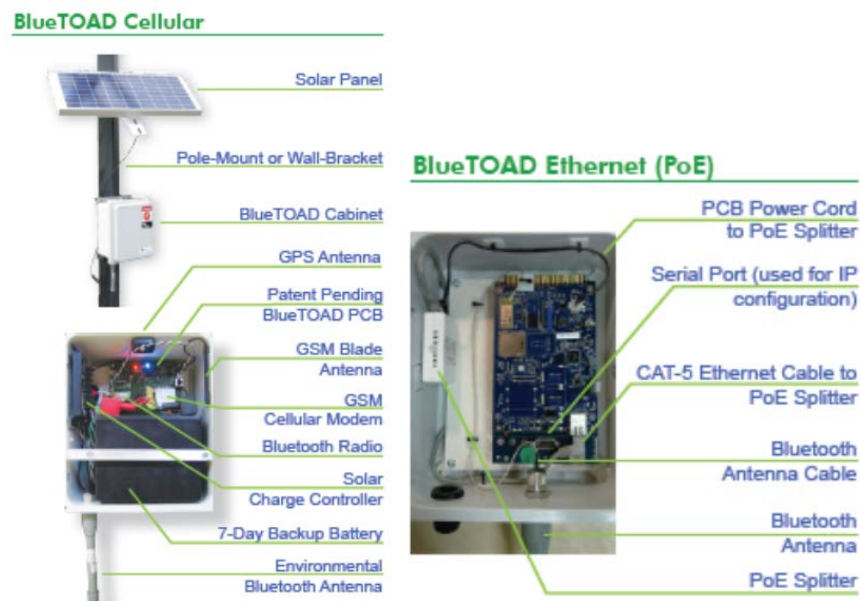
Figure 1-1 BlueTOAD Installation.

Data obtained by Bluetooth readers are transmitted via either the ethernet or 3G to a cloud-based host. Hard wiring is kept to a minimum, making temporary Bluetooth and/or Wi-Fi based TT measurement systems cost-effective. These can be used, for instance, to monitor traffic flows in work zones or to determine optimal timing and sequencing for traffic lights. The only requirements are an appropriate mounting point, a cellular data connection, and a 5W electrical supply. Alternatively, the system could be powered by a solar panel/battery combination for use in remote or temporary locations, such as an approach zone to roadwork. Units could also be plugged into an existing electrical and/or fiber infrastructure and utilize Power over Ethernet (PoE) technology. Unlike image-based TT detection (e.g., license plate recognition cameras), Bluetooth/Wi-Fi-based systems are unaffected by snow, ice, smoke, fog, or heavy rain.

Link TT is calculated when the MAC address matches a prescribed link origin and destination. SMS is then calculated based on TT along a given link. Abnormal data points (i.e., outliers) are removed using statistical filters and include illogical data pairs and any other matched pair that is outside the normally expected TT. This processing also filters out high speed outliers based on rarely found identical MAC addresses or multiple simultaneous MAC addresses from within a single vehicle, such as a bus. Data can be viewed in real-time or analyzed historically through a Web interface, which provides TT, speed, and MAC address detection counts.

BlueTOAD (or Bluetooth Travel-time Origination And Destination) is a currently available commercial product manufactured by TrafficCast for reading Bluetooth signals. Companion BlueARGUS software is used to compute TT, speed, and other performance metrics every 15-minutes.

Figure 1-1 illustrates a BlueTOAD installation.

1.3 Travel Time Reliability

Drivers become accustomed to everyday congestion and plan for it, leaving home early enough to get to work on time. Unexpected congestion, however, is a source of angst for travelers. For example, when a trip that typically takes 20 minutes takes an hour—with little or no warning, a motorist's day is significantly affected. He or she might be late for work, miss an appointment with a doctor, or pay a penalty for picking up kids late from childcare. A truck driver delayed by traffic congestion might deliver a late shipment to the manufacturer, disrupting just-in-time delivery and causing the shipping company to lose its competitive edge.

Travelers desire travel time reliability [TTR] (i.e., a consistency or dependability in travel time as measured from day to day or across different times of day. Motorists want predictability that a trip will take a half-hour today, a half-hour tomorrow, and a half-hour for the foreseeable future. Consistent TT has safety implications, as well, since

predictability in known to reduce risky driving behavior [5]. Thus, TTR not only improves motorists' experiences, but also has a positive impact on traffic safety.

Another view of TTR is based on probability of failure, which can be leveraged to characterize manufacturing and industrial processes. In this case, failure is defined in terms of TT relative to the number of times a given threshold is not achieved or exceeded. Some non-U.S. TTR research has defined the probability of failure in terms of traffic flow breakdown. A related concept, vulnerability, is a measure of transportation network imperviousness to breakdown conditions. Published literature includes several definitions of TTR, depending on the context in which the term is being used (See Table 1-1).

Table 1-1 Definitions of Travel Time Reliability

Reference	TRR Definition
Lida [6]	The probability of making trips on time.
Sisiopiku and Islam [7]	The degree of consistency of a particular mode, corridor, or route over a time period.
Elefteriadou and Cui [8]	The level of variability between the expected travel time (based on scheduled or average travel time) and the actual travel time experienced. Note that for facilities that are congested during most of the time, the expected travel time would be high and the difference between the two values (expected –actual travel time) would be small, labeling the facility as "reliable", when it is consistently congested.
Texas Transportation Institute [9]	Travel time reliability and variability are defined separately. Reliability is commonly used in reference to the level of consistency in transportation service; variability is the amount of inconsistency on operating conditions. To quantify the reliability the report recommends the Buffer Time, which is the amount of extra time that must be allowed for the traveler to achieve their destination in a high percentage of the trips. To quantify the variability, the report recommends the average travel time plus one or two standard deviations.

NCHRP Report 398 [10]	The impact of non-recurrent congestion on the transportation system.
NCHRP Report 399 [11]	A measure of the variability of travel time; it is stated that reliability could be presented as the standard deviation of travel time.
AASHTO's Freight Report [12]	The percent of on-time performance for a given time schedule.
TranSystems [13]	The probability of travel times meeting users' expectations. Reliability is the probability that a product or service performs adequately over the interval [0, t].
SHRP-2, Report S2-L03-RR-1 [14]	How travel times vary over time (e.g., hour-to-hour, day-to-day). The terms travel time variability and travel time reliability are used interchangeably.

1.4 Travel Time Reliability and Congestion

Traffic congestion results when traffic flow rate (i.e., demand) approaches or exceeds roadway capacity (i.e., supply). Figure 1-2 presents a conceptual model of the way in which seven sources of congestion interact and result in total congestion [14]. Reliability is an aspect of total congestion that is greatly influenced by such complex interactions of traffic demand, physical capacity, and roadway events. Although higher congestion generally leads to higher unreliability in TT, there may be instances when even though roadway congestion causes increased TT, the upsurge can be predicted with a high degree of certainty. Results of the SHRP-2 Reliability Project L03 [14] indicate that strategies and remedies that mitigate congestion should be helpful in reducing TT variability.
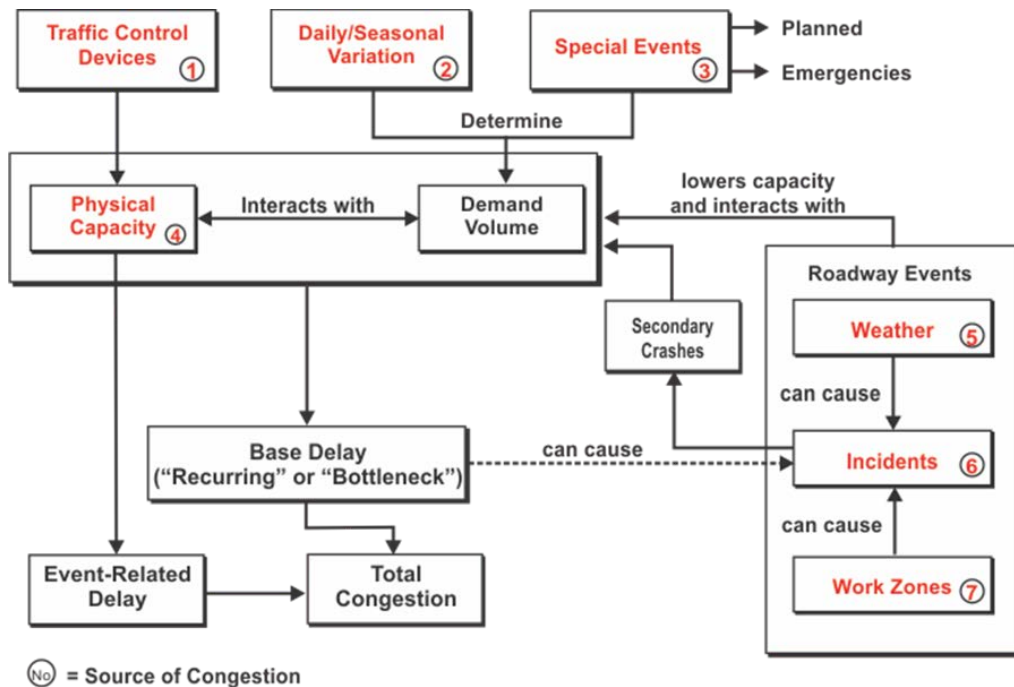
Figure 1-2 Congestion and Its Sources [14].

Following is a brief summary of seven sources of congestion [14].

1. **Physical bottlenecks (42%)** - Bottlenecks occur upstream of roadway segments with reduced capacity (e.g., lane drops, crash sites) or those affected by significant traffic movements (merging or weaving sections).
2. **Traffic incidents (39%)** - Traffic incidents (e.g., vehicular crashes, breakdowns, debris in travel lanes) disrupt normal flow of traffic, typically due to physically reducing the number of travel lanes.
3. **Weather (18%)** - Environmental conditions (e.g., fog, snow, and heavy rain) influence driver behavior that can negatively affect travel conditions/flow.
4. **Work zones (1%)** - Construction activities on the roadway, resulting in physical changes to the highway environment (e.g., reduction in the number/width of travel lanes; lane shift diversion, reduction or elimination of shoulder, and temporary roadway closure).
5. **Traffic-control devices (not measured)** - Intermittent interruptions of traffic flow by control devices (e.g., railroad grade crossing and poorly timed signal).
6. **Fluctuations in normal traffic demand (not measured)** – Daily, hourly, and sub-hourly variations in traffic demand causing flow rate exceeding capacity.

7. **Special events (not measured)** - Special event traffic fluctuations whereby flow in the vicinity of the event is significantly different from typical patterns (e.g., surges exceed capacity).

Figure 1-3 illustrates TT variation on the I-5 Freeway in San Diego, California, by time of day throughout a given year, excluding non-recurrent events, such as incidents, weather, unusual demand, and special events. Time of day is shown on the x-axis, and TT in minutes is shown on the y-axis. Clearly, this roadway segment is unreliable notwithstanding the influence of incidents and weather. Not only is there a variance in TT, but also in range of time (e.g., slightly during morning peak, and more pronounced during evening peak). Around midnight, minimum and maximum TT vary only 5 minutes (e.g., 55 versus 50 minutes); during weekday evening peak, TT varies 50 minutes notwithstanding additional influence of nonrecurring events (e.g., 100 versus 50 minutes).

Figure 1-4 shows TT without including non-recurrent events. Clearly, nonrecurring events have an impact, exemplified by a widening spread between minimum and maximum TT. Adverse weather serves as an example of the effect a non-recurrent event, especially during peak period travel. Traffic incidents also have an effect on TT reliability, as do special events and unusually high traffic demand.

National estimates of congestion by source are shown in Figure 1-5. FHWA estimates are based on consensus rather than analysis and are meant to be a snapshot rather than indicative of individual corridors or highways. For example, in rural conditions, delays are nearly always a function of events rather than a bottleneck. In urban conditions, especially roadways with predominant bottlenecks, most delays are determined by insufficient base capacity.
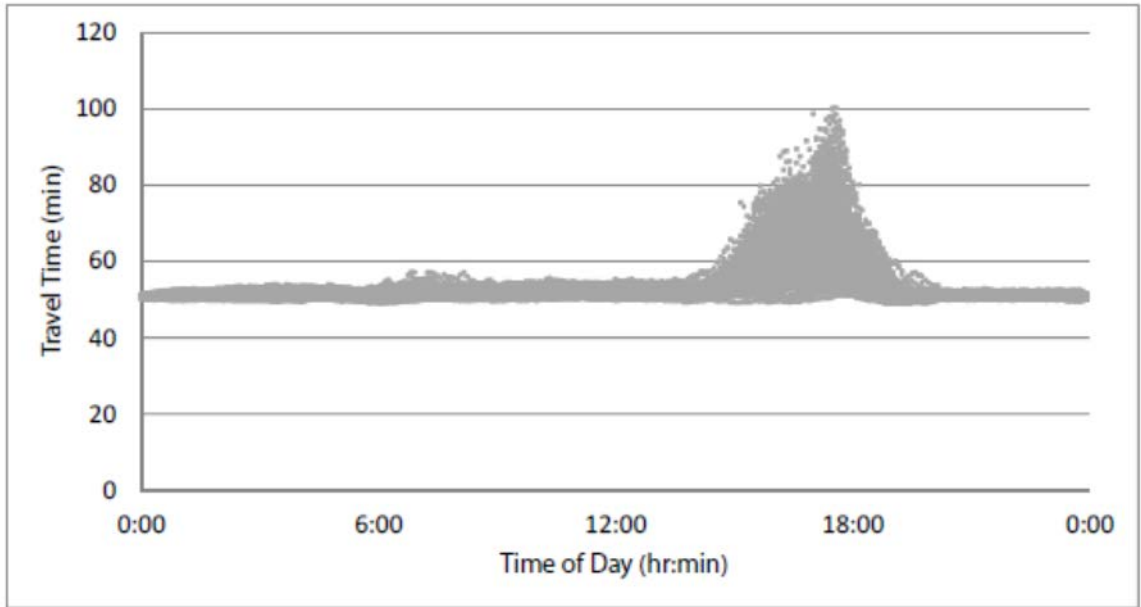
Figure 1-3 Variation in Travel Times by Time of Day Across a Year, Excluding Non-recurring Congestion [14].
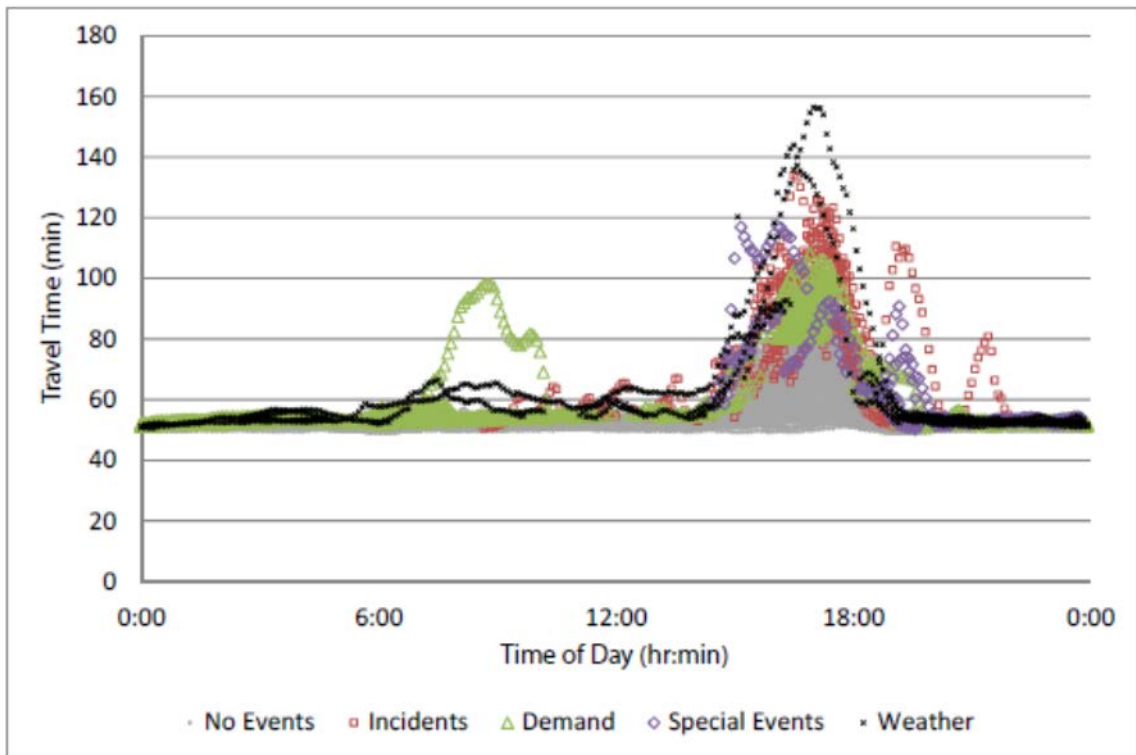
Figure 1-4 Variation in Travel Times by Time of Day Across a Year, Including Non-recurring Congestion [14].

10
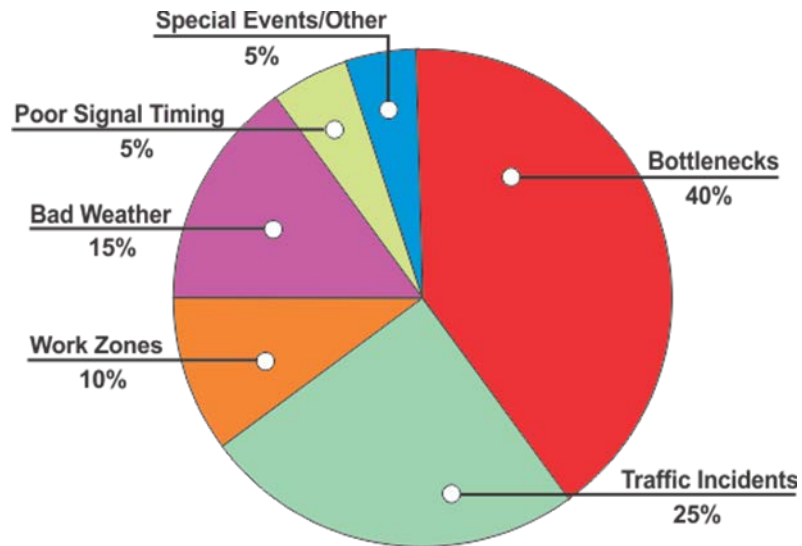
Figure 1-5 FHWA National Estimates of Congestion and Delay by Source [15].

1.5 Legislative and Regulatory Requirements

The Moving Ahead for Progress in the 21st Century (MAP-21) Act (Pub. L. 112-141) and the Fixing America's Surface Transportation (FAST) ACT (Pub. L. No. 114-94) established new requirements for performance management to ensure the most efficient investment of Federal transportation funds. Performance management increases accountability and transparency of Federal-aided highway programs and provides a framework for supporting improved investment decision-making through a focus on performance outcomes for key national transportation goals. Federal-aid highway fund recipients are mandated to make investments for achieving performance targets and advancing progress toward the following national goals:

• **Safety**: To achieve a significant reduction in traffic fatalities and serious injuries on all public roads.

• **Infrastructure condition**: To maintain the highway infrastructure asset system in a state of good repair.

• **Congestion reduction**: To achieve a significant reduction in congestion on the National Highway System (NHS).

• **System reliability**: To improve the efficiency of the surface transportation system.

• **Freight movement and economic vitality:** To improve the national freight network, strengthen the ability of rural communities to access national and international trade markets, and support regional economic development.

11

• **Environmental sustainability:** To enhance the performance of the transportation system while protecting and enhancing the natural environment.

• **Reduced project delivery delays**: To reduce project costs, promote jobs and the economy, and expedite the movement of people and goods by accelerating project completion through eliminating delays in the project development and delivery process, including reducing regulatory burdens and improving agencies' work practices.

On January 18, 2017, the FHWA published final rules for the last two national performance management measures in the Federal Register. One rule established regulations for assessing the condition and performance of bridges and of pavements on the Interstate and non-Interstate NHS. The other established regulations to assess the performance of the NHS, Freight Movement on the Interstate System, and the Congestion Mitigation and Air Quality Improvement (CMAQ) Program.

These National Performance Management Measures—Assessing Performance of the National Highway System, Freight Movement on the Interstate System, and Congestion Mitigation and Air Quality Improvement Program—mandate that states evaluate and report transportation system performance "more effectively and consistently," including TTR, excessive delay during peak hours, freight movement reliability and greenhouse gas and vehicle emissions by:

• Establishing a real-time system management information program,

• Monitoring traffic & travel conditions on major highways, and

• Sharing information to address congestion problems and facilitate traveler notifications.

Prior to MAP-21, there were no explicit requirements for state DOTs to demonstrate how their transportation programs supported national performance outcomes: measure condition or performance, establish targets and assess progress toward targets, or report on condition or performance in a nationally consistent manner that enabled FHWA to assess the entire system. Without such information, it is difficult for FHWA to examine the effectiveness of the Federal-aid highway program as a means to address surface transportation performance at a national level. MAP-21 regulatory rules:

• Propose requirements for establishing targets that can be aggregated at the national level,

• Recommend consistent reporting on roadway condition and performance, and

• Suggest a process for determining significant progress for state DOTs.

These new performance metrics will improve information available to state DOTs and help focus planning and programming decisions. Overall, the metrics are aimed at strategically targeting investment decisions and evaluating their impact. Regulations empower FHWA to better communicate a national performance story and more reliably assess impacts of Federal funding.

1.6 Travel Time Reliability Metrics

Like the wide range of definitions for TTR, there are a broad variety of techniques available for measuring reliability. Effective measures must capture commuters' experiences and should communicate information about the size and shape of the underlying TT distribution (i.e., TT history on roadways, corridors, or networks).

Figure 1-6 illustrates that travelers tend to recall worst-case scenario days spent in traffic rather than the average TT of their travels throughout the year [16]. One argument against using average TT to assess TTR is reported in Figure 1-7, which depicts results of a before-and-after study of incident management program benefits. Although average TT improvements might seem modest, TTR measured on the worst few days improved dramatically [16]. In fact, travelers arrived at their destinations on time more often or with fewer significant delays.

Four types of TTR measures have been proposed in the literature: 1) statistical measures of TT variability; 2) 80th, 90th; or 95th percentile TT; 3) TT buffer measures; and 4) tardy trip indicators [17]. Each is discussed in the following sections. Table 1-2 presents a summary of reliability metrics that are appropriate for general practice [14]. Some are shown in more detail in Figure 1-8 and Figure 1-9.

Statistical measures of TT variability. Percentage of variation serves as a statistical measure for quantifying TTR:

$$Percent\ of\ Variation = \frac{S_{TT}}{\overline{TT}} x100 \qquad \text{Eq. 1-2}$$

where:

S_{TT} = standard deviation of TT, minutes

$\overline{TT}$ = average TT, minutes

Although percentage of variation is easy to calculate and simple to interpret, it should be noted that early and late arrivals are considered equal in weight. This phenomenon serves as a significant drawback, primarily because travelers and shippers are primarily concerned with information regarding late arrivals.
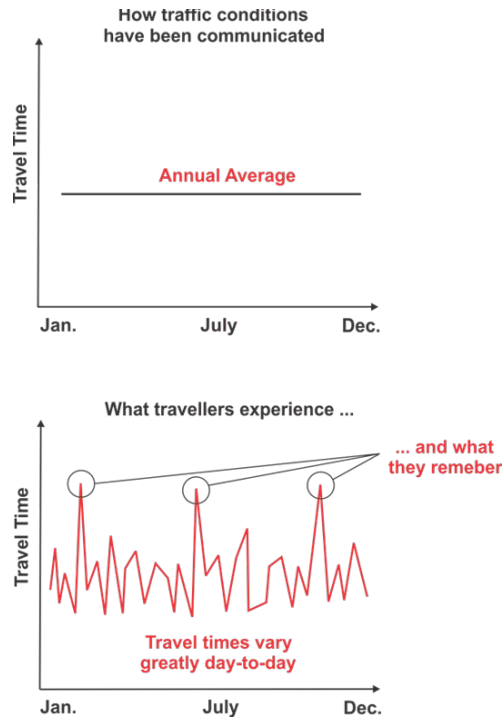
Figure 1-6 Average Travel Times Doesn't Tell the Full Story [16].
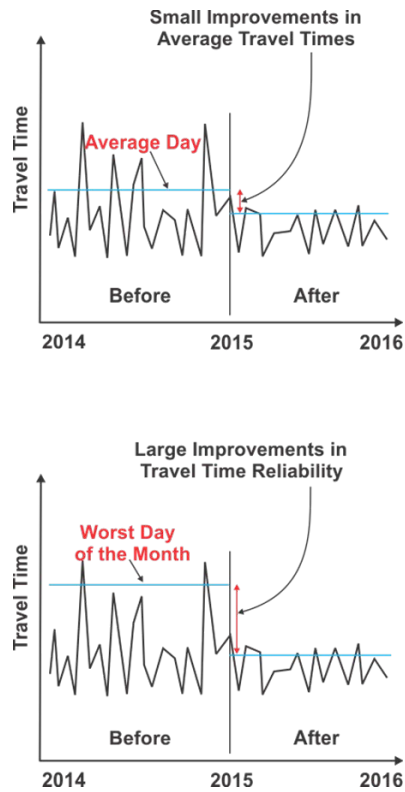
Figure 1-7 Travel Time Reliability Measures Demonstrate Traffic Management Benefits [16].

Table 1-2 Common Travel Time Reliability Metrics.

Reliability Performance Metric	Definition	Units
Buffer Index	Difference between 95th percentile travel time index (TTI) and average TTI, normalized by average TTI; Difference between 95th percentile TTI and median TTI, normalized by median TTI	%
Failure and on-time measures	Percentage of trips with TT <1.1 median TT (MTT) and <1.25 MTT; Percentage of trips with space mean speed less than 50-, 45-, and 30 mph	%
Planning Time Index	95th percentile TTI	None
80th percentile TTI	Self-explanatory	None
Skew statistic	(90th percentile TTI - median)/(median - 10th percentile TTI)	None
Misery Index (modified)	Average of the highest 5% of TT / free-flow TT	None
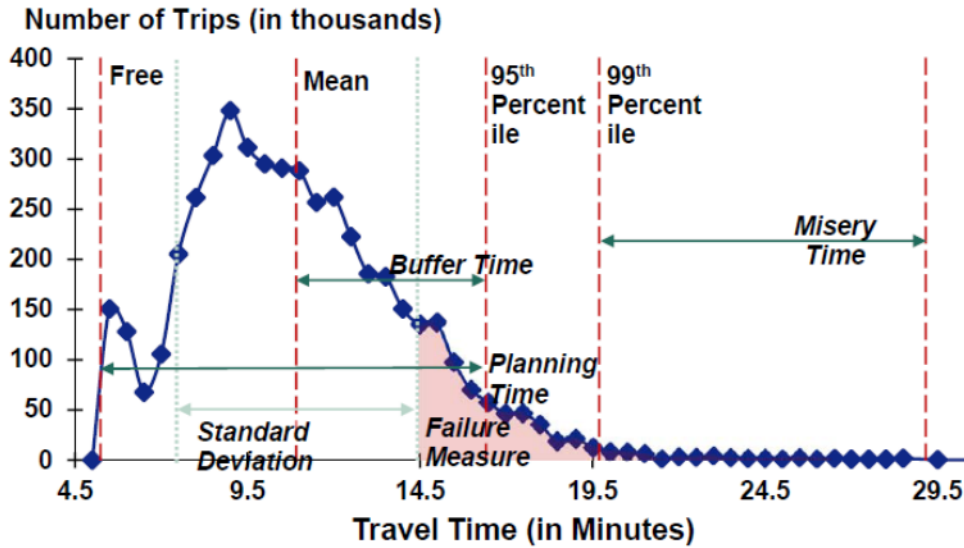
Figure 1-8 Travel Time Distribution is the Basis for Defining Reliability Metrics [18].
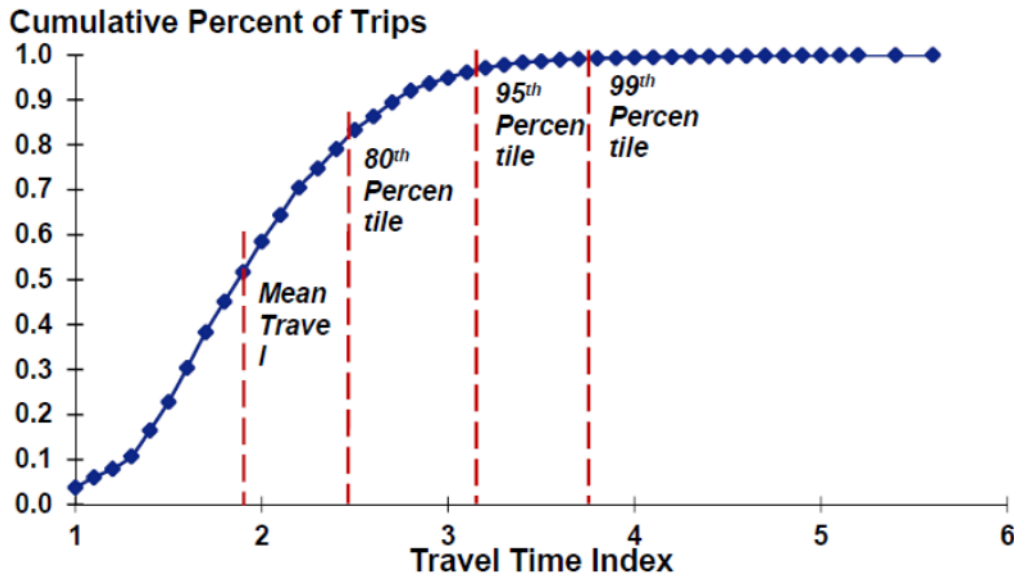
Figure 1-9 Cumulative Travel Time Distribution and Travel Time Indices [18].

90th or 95th percentile TT (i.e., planning time). The 90th or 95th percentile TT method is considered the easiest for measuring TTP of a given road network. The first and second worst TT recorded over the period of a month are used to mark the 95th or 90th percentile TT, respectively. Worst case scenarios are typically the result of non-recurring congestion (i.e., traffic crashes, inclement weather, construction work, and special events). Hence, if travelers know the 90th or 95th percentile TT of a route, they

16

can plan accordingly and reach their destinations on time. Notably, this measure is reported in minutes and is used in computing reliability indices, such as the buffer index.

Buffer time and buffer time index. Buffer time (BT) is the extra time travelers must add to their TT to arrive at their destination on time:

$$BT = TT_{95} - \overline{TT}$$
Eq. 1-3

where:

BT = buffer time, minutes

TT_{95} = 95th percentile TT, minutes

$\overline{TT}$ = Average TT, minutes

Buffer Time Index (BTI) is defined by the following equation:

$$BTI = \frac{TT_{95} - \overline{TT}}{\overline{TT}}$$
Eq. 1-4

For example, a buffer time index of 40% indicates that a trip with 20-minute average TT requires a traveler to leave 8 minutes early to ensure on-time arrival:

Average TT: 20 minutes

BTI: 40 percent

BT: 20 minutes × 0.40 = 8 minutes

Given this information, the traveler should allow 28 minutes total TT to ensure on-time arrival 95 percent of the time.

SHRP-2 Project S2-L03 suggests that BTI is too erratic and unstable to be considered for the primary reliability metric for tracking performance trends or for studying the effects of improvements [14]. However, as a secondary metric, BTI provides useful information, meaning that rather than being disregarded, BTI should be included in a suite of reliability performance metrics [14].

Planning time index. The planning time index (PTI) represents TT a traveler should allow to ensure on-time arrival. PTI is the ratio of 95th percentile TT to free-flow TT. While BT represents the additional time necessary to consider for on time arrival, PTI indicates TT and represents the 95% percentile TT. For example, a PTI of 1.60 indicates that a trip with 15-minute TT in light traffic requires a traveler to allow 24 minutes TT to ensure on-time arrival 95 percent of the time.

Free-flow TT = 15 minutes

PTI = 1.60

PT = 15 minutes × 1.60 = 24 minutes

PTI can be directly compared to TT *index* (TTI), which is a measure of congestion (i.e., average additional TT during congestion compared with TT during light traffic). TTI is the ratio of average TT during peak-periods to free-flow TT. Figure 1-10 illustrates the relationship between TTI, PTI, and BT.

Misery index. The misery index focuses on trips with later than expected arrival times (i.e., "How bad are the worst days" [19] for 20% of trips). The misery index compares average TT of late-arrival trips against average TT during normal conditions in an effort to measure negative aspects of trip unreliability:

$$BTI = \frac{\overline{TT_{80}} - \overline{TT}}{\overline{TT}}$$ **Eq. 1-5**

where:

$\overline{TT_{80}}$ = Average TT for the longest 20% of trips, minutes

$\overline{TT}$ = Average TT for all trips, minutes
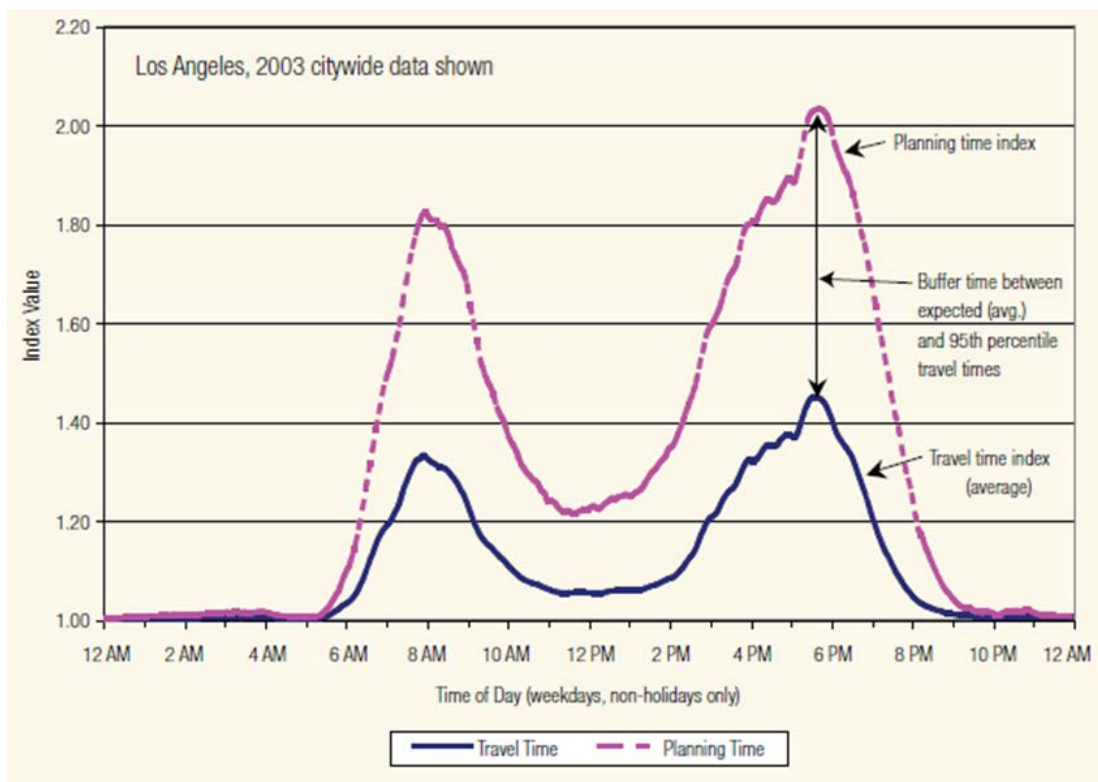
Figure 1-10 Relationship of Travel Time Index, Planning Time Index and Buffer Time [7].

18

Performance measures discussed earlier provide different perspectives and additional insights when used with multiple time periods. For example, the 95th percentile TT can be computed for an entire peak period or for each specific hour within a specified peak period. Comparing the way in which these measures change over the course of a day illustrates how reliability fluctuates during the day. Tracking changes in measures according to time of day can be used to assess the benefits that travel demand management programs are likely to produce in terms of travel reliability improvements and also when incident-response resources are most needed.

1.7 Travel Time Reliability Monitoring System (TTRMS)

Figure 1-11 illustrates the seven steps involved in establishing a travel time reliability monitoring system (TTRMS) and how to put TTR information to work for travelers and traffic managers [20].
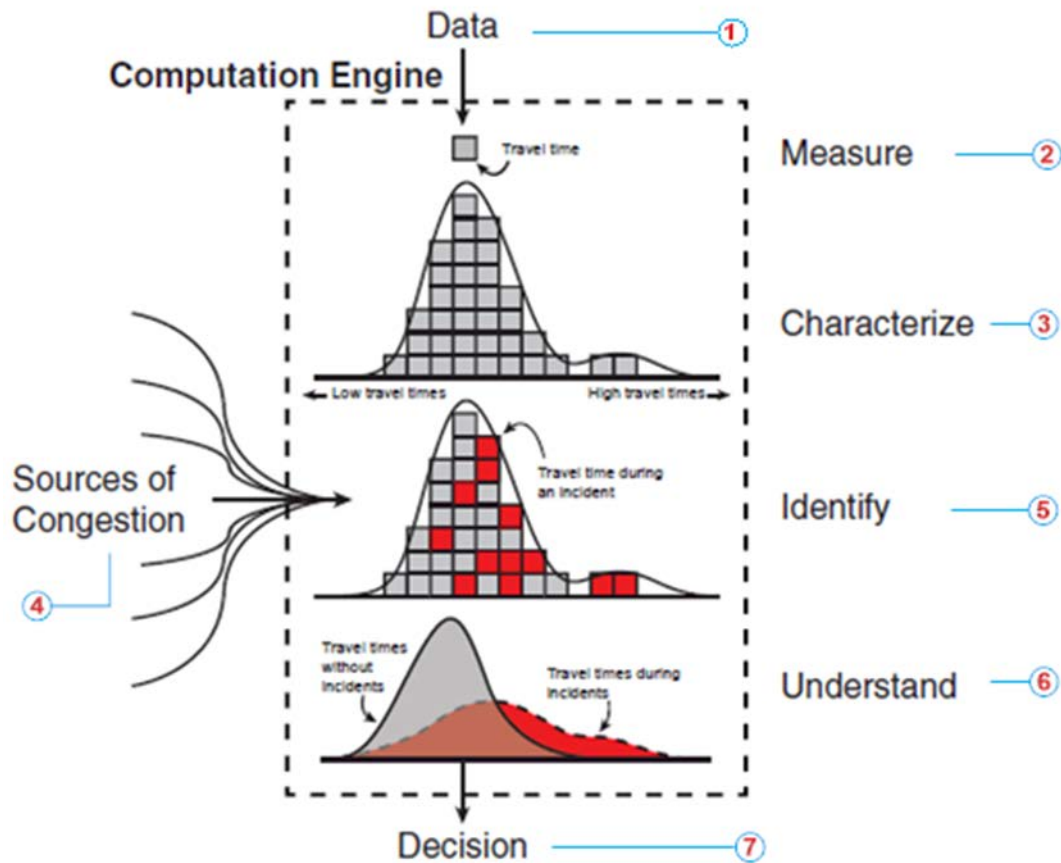
Figure 1-11 Information Flow in Travel Time Reliability Monitoring System [20].

Following is a brief discussion of each step:

1. Collect and Manage Traffic Data

The first step in developing TTRMS is acquiring/storing traffic data collected from infrastructure-based sources and vehicle-based sources. Data should be both mode neutral (e.g., freeway lane data) and mode specific (e.g., transit data).

Infrastructure-based sources include loop detectors, video image processors, wireless magnetometer detectors, and radar detectors. These technologies are able to collect single-point vehicle count and lane occupancy data, as well as double-point speed data. Collected data is anonymous (i.e., specific vehicle cannot be identified).

Vehicle-based detectors collect data about a vehicle when it passes either a fixed point, as is the case for an automated vehicle identification (AVI) system, or as it travels along a path for automated vehicle location (AVL). AVI data collection sources include Bluetooth readers, electronic toll tag readers, and license plate readers, detecting vehicles passing sensor locations. Data are post-processed for matching information from a vehicle as it passes successive sensors. Doing so allows direct computation of TT between two points. AVL data collection sources identify GPS traceable paths for individual vehicles as they travel through a roadway system.

2. Measure Travel Times

The second step in developing TTRMS is measuring TT at the route level. This process involves imputing missing data, computing segment TT, and then computing route TT. These are described in detail below.

Impute missing values. Sensor coverage can often be incomplete due to gaps in system coverage or because of an individual sensor malfunction. Missing data present a major challenge for producing useful TTR performance measures. SHRP-2 Program Report S2-L02-RR-2 presents statistical techniques for identifying malfunctioning detectors, discarding poor data, and filling in missing data with imputed values. The report also presents methods for collecting, filtering, and imputating AVI and AVL data.

Compute segment TT. For infrastructure-based detectors, segment TT estimates are based on average speeds of vehicles traversing the segment. For double-loop detectors, speeds are measured directly. However, for single-loop detectors, speeds are estimated using tools like a g-factor, which combines an assumed vehicle length with the flow and occupancy data gathered by single-loop detector [20].

Unlike infrastructure-based detectors, vehicle-based detectors (e.g., AVI and AVL) generate direct measurements of individual vehicle TT from one location to another, requiring detector data to match network data.

Compute route TT. Although estimating average route TT from infrastructure-based data is straight forward, determining route TT distributions from infrastructure-based sensors is difficult. Limited information about specific vehicles is available on the

network. SHRP-2 Program Report S2-L02-RR-2 presents two methods for constructing route TT from infrastructure-based sensors: 1) Monte Carlo simulation with link incidence matrices, and 2) Monte Carlo simulation with a prediction technique using probe vehicles and point queue estimations [20].

Constructing route TT distributions from vehicle-based data can be done directly if ample data are available. Given the absence of sufficient data, techniques described for infrastructure-based sensors can be employed.

3. Characterize Observed Travel Times

Figure 11 illustrates that characterization involves labeling each TT observation based on operating conditions when TT was observed. For example, TT might have been observed late at night under light traffic conditions free from a non-recurring event, or it might have observed during a heavily congested afternoon peak immediately following an incident. The objective of characterization is assigning TT observations into bins composed of similar operating conditions.

4. Collect, Manage, and Impute Non-recurring Event Data

Non-recurring event data come in a variety of forms, as previously mentioned. Some TTRM systems integrate non-recurring event data into a single database (e.g., Georgia DOT Navigator system). In others, multiple data sources are post¬-processed for integrating various non-recurring event sources into a single database (e.g., San Diego's performance measurement system [PeMS]). PeMS integrates incident data from three sources: 1) the statewide Traffic Accident and Surveillance Analysis System, 2) lane closure data from Caltrans, and 3) weather data from the Automated Weather Observing System reported for the San Diego International Airport.

Integrating non-recurring event data can be challenging and often involves separate analysis for properly integrating and assigning event data to correct time periods. For example, assigning incident data to time periods is not straightforward, as the impact of an incident on traffic might extend well beyond the time period during which the incident occurs. Weather data presents similar challenges. In some cases, imputing non-recurring event data is required for developing consistent event reporting across time periods under analysis. A common example includes achieving consistency in the way in which incidents are recorded.

5. Identify Sources of Congestion and Unreliability

Once route TT calculations or distributions have been assembled, data can be analyzed in conjunction with non-recurring event data to identify sources of unreliability. SHRP-2 Program Report S2-L02-RR-2 presents two methods of congestion source identification: 1) tagging and 2) statistical [14].

A tagging approach matches non-recurring event data with TT data during the data collection process. Non-recurrent event data are captured in real time and can be archived into databases tailored to each event type. This information can then be matched to TT data for analysis and categorization purposes. Recurring congestion levels are identified and tagged to TT observations by time of day, allowing each observation to be tagged with a flow regime.

A statistical approach identifies congestion sources in two steps. First, unusual TT requiring explanation are identified. Second, evidence of nonrecurring events likely to have caused unusual TT is sought after. Information is collected for each event with an unusual TT value. Notably it is possible for causal events to be overlooked, however, as these cause no significant impact.

6. Understand the Impact of the Sources of Unreliability

As discussed earlier, various metrics can be used to quantify source impact of unreliability based on distributions developed in Step-5 for specific facilities or routes. Examples of such metrics include the BTI, PTI, and TTI.

SHRP-2 Program Report S2-L02-RR-2 presents a methodology that uses semi-variance measures for identifying reliability impacts of congestion. Semi-variance (σ_r^2) is a one-sided variance metric that uses a reference value r instead of the mean as the basis for calculation. Only observations x_i greater than (or less than) the reference value are used:

$$\sigma_r^2 = \frac{1}{n}\sum_{i=1}^{n}(x_i - r)^2 \qquad x_i \geq r \qquad\qquad \textbf{Eq. 1-6}$$

For TTR analysis, the typical value assigned to r is the minimum travel value observed for the entire study period (e.g., a year). Low semi-variance values indicate high reliability on a route. Comparing semi-variance values throughout the day can be used to identify peak time periods and how reliability fluctuates throughout the day.

TTR metrics can be used by different transportation system managers for various purposes (e.g., transportation agency planning and programming decisions, as well as prioritizing improvements to transportation facilities based on relative impacts).

Step 7. Make Decisions

The final step in developing TTRMS is leveraging knowledge gained from the analysis for decision-making about actions making a significant impact on TTR. Key questions can include:

• When will investments in capacity improvements be necessary, given the current distribution of TT?

• Are proposed operational improvement actions expected to better TT and TTR?

TTR has been the subject of much research in recent years. Appendix-A presents a summary of notable studies cited in published literature.

1.8 Research Motivation

The reported research had four major goals, which are listed below:

- The *first goal* was developing an inexpensive system for monitoring traffic flow on highways and roadways.

- The *second goal* was designing a versatile system that permitted researchers to conduct speed reliability and origin/destination studies, among other investigations.

- The *third goal* was generating probabilistic model(s) for predicting and detecting traffic flow changes due to weather, poor road surface conditions, road incidents, and congestion.

- The *fourth goal* was investigating various schemes for proactively preventing road congestion.

1.9 Report Structure

This report consists of eight chapters, which are organized as follows:

Chapter 1: Includes a general introduction of the scope of this report, including a discussion about measurement techniques used for collecting travel time (TT); travel time reliability (TTR) metrics and monitoring system; requirements for traffic performance management; and the motivation for this research.

Chapter 2: Includes development of an accurate Bluetooth station used for collecting travel time (TT). This chapter includes a description of the system and field testing.

Chapter 3: Describes a set of processes that must be applied on the measurements to estimate TT. This chapter also introduces improvements to Bluetooth system, and it compares it with the inductive loop detector (ILD) traffic monitoring system.

Chapter 4: Includes information necessary to understand the framework for processing the NPMRDS dataset, including limitations and challenges associated with utilizing the dataset.

Chapter 5: Describes methods and processes for anomaly detection and outlier removal, which are used to obtain a cleansed NPRMDS dataset.

Chapter 6: Details the use of NPMRDS to compute required performance measures, as defined in 23 CFR Part 490 of Federal Register, vol. 82, no. 11.

Chapter 7: Includes a description of logit, probit and artificial neural network (ANN) models, which were designed for incident classification. This chapter also includes a description of a Bayesian model for identifying non-recurrent congestion.

Chapter 8: Presents research outcome and makes recommendations for further research work.

2. BLUETOOTH-STATION DEPLOYMENT

2.1 Introduction

Developing an accurate Bluetooth station for collecting TT was completed and field-tested at multiple locations in the vicinity of Oklahoma City (OKC) and Tulsa. A description of the system and field testing is available in the next section.

The proposed TT system consists of Bluetooth stations for detecting Bluetooth devices associated with vehicles using Ubertooth-one [21]—an open source 2.4 GHz wireless development platform used for Bluetooth sniffing. Each Bluetooth station is connected to a Linux box (i.e., Beaglebone) that reads data collected by Ubertooth-one before transmitting the data to a back-end server, where it is stored and processed in real-time. Figure 2-1 depicts the overall proposed system architecture.
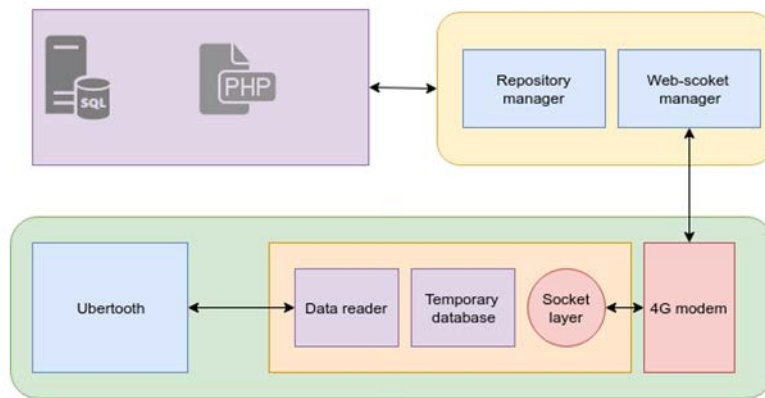
Figure 2-1 System Architecture.

2.2 Removing Unwanted Duplicate LAPs

The OU research team configured system hardware to sniff Bluetooth device LAP for passing vehicles. Since this task is performed in milliseconds and estimated time for a vehicle to remain in the Ubertooth sniffing zone is approximately one second, duplicate records are possible. Based on experiments, the team determined Bluetooth device LAP will be detected between six and 10 times during the time the vehicle is in the sniffing zone (i.e., number of detections for an LAP [Dn] equals vehicle time in sniffing zone [Tv] divided by time required to detect an LAP [Td],—Dn = Tv/Td). For example, given average time of vehicles in sniffing zone is 1000 milliseconds and average time of LAP detection is 135 milliseconds, Dn = Tv/Td = 1000/135 = 7.

Modifications were made to eliminate false data before transmission to server. Defining a buffer permits 128 stored LAPs. For each newly detected Bluetooth device, a window search inside the buffer checks for duplicates among the most recent 32 LAPs. Two factors must be considered: 1) eliminate Ubertooth dongle LAP and 2) determine

when buffer index is shorter than searching window size length (i.e., index of buffer < size of search window 32). Only then can the search operation continue to look for duplicates among LAPs stored in the end of the buffer.

Applying this method ensures that expected time for detecting 32 unique LAPs will exceed the time a vehicle remains in the sniffing zone. For a three-lane highway segment with vehicles spaced at a safe distance, time required for 32 vehicles to pass the sniffing zone (T32v) will be greater than the time one vehicle remains in the detecting zone (T1v)—T32v > T1v.

Buffer size required to eliminate duplicate LAPS should be configured based on sniffing zone and selected antenna. This method for eliminating duplicates demonstrated a sharp increase in data accuracy. Figure 2-2 shows a flowchart of processes implemented to remove duplicate Bluetooth IDs.
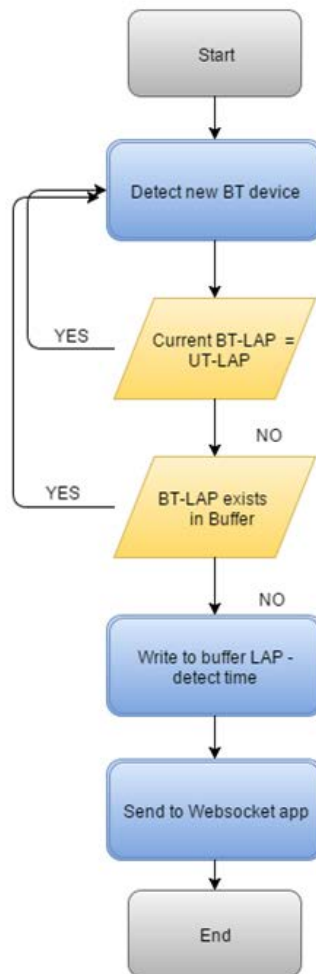
Figure 2-2 Flowchart of Bluetooth ID Duplicate Removal.

2.3 Real-time Communication System

One primary objective for this project was developing and deploying a Real-Time Traffic Monitoring System (RTTMS). The research team employed WebSocket for facilitating communication between REECE and server, which guaranteed detecting and calculating TT in real time, The WebSocket Protocol is an independent TCP-based protocol that provides full-duplex communication channels over a single TCP connection. Although WebSocket is designed for implementation in web browsers and web servers, the protocol can also be used by any client or server application. Its only relationship to HTTP is that its handshake is interpreted by HTTP servers as an Upgrade request. The protocol improves interaction between a station and a website, facilitating live content and the creation of real-time data. This functionality is made possible by establishing a standardized method for the server to send content free from client solicitation to the browser, and then allow messages to pass back and forth while maintaining an open connection. In this way, an ongoing, two-way (i.e., bi-directional) conversation is possible between a browser and the server [22].

2.4 Websocket Message Types

The objective of the following messages is establishing a secure connection between server and stations, guaranteeing real-time data flow for calculating TT changes and detecting various activity (e.g., roadway blocking, construction, weather effects) in short time. Messages also manage connection loss between stations and server by performing backups when connection is recovered. For example:

●Station Registration Message (authentication): Message is sent only on the station's first deployment and consists of station ID and location, using latitude and longitude.

●Bluetooth Single Message (real-time detection): Given that a Bluetooth device is detected, LAP and detection time stamp will be accurate.

●Multi Bluetooth Message (detection back up when connection failed): Message sends a backup of detected LAPs when connection between REECE and server is not working.

2.5 Back-end Processing and Storage (Server Side)

In order for the base station to receive, process, and store data arriving from Bluetooth stations, the research team installed and configured a Microsoft Windows server in the OU network, whereby Bluetooth stations can gain access using their unique IP address. To support real-time communication between server and Bluetooth stations, the team utilized a WebSocket connection for opening bidirectional

communication. WebSocket is deployed on a specific server port so that each station can access the server by way of its IP address and this particular port.

A database was designed and implemented using Microsoft SQL server for storing data received from Bluetooth stations onto the server. The database is composed of tables representing highway, station, detected vehicles, and detected passing time data, among other information. Figure 2-3 depicts the database schema diagram.

A web application using PHP was developed to maintain WebSocket connection between server and station nodes and to listen to a specific port. Given that a message arrives on the port, the application will verify message type (e.g., registration, single data, multiple data) and store the message in the database for data processing and analysis at a later time. Figure 2-4 depicts the connection and message transferring sequence between server and station node.

Any Bluetooth station can communicate with the server via the three types of messages named above. Given that a Bluetooth station opens socket connection with the server, an empty station object will be created and stored in memory; the object will contain information only about the connection (e.g., station IP address). It is important to know that Bluetooth station IP addresses are not static and that the station cannot send data until it sends a registration message containing information like station ID, serial number, highway and GPS location, and a sample registration message, as illustrated in the JSON messages shown in Figure 2-4.

The server uses the registration message to validate that the communicating station is authorized by comparing Bluetooth station ID and serial number with predefined information stored in the database. Given that the information matches, the Bluetooth station object will be flagged as authorized and the station can begin sending information to the server. In the event that the station is not authorized, the connection between the server and the Bluetooth station is closed and the station object is deleted from the memory. If a Bluetooth station detects a Bluetooth device, the station will send a detection JASON message.
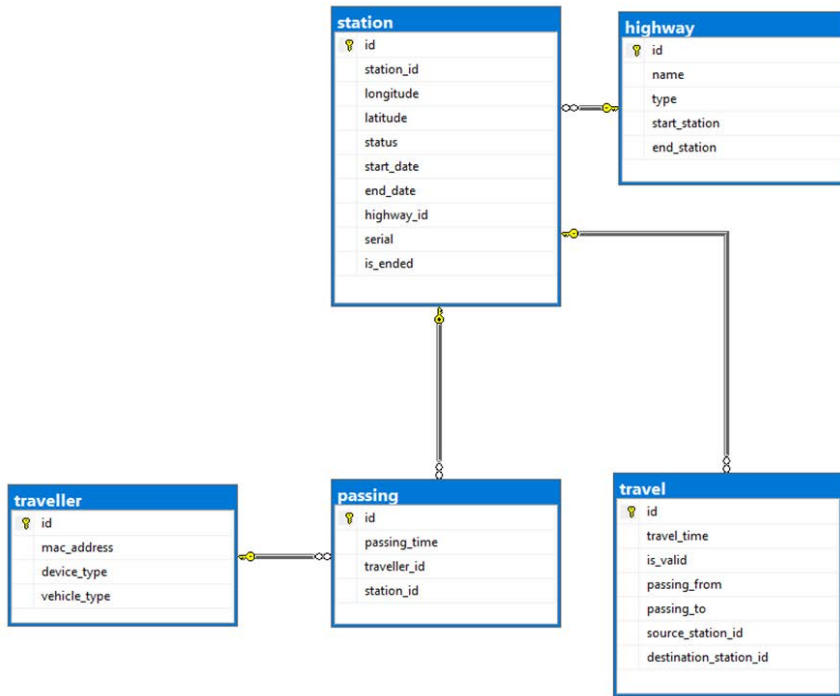
Figure 2-3 Database Schema.
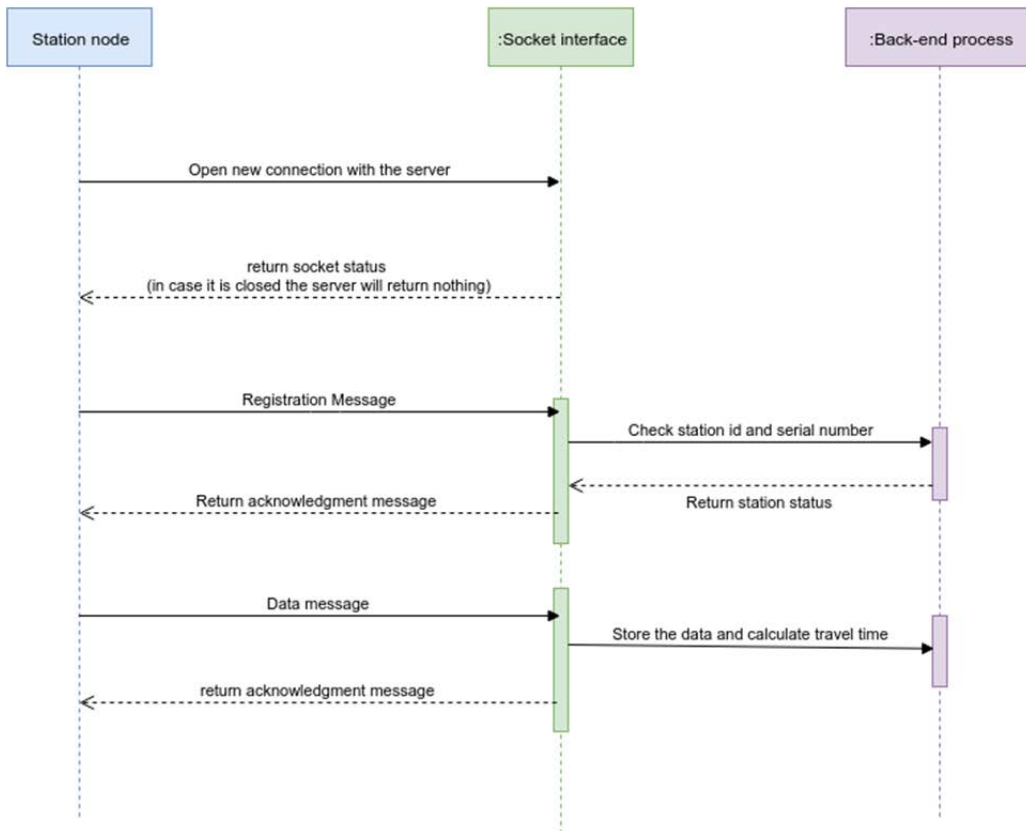
Figure 2-4 Message Exchange Between Server and Station.

2.6 Deployments and Analysis Results

To ensure accurate TT estimation, many experiments were conducted for collecting and analyzing travel data. Travel data was then compared with information provided from HERE and ODOT radar. Using single and multiple Bluetooth stations, we were able to estimate number of vehicles, TT, and speed. Data statistics, modeling, and prediction results are discussed in the following section.

2.6.1 Four Bluetooth Stations Deployed in Oklahoma City

Analysis of a single site Bluetooth station deployment. Data analysis compared the number of vehicles that a station was able to detect with a reference data source, like HERE or ODOT radar data (i.e., 7,688 detected vehicles). Statistical information was extracted from data collected between 10/18/2016 and 10/25/2016.

Deployment encountered a number of problems. A list is provided below.

1. Aircard Sprint Franklin U772 was not compatible with the REECE OS. The connection between the REECE and the server was dropped most of the time, and mounting errors caused the REECE system kernel to enter panic mode.

2. Station clearing system-logs were not implemented, causing the SD cards to reach full capacity and stop working.

3. Units were positioned too far from one another and provided misleading information for calculating TT.

2.6.2 Three Bluetooth Stations Deployed in Tulsa, OK

Analysis of a single site Bluetooth station deployment. Software adjustments were made, and a new deployment was subsequently conducted. A single Bluetooth station was deployed to collect data on OK highways I-44 and 169 between 12/10/2016 and 01/06/2017. 115,256 vehicles were detected. Figure 2-5 (a) shows detected LAPs binned to collection date. Mean was 3974, and median value was 4500. Saturday and Sunday had the lowest rates; the number of vehicles increased during business days. Thursday traffic rates were the highest. Figure 2-5 (b) shows detected vehicles on a single day and reflects distribution of detection over 24 hours. Traffic counts increased between 7 and 8 a.m. and after 5 p.m.

Analysis of TT comparing Oklahoma City, OK with Tulsa, OK. During the experiment, the proposed system matched 4740 records from two sites over an 18-day period. Figure 2-6 shows the distance between sites. Calculated TT mean was 224.37s (or 3 minutes and 44 seconds), and median was 222s. Figure 2-7 shows TT distribution. Daily average for matched Bluetooth IDs was 237, and median was 196, as shown in Figure 2-8.

(a)

(b)
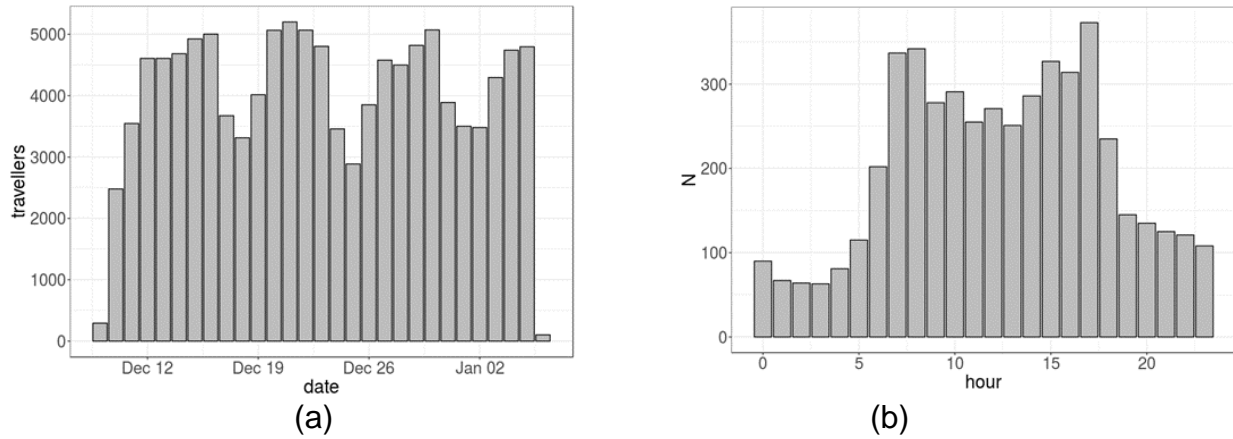
Figure 2-5 (a) Daily Bluetooth ID's Detect by One Site; (b) Bluetooth ID's Distribution During One 24 Hour Period.
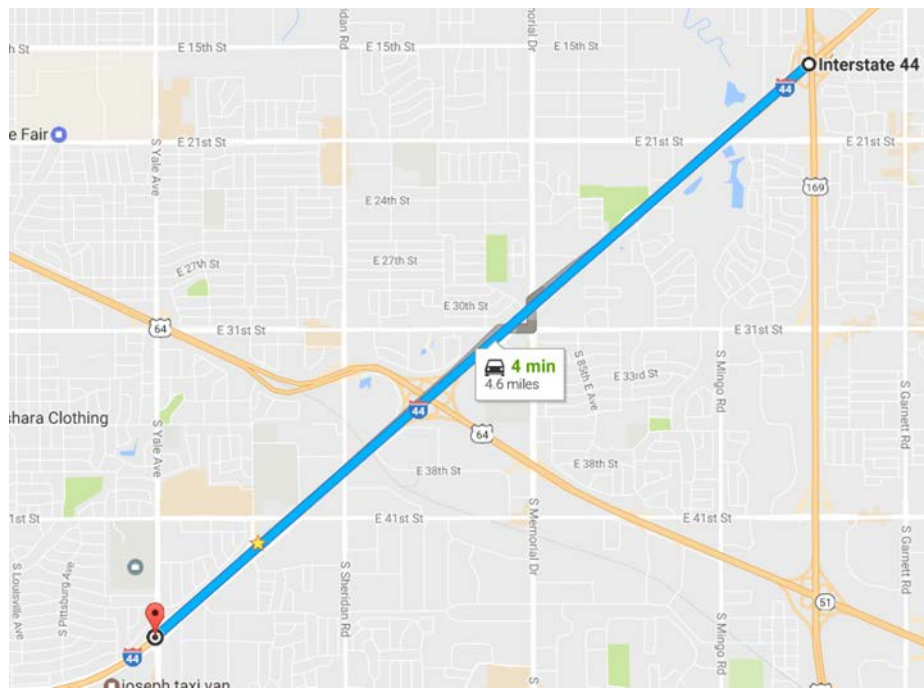
Figure 2-6 Deployment Sites and Separation Distance.

Several improvements were made during this deployment. These are listed below.

1. When comparing the OKC and Tulsa deployments, for the latter the OU research team used stable AC341u Aircards, ensuring that the connection between stations and the server was operational most of the time.

2. Reducing the distance between Bluetooth stations increased the number of matched Bluetooth IDs and accurate TTs.

31

3. Limiting system log size prevented the SD card from reaching full capacity, requiring less frequent site maintenance.
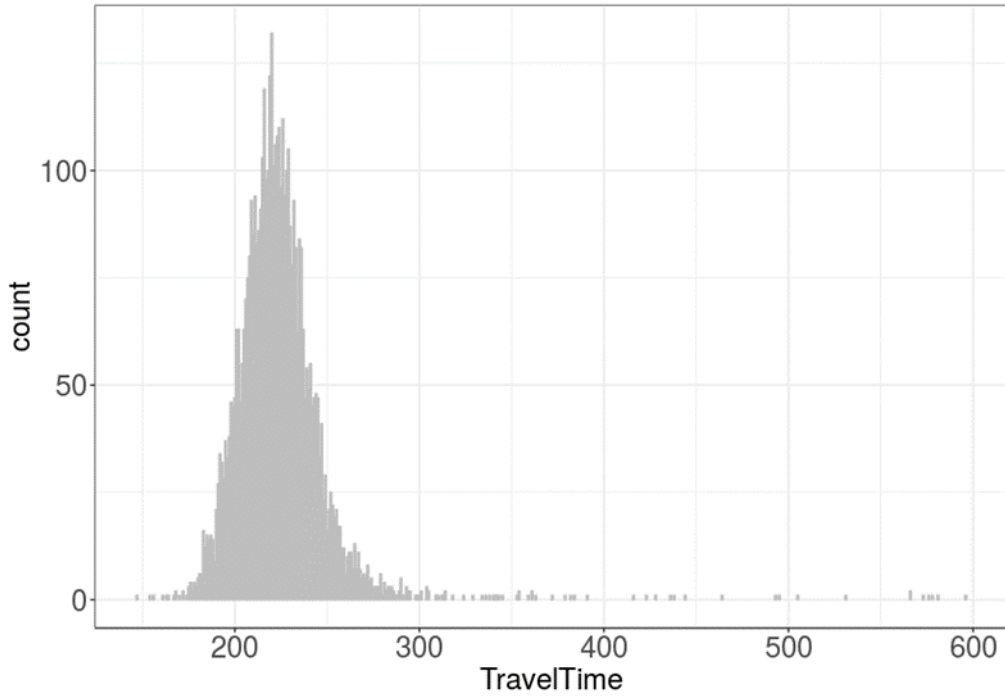
Figure 2-7 TT Distribution.
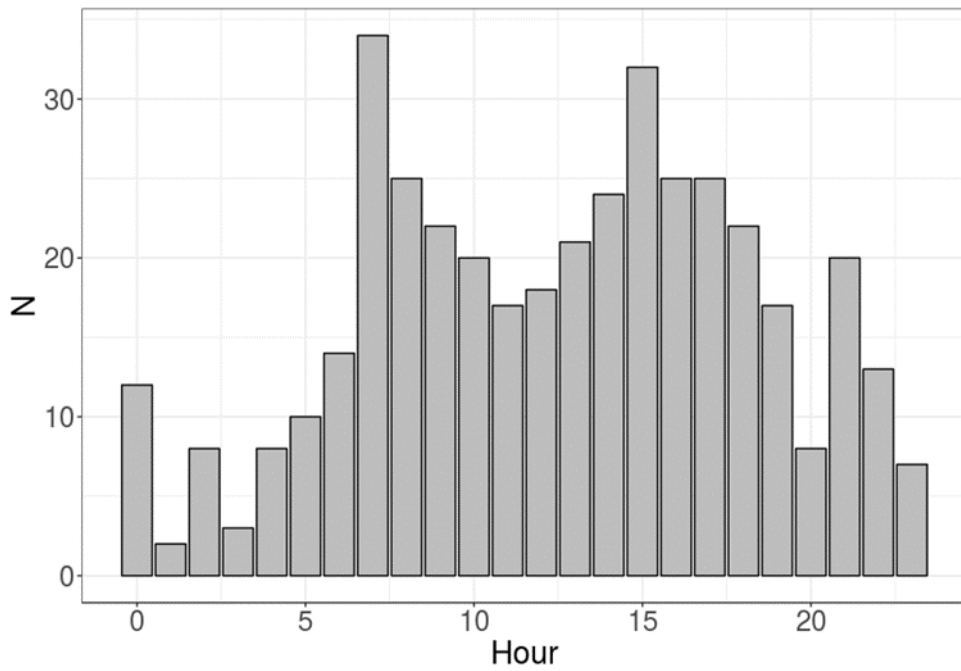
Figure 2-8 Matched Bluetooth Ids in Number Over 24-Hour Period.

3. INTEGRATION OF BLUETOOTH TRAVEL TIME MEASUREMENTS INTO ODOT TRAVEL TIME SYSTEM

To estimate TT based on detected vehicles traveling from checkpoint A to checkpoint B, a set of processes must be applied on the measurements. Figure 3-1 represents a typical Bluetooth traffic monitoring system. Multiple Ubertooth sniffers were deployed with variant distances on highways for detecting vehicle MACs.
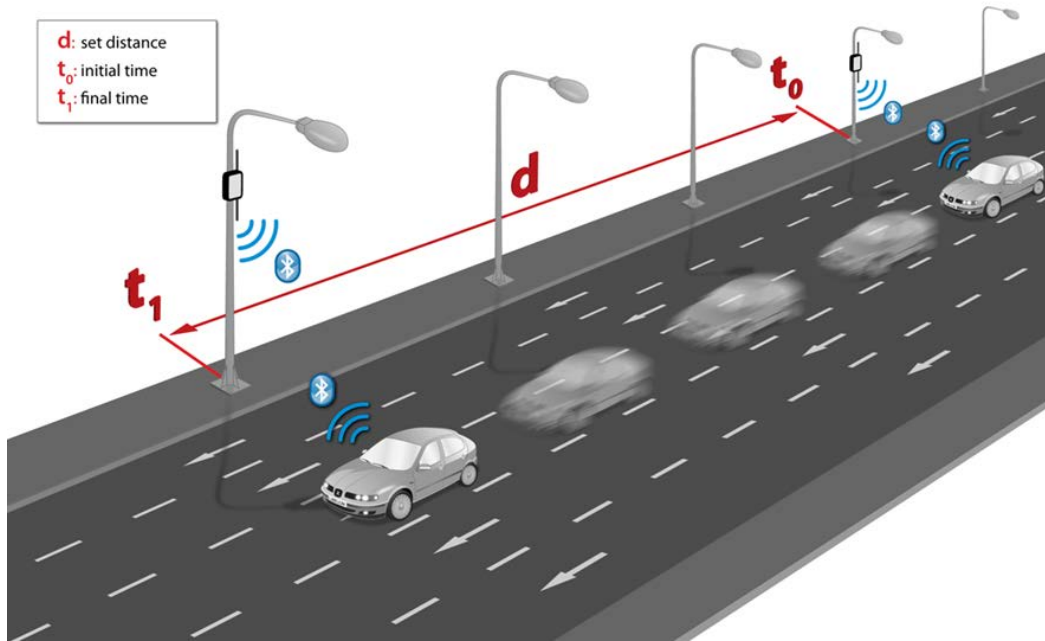
Figure 3-1 Bluetooth Traffic Monitoring System.

3.1 Removing Unwanted Duplicated MACs

Ubertooth was configured to sniff Bluetooth device MACs traveling on the highway. Since sniffing MACs occurs in just microseconds and estimated time for a vehicle to remain in the Ubertooth sniffing zone is more than 1 second, the same MAC might be detected multiple times. Consequently, modifications to the proposed system were made to eliminate duplicated data before uploading to the cloud. A buffer can store 128 MACs. Hence, for every newly detected Bluetooth device, a window search occurs inside the buffer to identify duplicates among the last 32 MACs. Two considerations were made. First, eliminate Ubertooth dongle MAC. Second, state when the index of buffer is smaller than the size of the searching window (i.e., index of the buffer < size of search window 32). A search operation continues to look for duplicates among LAPs stored in the end of the buffer. Figure 2-2 illustrates the flowchart for eliminating Bluetooth duplicates.

Collected data is saved on REECE before transmitting information to the cloud using a simple MySQL lite database. Each MAC address is accompanied by a time stamp and unique ID. The database table structure is shown in Figure 3-2.

Figure 3-2 Bluetooth MySQL Database on REECE.

The database consists of one table with six columns, as indicated below:

- Seq: Sequence of Bluetooth device labelled in the database

- MAC: MAC of detected Bluetooth device

- Det_TIME: Detection time of Bluetooth device

- Trans_TIME: Transmission time of information packet to the server

- Exp_TIME: Time to determine unnecessary transmission of detected Bluetooth device information; fixed value not in use

- ACK_TIME: Acknowledgment time wherein REECE receives a message from the cloud containing sent packet sequence

3.2 Vehicle Reidentification

A vehicle can be re-identified by searching for the same MAC address at consecutive checkpoints. Matched MAC addresses provide a TT value based on differences in detection time. Vehicle speed is based on known distance between checkpoints.

TT per vehicle can be calculated using the following equation:

$$TT_{per\ vehicle} = DT_b - DT_a \qquad \text{**Eq. 3-1**}$$

where DT is the detection time at one checkpoint.

Outliers can occur when one vehicle travels between two points on a different journey. For an accurate estimation, outliers must be identified and removed. The following algorithm is proposed for this purpose.

- Find TT distribution of observed segment.
- Calculate mean TT and SD σ.
- TT is considered an outlier given it meets the following equation:

$$TT_{per\ vehicle} > TT_{mean} + 2\sigma$$ **Eq. 3-2**

3.3 Travel Time Estimation

TT can be estimated by finding the mean of the distribution of TT per vehicle measurements.

Experiments and analysis results. A number of experiments were conducted to collect and analyze travel data for achieving accurate TT estimation. Using single and multiple Bluetooth stations, number of vehicles, TT, and speed estimation can be estimated.

Deployment was tested during March 2017 in Tulsa, OK. Details are summarized below.

1. Testing deployment had seven units running throughout the city of Tulsa, OK during a 10-day period.
2. TT calculated between the selected locations were approximately equal to Google TT estimates.
3. Traveling vehicles between locations were detected at distances of 5 and 10 miles.

Data insights were made following data collection. Daily average of detected vehicles was over 5.000 per day. Table 3-1 provides detailed information for each unit. Figure 3-3 shows the location of units deployed throughout the city of Tulsa, OK.

Table 3-1 Tulsa, OK Deployments.

station ID	Daily average Detected Vehicles	Antenna	Location and Distance from Highway
BT-054	8790	5 dbi internal	Side highway, apx 1 meter far
BT-061	5140	5 dbi internal	Under Bridge , apx 8 meters far
BT-062	4560	3 dbi internal	Above highway, apx 15 meters far
BT-063	6010	3 dbi internal	Side highway, apx 1 meter far
BT-064	3950	5 dbi internal (tilted)	Side highway, apx 1 meter far
BT-065	6160	3 dbi internal	Side highway, apx 1 meter far
BT-066	5550	3 dbi internal	Above highway, apx 5 meters far
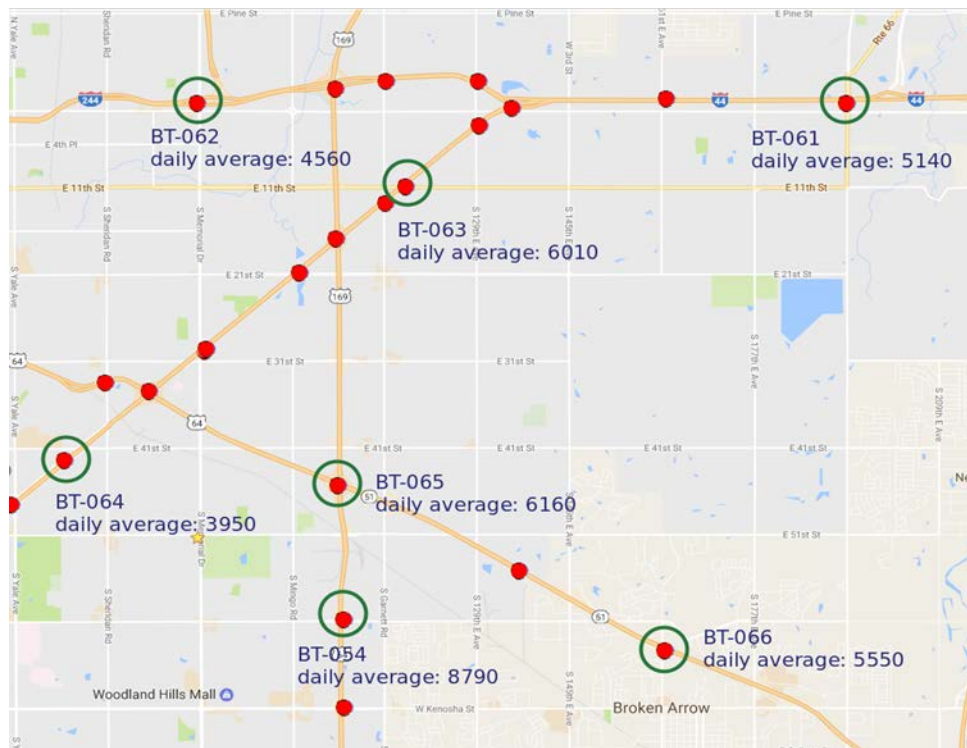
Figure 3-3 Locations of Deployed Units in Tulsa, OK.
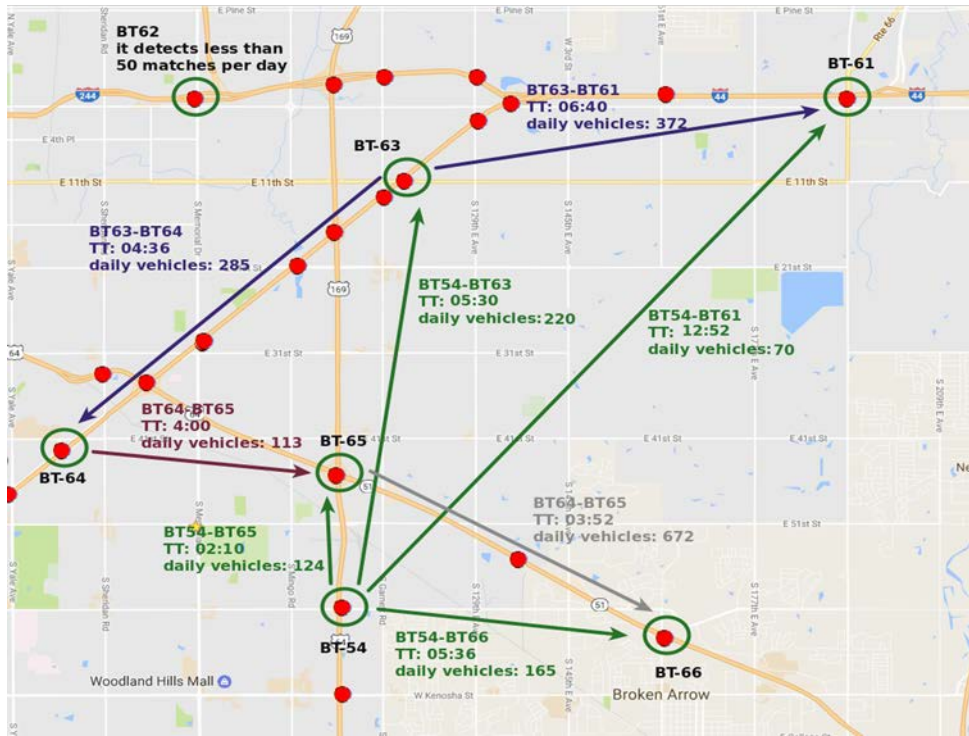
Figure 3-4 Average TT and Average Daily Detected Vehicles Between Two Locations.

Deployment-calculated TT was approximately equal to Google TT estimates. An average of over 200 vehicles were detected per day between two locations among all deployed units. Number of detected vehicles depends on a number of factors, including:

- distance between the two locations,

- traffic flow,

- attractions approximate to deployed units (e.g., downtown, main apartments complexes, city exits), and

- antenna type/distance between cabinet and the highway.

Figure 3-4 and Table 3-2 provide detailed information for detected vehicles traveling between two locations.

Table 3-2 Average Travel Time and Average Daily Detected Vehicles.

Units	Average TT	Average daily detected vehicles
BT-054 BT-061	**12:52**	**70**
BT-054 BT-062	07:35	34
BT-054 BT-063	**05:30**	**220**
BT-054 BT-064	06:21	67
BT-054 BT-065	**02:10**	**124**
BT-054 BT-066	**05:36**	**165**
BT-061 BT-062	08:00	45
BT-061 BT-063	**06:40**	**372**
BT-061 BT-064	10:30	25
BT-061 BT-065	11:05	4
BT-061 BT-066	13:20	6
BT-062 BT-063	07:44	8
BT-062 BT-064	07:38	10
BT-062 BT-065	06:40	38
BT-062 BT-066	10:00	11
BT-063 BT-064	**04:36**	**285**
BT-063 BT-065	05:10	22
BT-063 BT-066	08:50	9
BT-064 BT-065	**04:00**	**113**
BT-064 BT-066	07:34	55
BT-065 BT-066	**03:52**	**672**

3.4 Study of Travel Time Between Two Units

In this section the results of data collected between two different road segments will be discussed.

3.4.1 TT between units Bluetooth -061 and Bluetooth -063

Distance between units Bluetooth-061 and Bluetooth-063 was 5.2 miles, as shown in Figure 3-5. Figure 3-6 through Figure 3-9 illustrate TT distribution, daily number of detected vehicles, hourly number of detected vehicles on a single day, and hourly average TT on a single day. Bluetooth sniffers detected an average of 372 vehicles/day and calculated TT of 06:40, which is one minute longer than Google estimates. Of note is that road work may have had an effect on the difference between the two values. During rush hour (i.e., 2 to 6 p.m.), the hourly rate of detected vehicles was approximately 40.
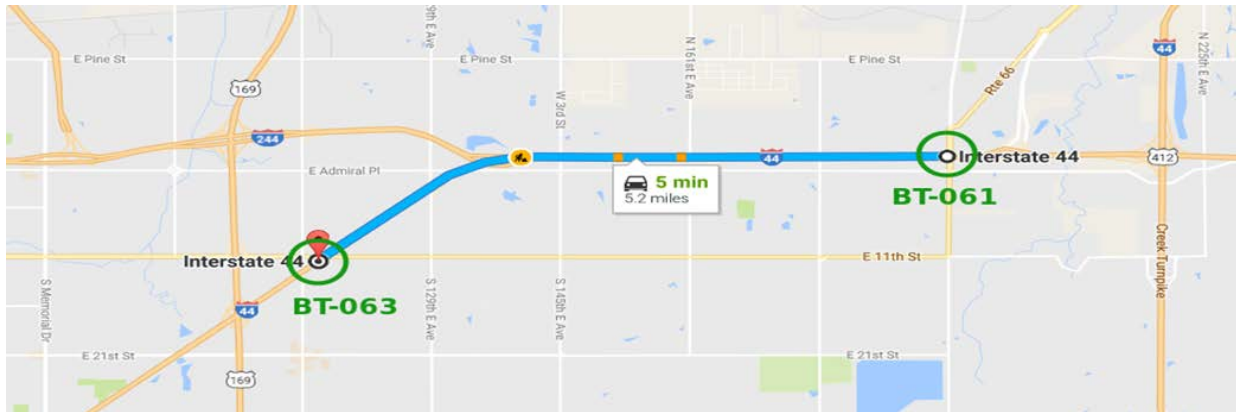
Figure 3-5 Bluetooth Monitoring System for 5.2-mile Distance on I-44 in Tulsa, OK.
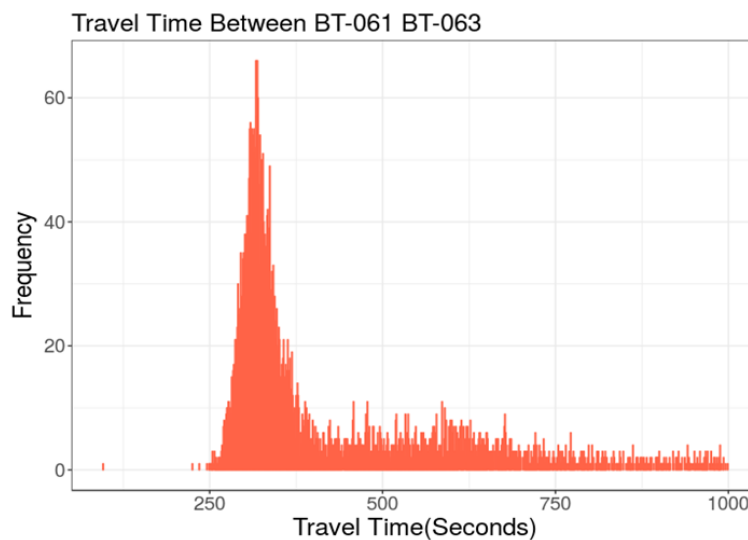
Figure 3-6 TT Distribution.

39
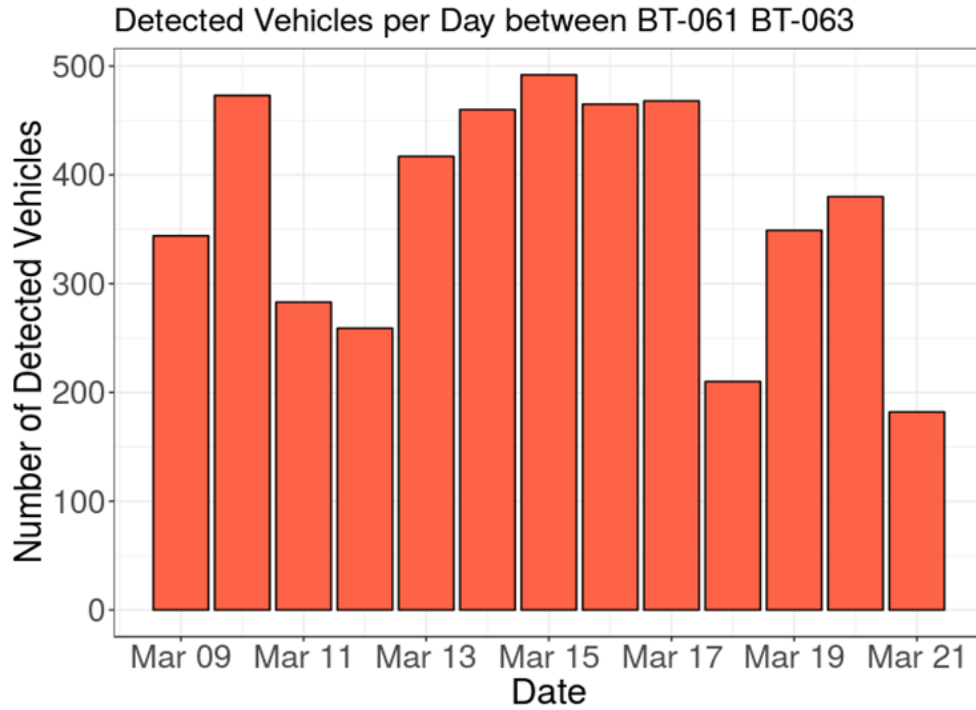
Figure 3-7 TT Values Based on Bluetooth on I-44 in Tulsa, OK.
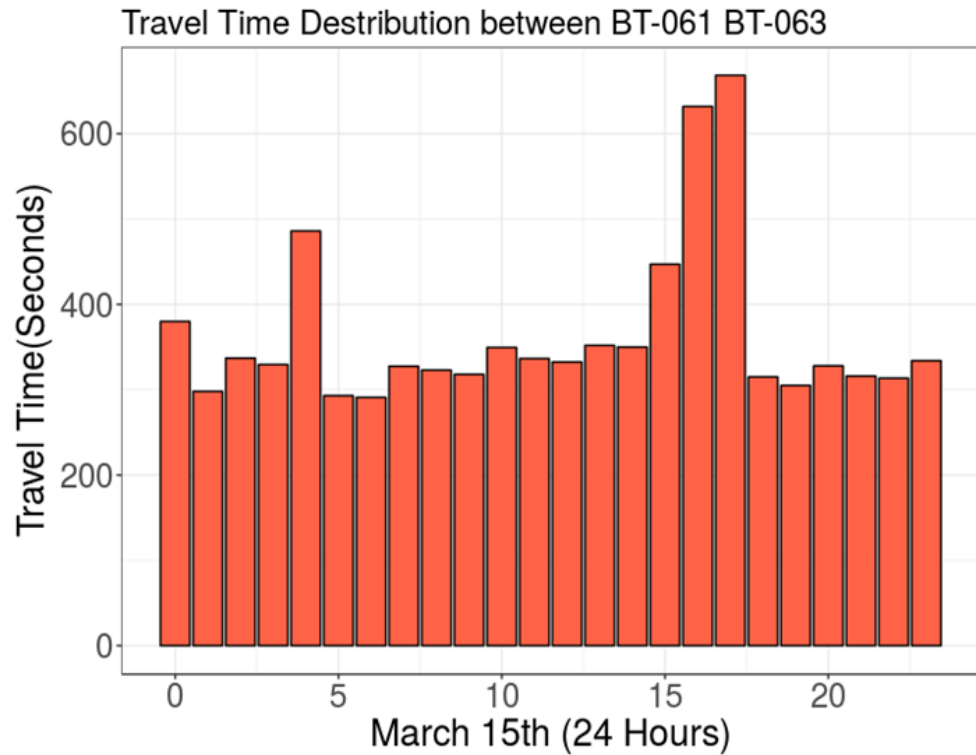
Figure 3-8 Hourly Average TT on a Single Day.
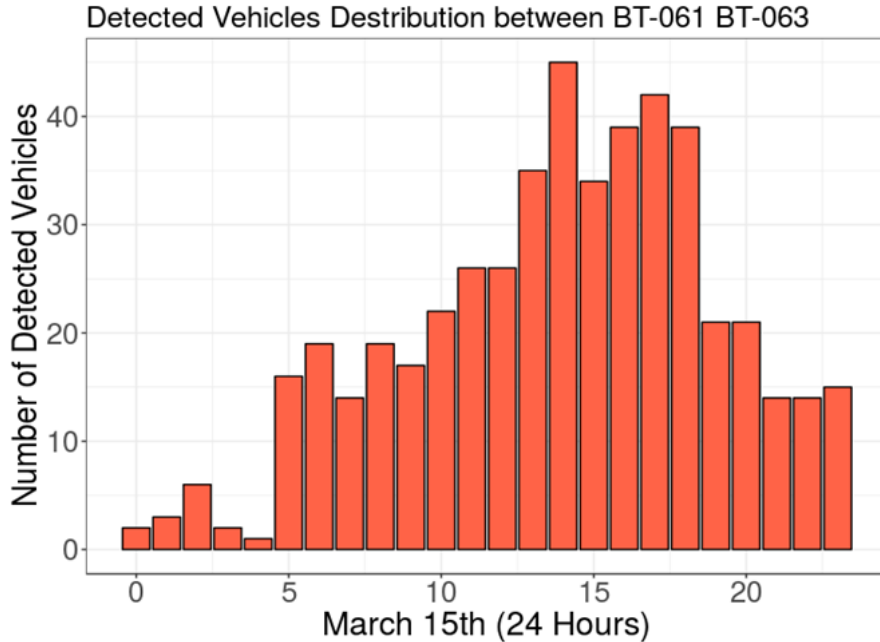
Figure 3-9 Hourly Number of Detected Vehicles on a Single Day.

3.4.2 Units Bluetooth-065 and Bluetooth-066

The distance between units Bluetooth-065 and Bluetooth-066 is 4.1 miles. Bluetooth sniffers detected an average of 672 vehicles/day and calculated TT of 03:52, which was the same as the Google estimate. During rush hour (i.e., 3 to 5 p.m.), the hourly rate of detected vehicles was approximately 70. Figure 3-10 through Figure 3-14 illustrate the segment location, TT distribution, daily number of detected vehicles, hourly number of detected vehicles on a single day, and hourly average TT on a single day.
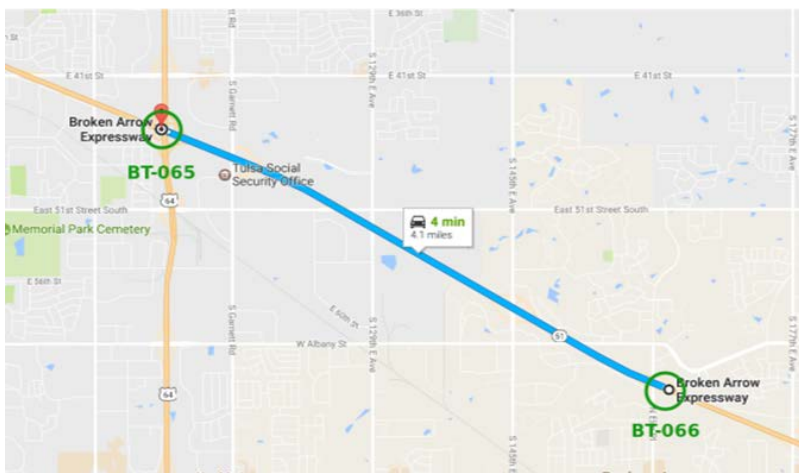
Figure 3-10 Bluetooth Monitoring System for 4.1-mile Distance on BA-Expressway in Tulsa, OK.

41
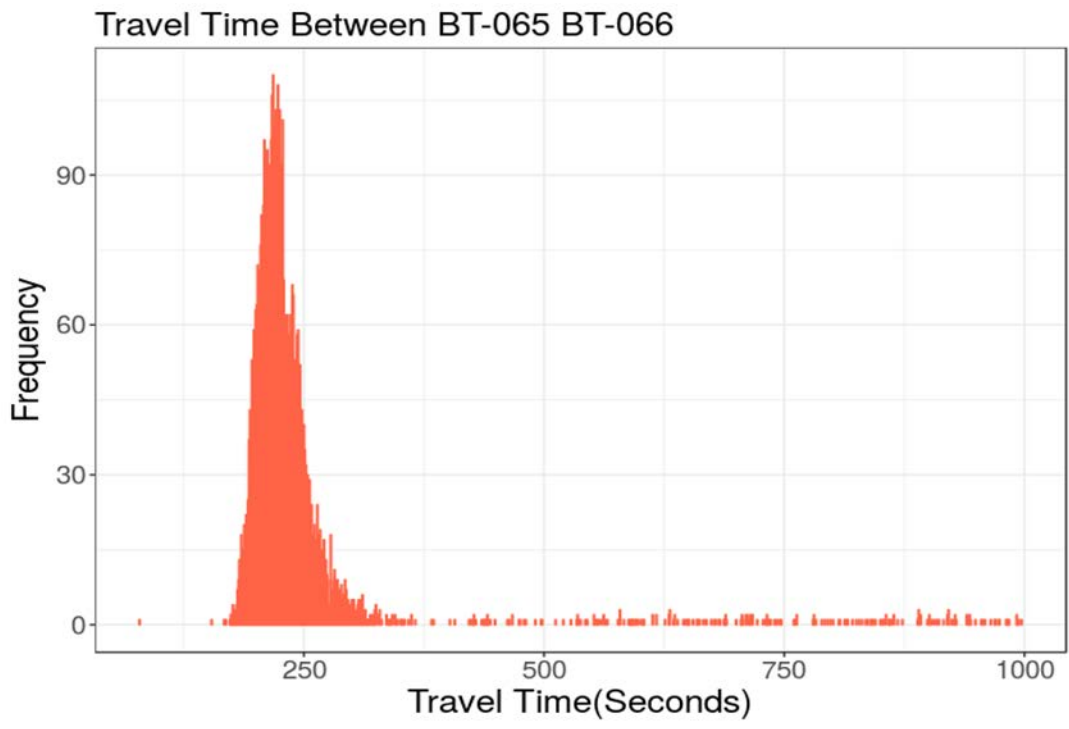
Figure 3-11 TT Values Based on Bluetooth on BA-Expressway in Tulsa, OK.
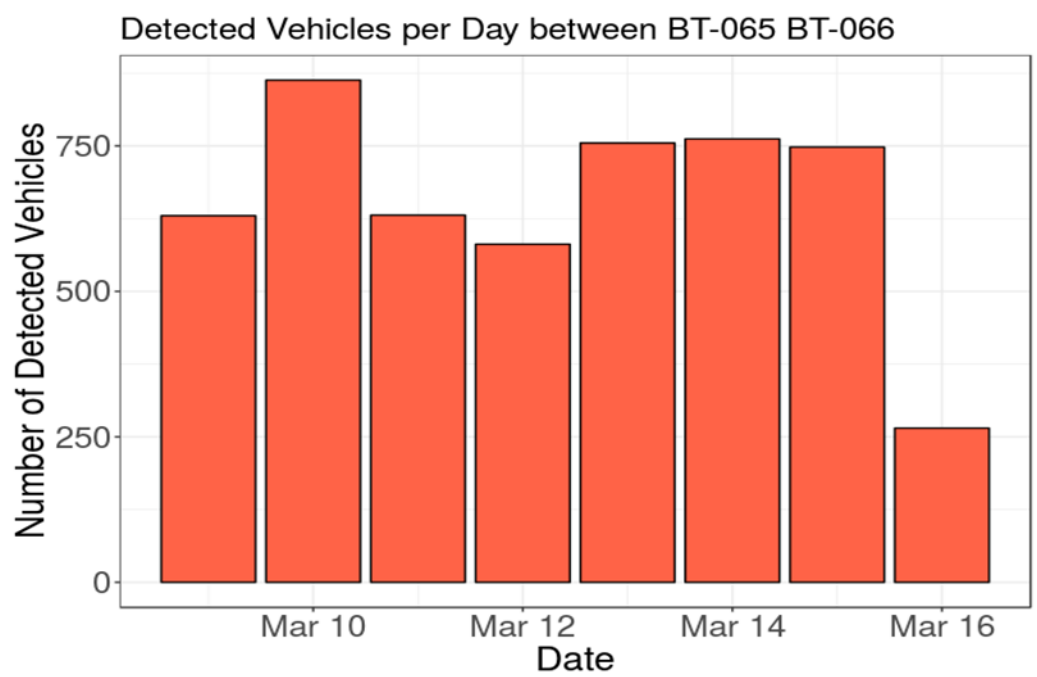
Figure 3-12 Number of Detected Vehicles on a 4.1-Mile Segment over a 5 Day Period.
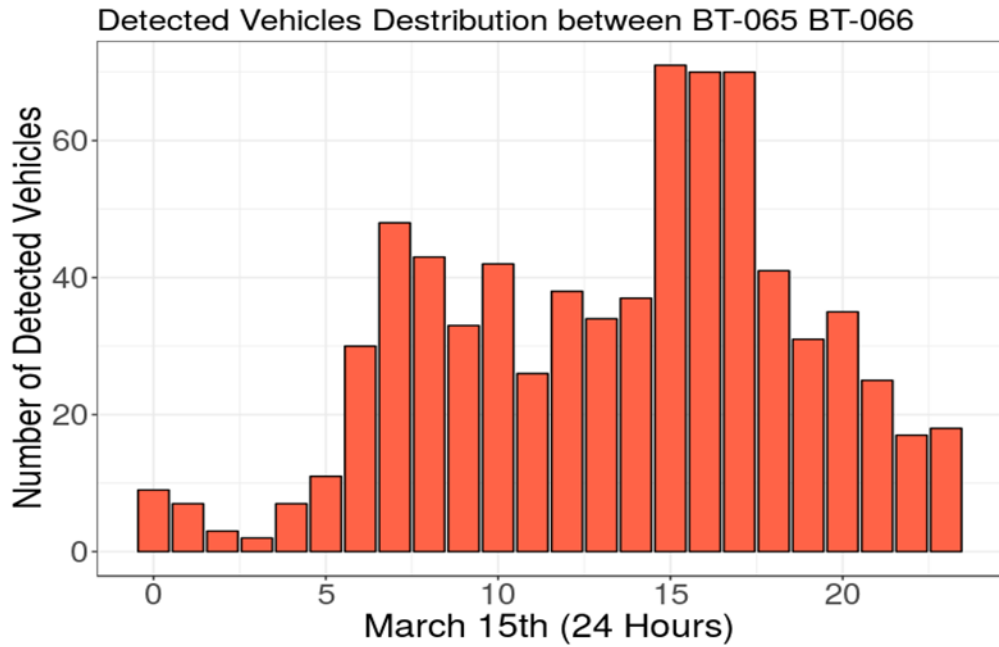
Figure 3-13 Hourly Number of Detected Vehicles on a Single Day.
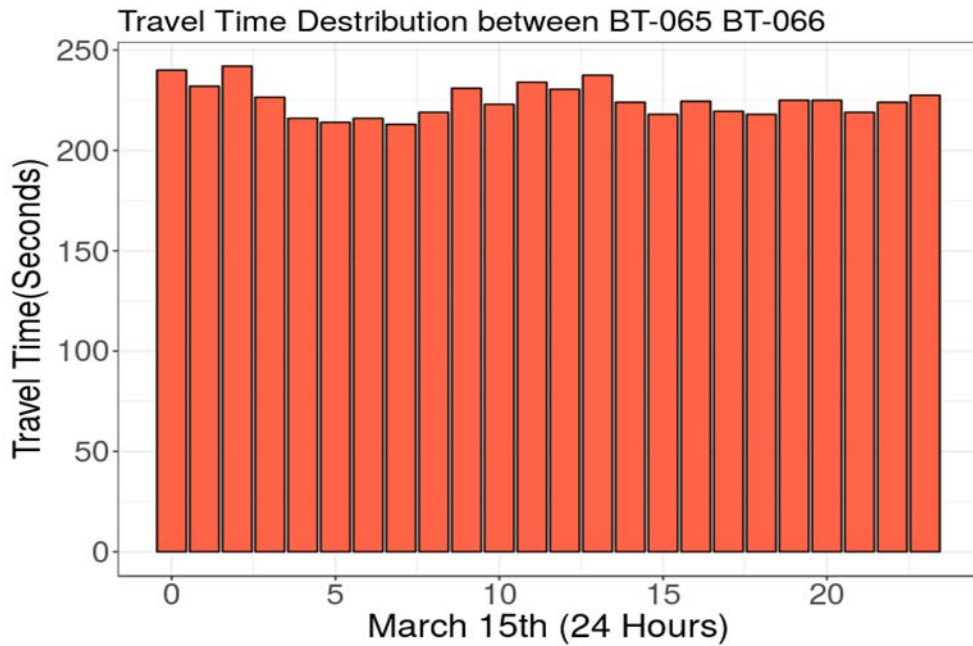
Figure 3-14 Hourly Average TT on a Single Day.

No major changes were detected in TT between the two locations over a period of 24 hours.

3.5 Improvements to Bluetooth System

Previous experiments have shown that the number of vehicles detected between two locations is extremely low. An alternate antenna was tested to improve traffic system penetration. Figure 3-15 and Figure 3-16 depicts two antennas considered for Bluetooth detection. Figure 3-15 shows an antenna used in previous experiments, which is an internal omni-directional antenna with 5dBi gain and 50 Ω impedance. Figure 3-16 shows an alternative antenna (TP-Link TL-ANT2414A), which is an external directional antenna with 14dBi and 50 Ω impedance.

Figure 3-15 Internal Omni-directional Antenna

Figure 3-16 External Directional Antenna

Figure 3-17 and Figure 3-18 show a substantial change in the number of detected vehicles when using an external directional 14dBi antenna instead of an internal 5dBi antenna.
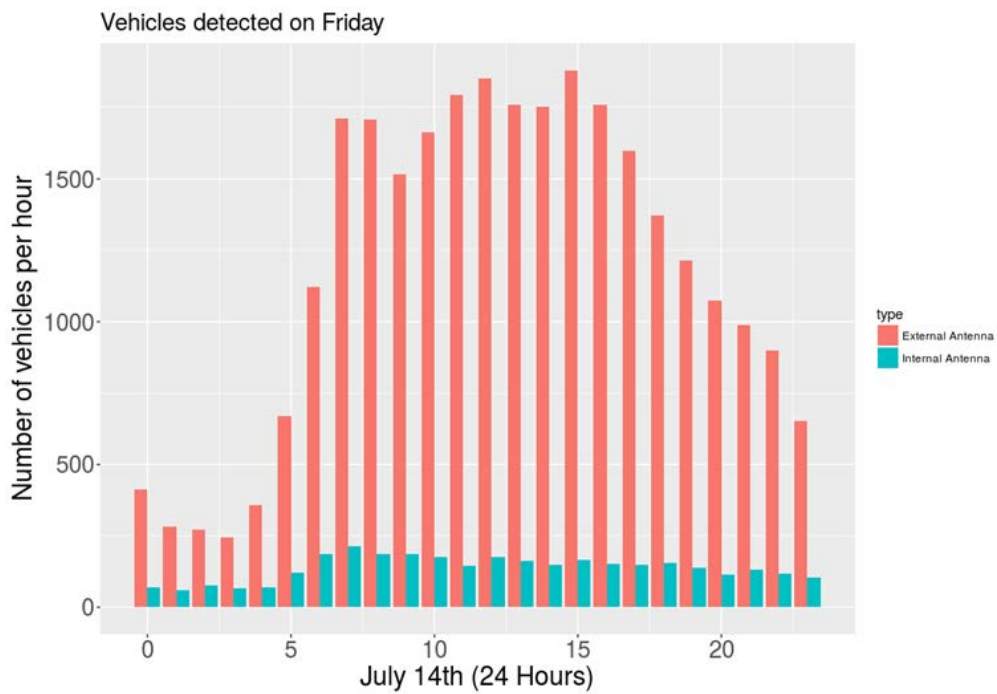
Figure 3-17 Hourly Number of Detected Bluetooth Devices on a Single Site.
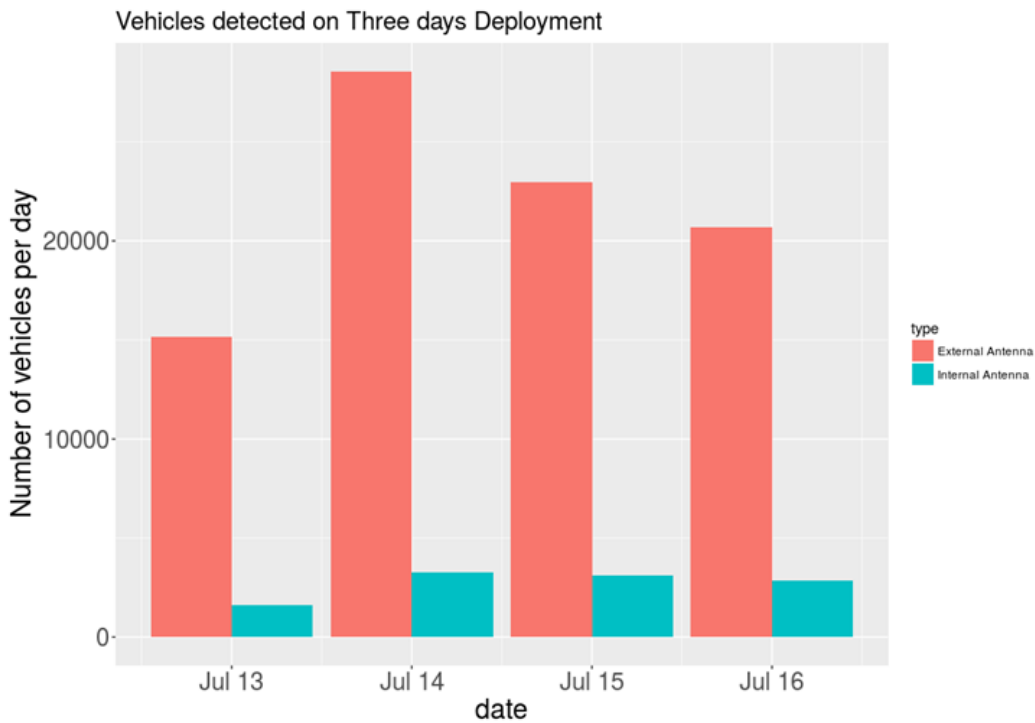
Figure 3-18 Daily Number of Detected Bluetooth Devices on a Single Site.

3.6 Inductive Loop Detectors for Travel Time Estimation

An inductive loop, shown in Figure 3-19, consists of wire "coiled" to form a loop shaped as a square, circle, or rectangle for installation into or under the roadway surface. Inductive loops work like a metal detector, measuring the change in magnetic field when objects pass over. As a vehicle drives over a loop sensor, the loop field changes so that the detection device detects the presence of an object (e.g., vehicle). Inductive loops are referred to as presence detectors. Traffic detection devices are often used in combination with axle sensors to collect classification data, such as vehicle speed and length.
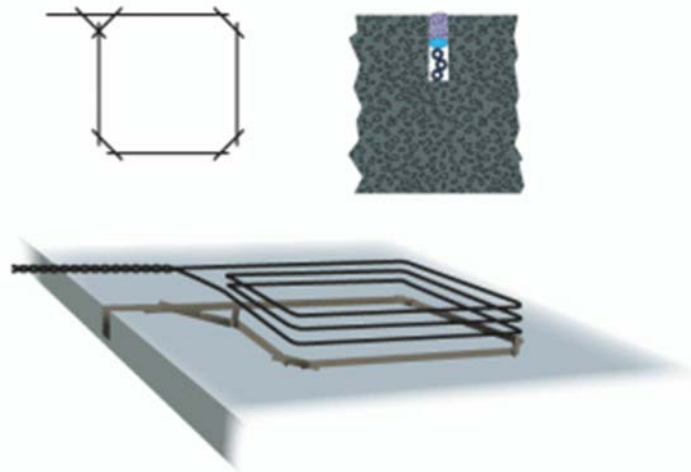
Figure 3-19 Square Inductive Loop.

Two commonly used shapes for inductive loops are round and square/rectangular. Many loop designers have theorized that a circular shape provides optimum detection because a uniform magnetic field is produced without dead spots. Proponents of the round loop argue that the circular design maximizes loop sensitivity for detecting both motorcycles and high-bed trucks, while eliminating splash over from adjacent lanes. Other cited advantages include elimination of sharp corners and reduction in wire stress. Modern techniques have mitigated difficulties associated with cutting a circular shape in the pavement.

An inductive loop is composed of a continuous length of wire that enters and exits from the same point. Both ends are connected to the loop extension cable, which in turn connects to the vehicle detector. The detector powers the loop, causing a magnetic field in the loop area. The loop resonates at a constant frequency that is monitored by the detector. A base frequency is established when there is no vehicle atop the loop. When a large metal object, such as a vehicle, passes over the loop, resonate frequency increases. The change is sensed and, depending on the design of the detector, forces a

normally open relay to close. The relay will remain closed until the vehicle leaves the loop and the frequency returns to the base level.

3.6.1 Study of the Inductive Loop Signature

Generated ILD signals vary from one vehicle to another. Accordingly, an ILD signature depends on vehicle length, metal surface, speed, and the way in which a vehicle will pass over a loop. Figure 3-20 shows the difference in signatures between SUV and sedan vehicles (e.g., variance in signature length and amplitude of the magnetic field). While the sedan has one peak point, an SUV has two. Also, it is important to note that signatures of the same vehicle will not be identical on another loop. In Figure 3-20, the red and blue signatures for each vehicle represent the signature detected on the lead and lag loops, respectfully, with an 8-foot distance between them. Variations will increase for longer distances between two loops, hence, magnetic field strength will vary among vehicles of the same class. ILD signals have many applications in length-based vehicle classifications due to accurate measure of vehicle length.

Loop Shutdown. Two phenomena are cause for possible inductive loop malfunction:

- Lightning strike: Given that lightning strikes relatively close to a road-embedded loop, it is possible that a large static charge will be transmitted through the loops into the loop board circuitry. Although the loop board is equipped with a certain level of electronic protection against this type of event, lightning strikes might cause the loop board to lock up or shut down. A strike is unlikely to cause damage to a unit that is grounded.
- Electrical noise: Similar to a lightning strike, other sources of strong electronic signals could cause the loop board to detune.

In some cases, inductive loops do not shutdown even though they add noise to the ILD signals and require retuning to fix an issue. Figure 3-21 illustrates various noisy signatures.
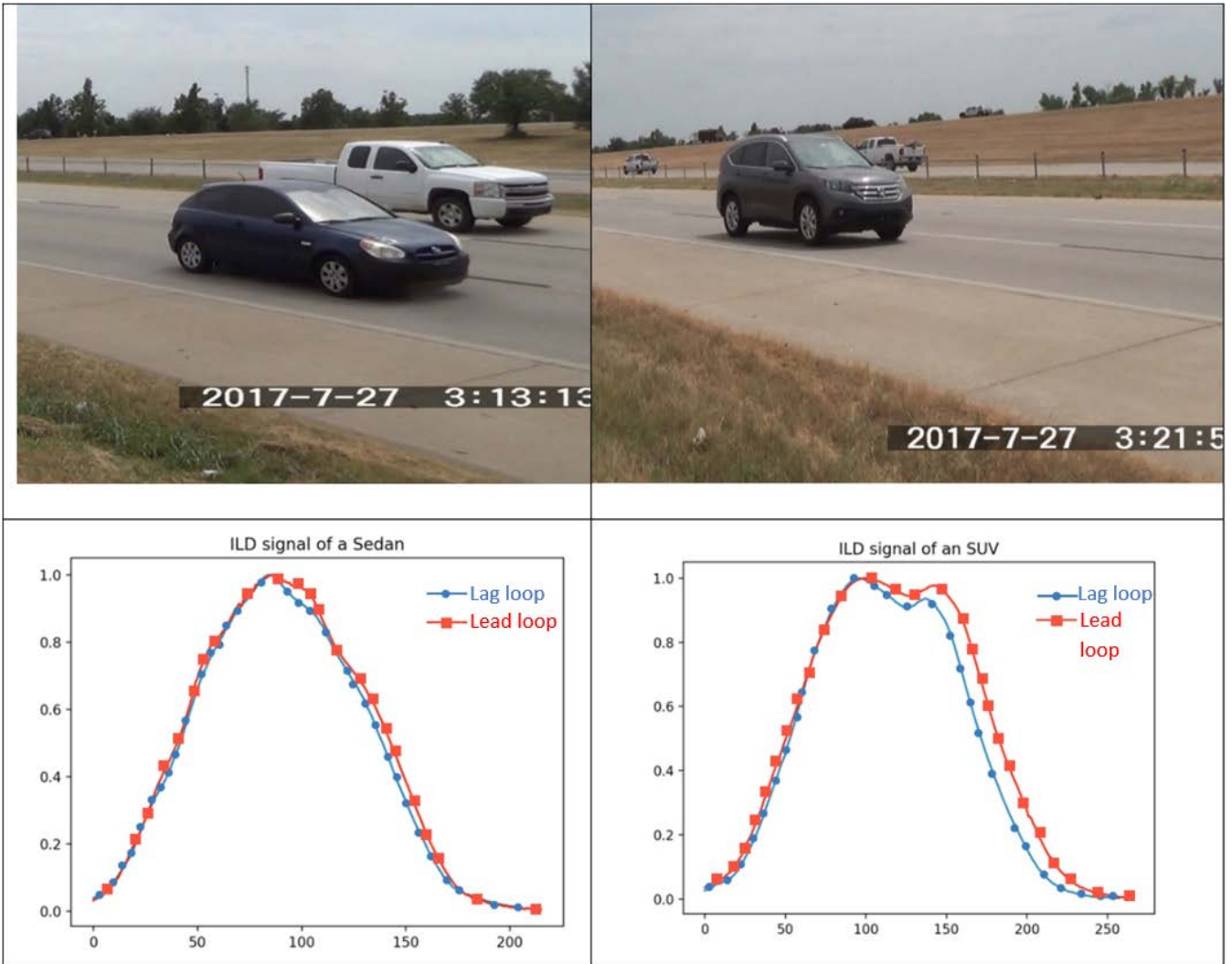
Figure 3-20 ILD Signatures of Two Vehicles.
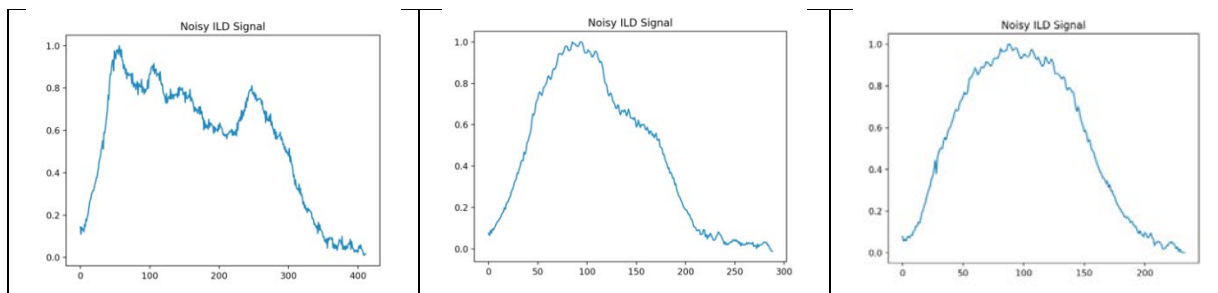
Figure 3-21 Noisy ILD signals.

3.6.2 Phoenix II Diamond Traffic

Phoenix II (See Figure 3-22) is a multi-lane, time interval counter/classifier designed for permanent installations or large portable applications. The classifier can count from one to eight lanes using axle sensors; 16 lanes with loops; or one to eight lanes with gap, headway, and speed by axle type. The system can be fitted with four road tube sensors, two to eight remote inputs, four to 16 presence inductive loop sensors, and four to eight piezo or resistive sensor inputs.

When Phoenix II is activated in vehicle output in comma delimited output (VO=CMA), the classifier generates signatures as a string of time-series data samples, separating each vehicle signature by CR/LF.

Figure 3-22 Phoenix II Diamond Traffic Unit.

Deployment setup. The following steps are necessary for deployment.

- Phoenix II Diamond Traffic with 1KB sampling rate is connected to a standard 6' by 6' rectangular inductive loop.

- REECE is connected over RS-232 with Phoenix II and over ethernet to the cloud.

Figure 3-23 illustrates the ILD Traffic Monitoring System setup at Hefner parkway in Oklahoma City, OK.
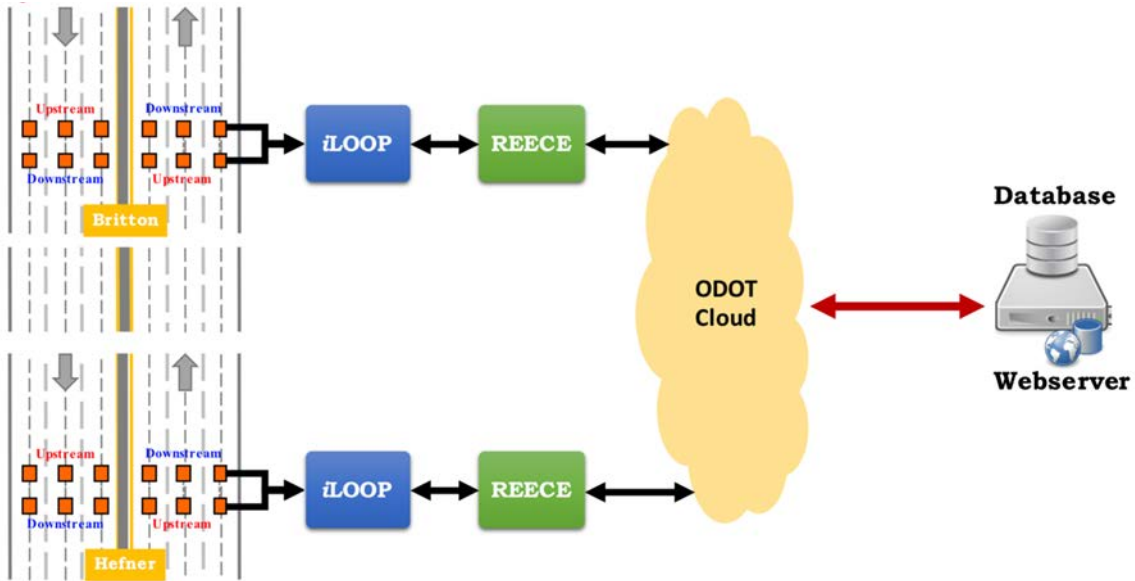
Figure 3-23 ILD Traffic Monitoring System.

Preprocessing the data. Signature re-identification is accomplished in the following manner.

1. Data cleaning to ignore incomplete or distorted signatures

2. Speed-based normalization on the time domain

3. Vehicle length estimation

4. Amplitude Normalization between 0 and 1

Vehicle reidentification and TT estimation

1. Comparing signatures with time window less than 300 seconds

2. Comparing signatures with vehicle length difference less than 40 cm

3. Vehicle re-identification by way of matching signatures via either Pearson Correlation or Relative Entropy

4. TT calculation indicating time difference between the best matched signatures

5. Data spike detection

6. TT estimation given mean value of spike data

    Data cleaning. Some signatures were interrupted due to vehicle lane change or hardware fault in the loops. All signatures contained interruptions that were deleted from the data.

50

Speed-based normalization. Signature length is dependent upon vehicle length and speed. Test setups had two convolutional loops: one at the upstream location and another at the downstream location. Distance between loops was 8ft, and detection time at each loop was provided by Phoenix II. Speed can be calculated using the following equation:

$$V = \frac{Distance}{T_2 - T_1}$$

Eq. 3-3

where *distance* is the amount of separation between two loops at one site; T_1 represents detection time at the first loop; and T_2 represents detection time at the second loop.

A signature can be normalized by fixing the speed for all vehicles to 60 mph so that a new signature length can be calculated from the fixed speed.

$$l_{normalized} = \frac{l_{original} \times v_{60\ mph}}{V}$$

Eq. 3-4

where *V* is vehicle speed; $l_{original}$ is signature length at speed (V); $v_{60\ mph}$ is the fixed speed for all vehicles at 60 mph; and $l_{normalized}$ is speed normalized signature length.

Cubic spline interpolation was applied to shrink (or compress) the signature to the normalized length. This process is a polynomial method that provides a smoother and smaller error when compared with other polynomials [6].

The tested device suffered from hardware issues. Signatures on four lanes were undetectable on both convolutional loops. To mitigate this problem, the research group determined that one lane detected 90% of vehicles on both loops, thus was subsequently selected for the study. Vehicle speeds undetectable on both loops were estimated based on speed mean of all detected signatures in the same minute. Figure 3-24 through Figure 3-27 compare number of detected vehicles between the two loops on a single site and number of detected vehicles between the two sites.
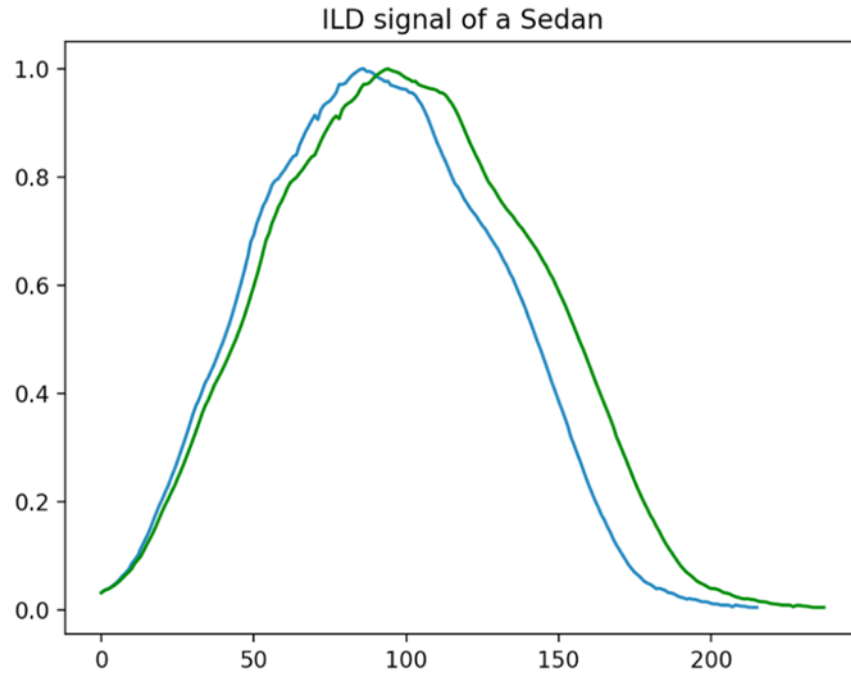
Figure 3-24 Normalized Signature.
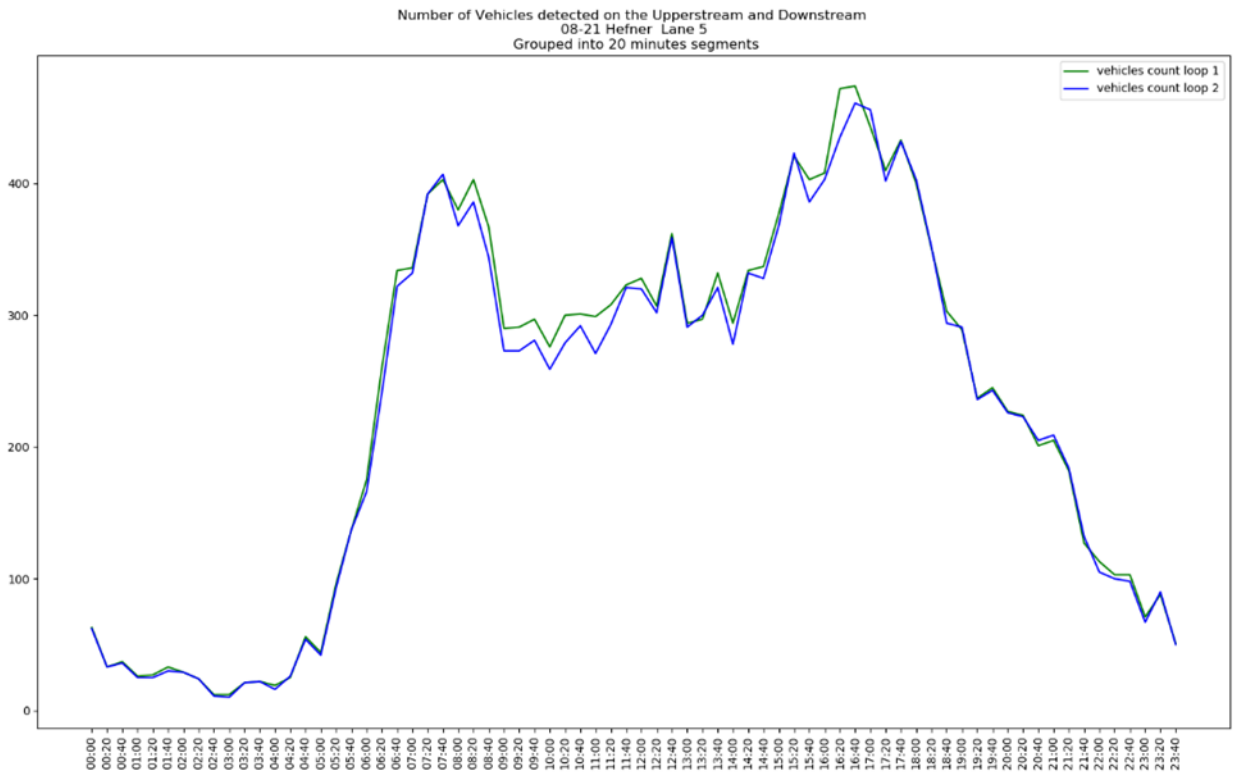
Figure 3-25 Number of Vehicles Detected on Both Loops at Britton Site.
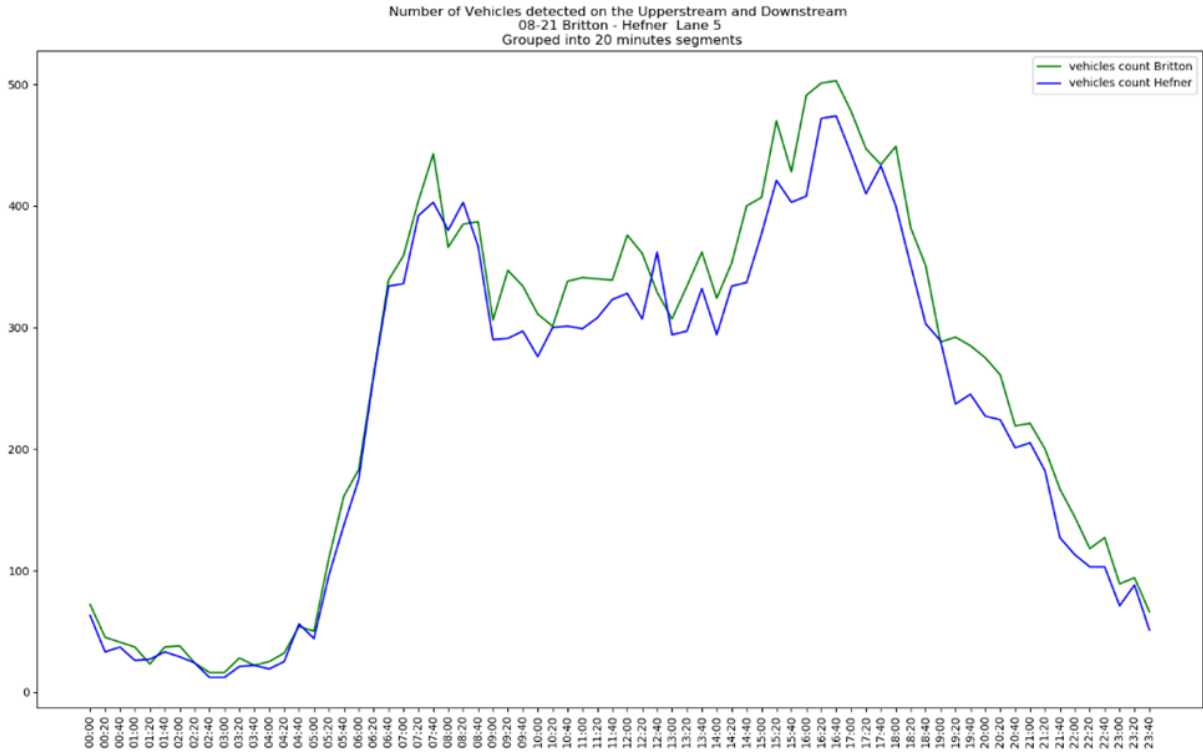
Figure 3-26 Number of Vehicles Detected on Both Loops at Hefner Site.
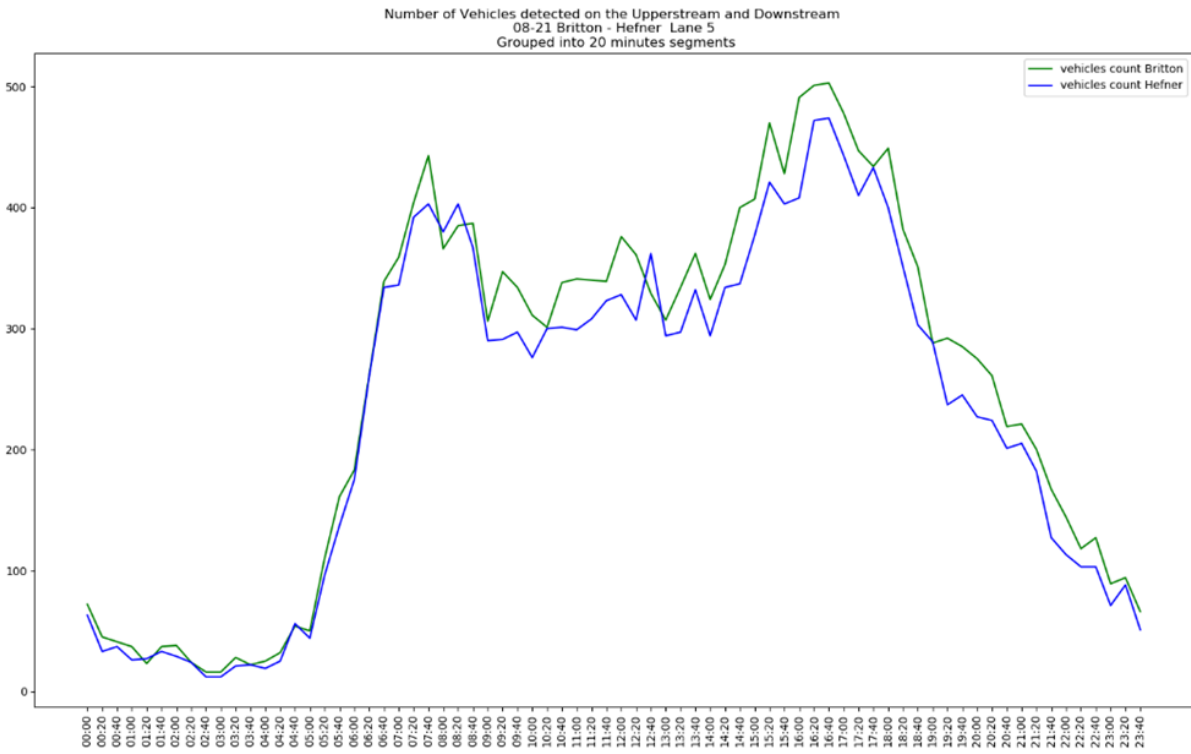
Figure 3-27 Number of Detected Vehicles on Britton and Hefner sites.

Vehicle length estimation. After normalizing signature length based on speed, vehicle length can be estimated from signature length. Phoenix II sampling rate is 1000/s; therefore, signature length can be considered the time required for a vehicle to cross over a loop. Based on this, vehicle length can be estimated from the following formula:

Vehicle Length = Vehicle Speed x Signature Length **Eq. 3-5**

Vehicle reidentification. Two methods were tested to determine the most correlated signatures (e.g., Pearson Correlation or Relative Entropy). Pearson Correlation depends on signature shape and was used to find linear dependences between the two signatures. Two signatures are correlated if they are similar in slope rates:

$$r = \frac{n\sum(xy) - (\sum x)(\sum y)}{\sqrt{(n\sum x^2 - (\sum x)^2)(n\sum y^2 - (\sum y)^2)}}$$ **Eq. 3-6**

where n is the number of samples (i.e., signature length). When r =1, signals are identical and correlated. TT and corelated signatures using Pearson correlation are shown in Figure 3-28 and Figure 3-29, respectively.
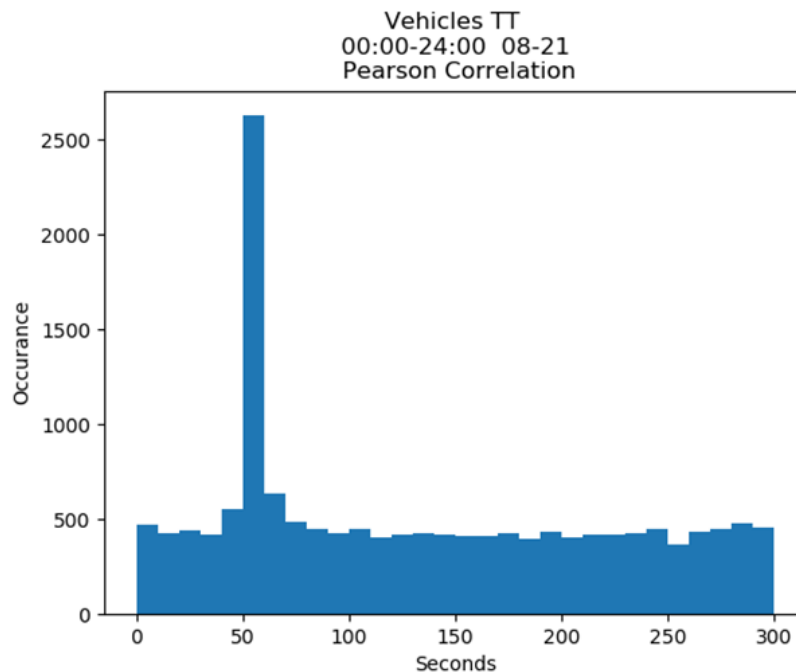
Figure 3-28 TT Using Pearson's r Correlation.
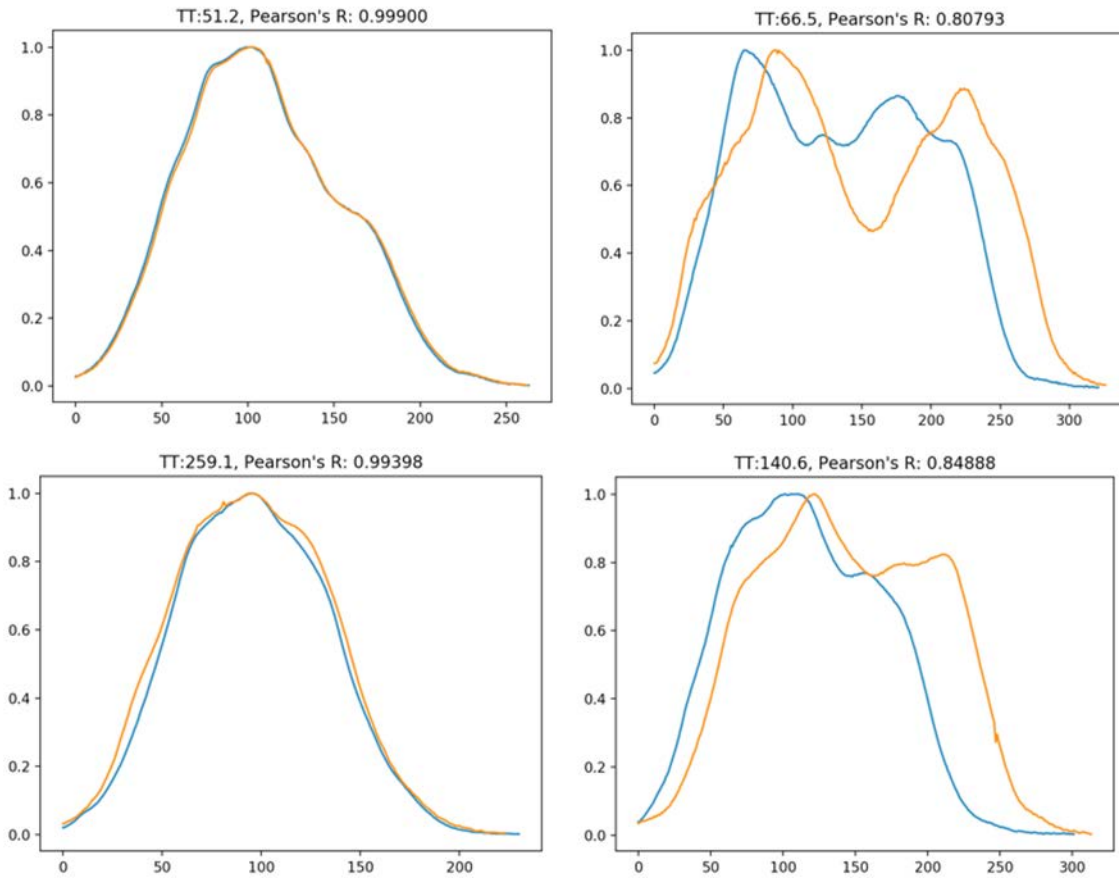
Figure 3-29 Correlated Signatures Using Pearson Correlation.

Since the amount of vehicle metal is invariant, Relative Entropy assumes signatures of the same vehicle will have the same value for area under the curve. However, slope rate and strength of magnetic field can change based on the way a vehicle is passing over the loop. Relative Entropy was used to compute relativity of the pdf value between two signatures:

$$d = \sum_{k}^{n} p_k \, log_2\left(\frac{p_k}{q_k}\right)$$

Eq. 3-7

where p_k, q_k = probability functions for both signatures. When d = 0 =>, both signatures have identical PDF values and are correlated. TT and corelated signatures using Relative Entropy correlation are shown in Figure 3-30 and Figure 3-31, respectively. Correlated signatures using Pearson Correlation and Relative Entropy are shown in Figure 3-32. Both methods were successful in re-identifying vehicle signatures. Relative Entropy was characterized with higher noise values than Pearson Correlation. Both methods were applied to achieve an improvement in vehicle signature correlation.
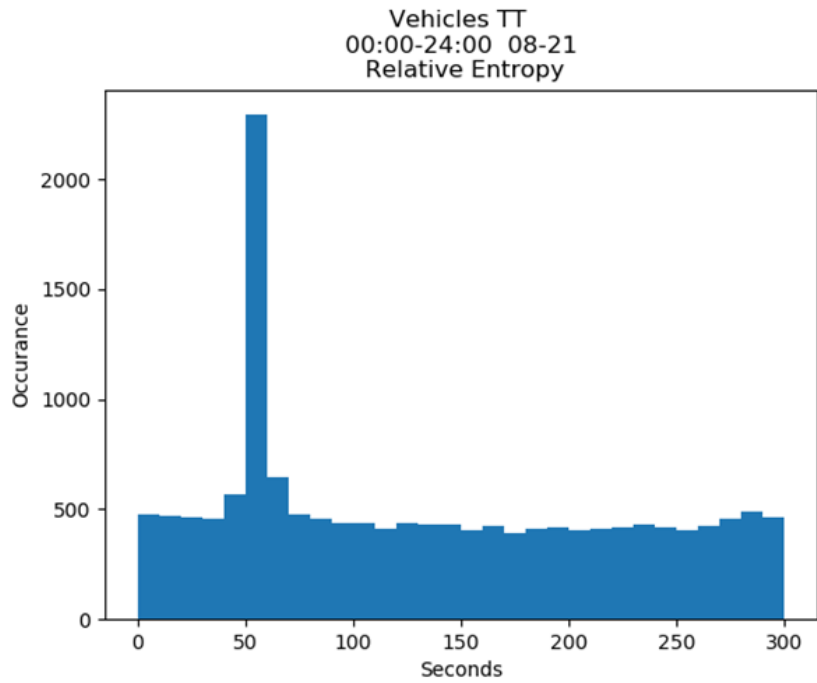
Figure 3-30 TT Using Relative Entropy.
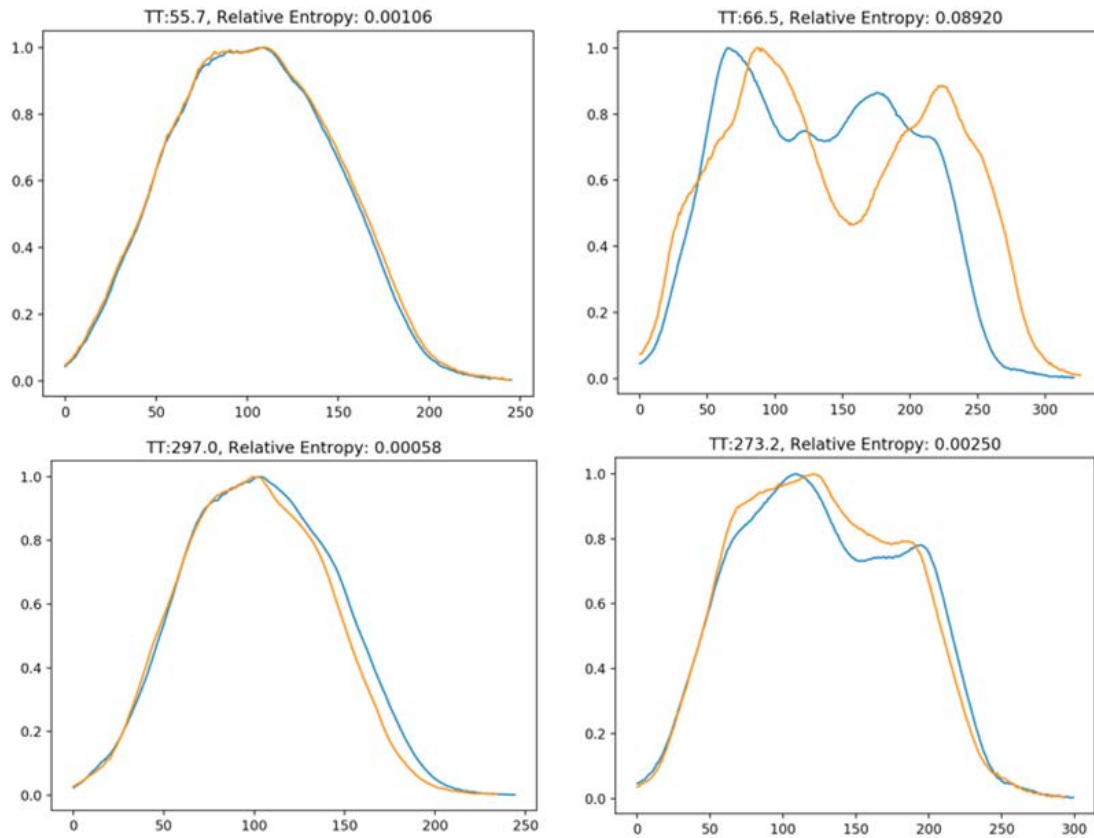
Figure 3-31 Correlated Signatures Using Relative Entropy.
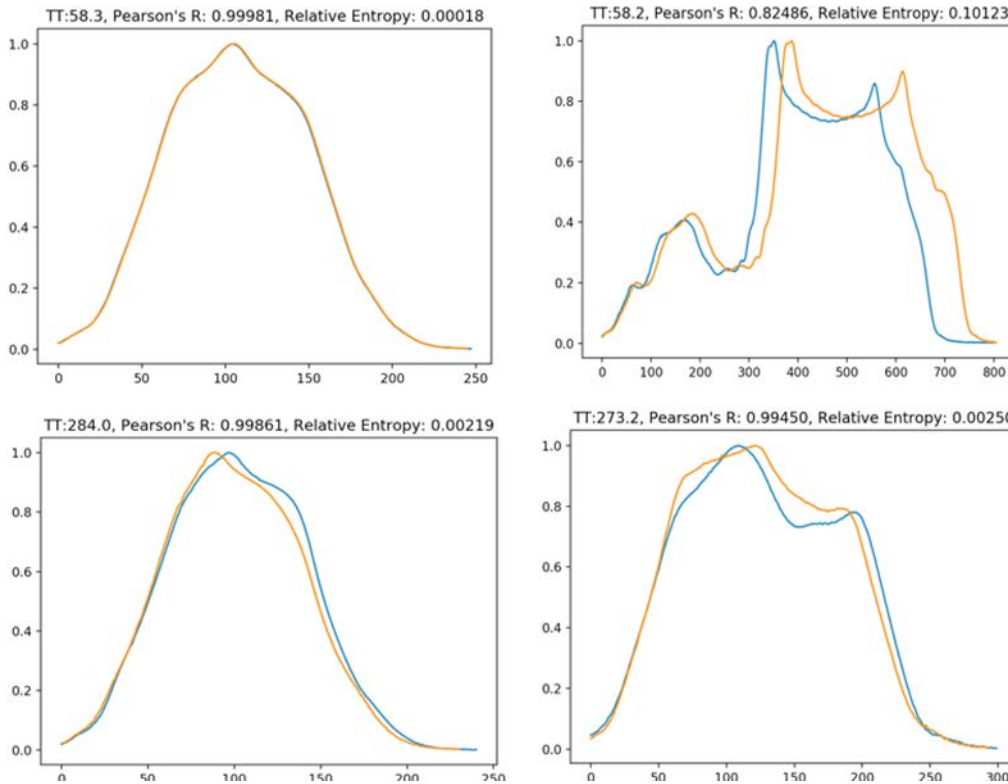
Figure 3-32 Correlated Signatures Using Pearson Correlation and Relative Entropy.

Figure 3-33 and Figure 3-34 show TT values of ILD traffic monitoring systems divided into five periods: 00:00 to 07:00, 07:00 to 10:00, 10:00 to 16:00, 16:00 to 20:00, 20:00 to 24:00. The percentage under each graph represents total number of vehicles with TT between 45 and 70 mph compared to total number of re-identified vehicles. Clearly, noise ratio increases during rush hour periods from 7 to 10 a.m. and 4 to 8 p.m.
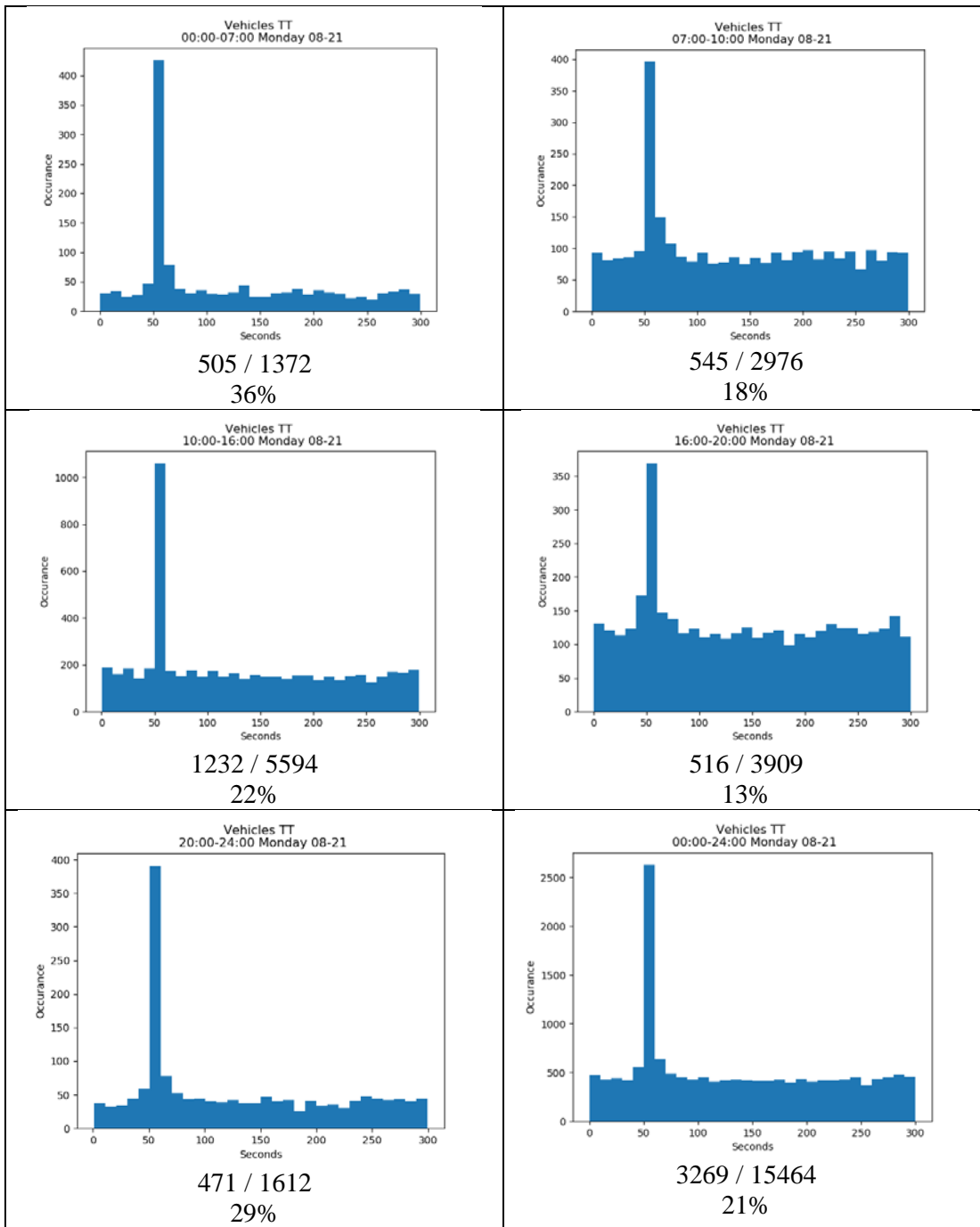
Figure 3-33 Travel Time Values of ILD Traffic Monitoring System on Monday.
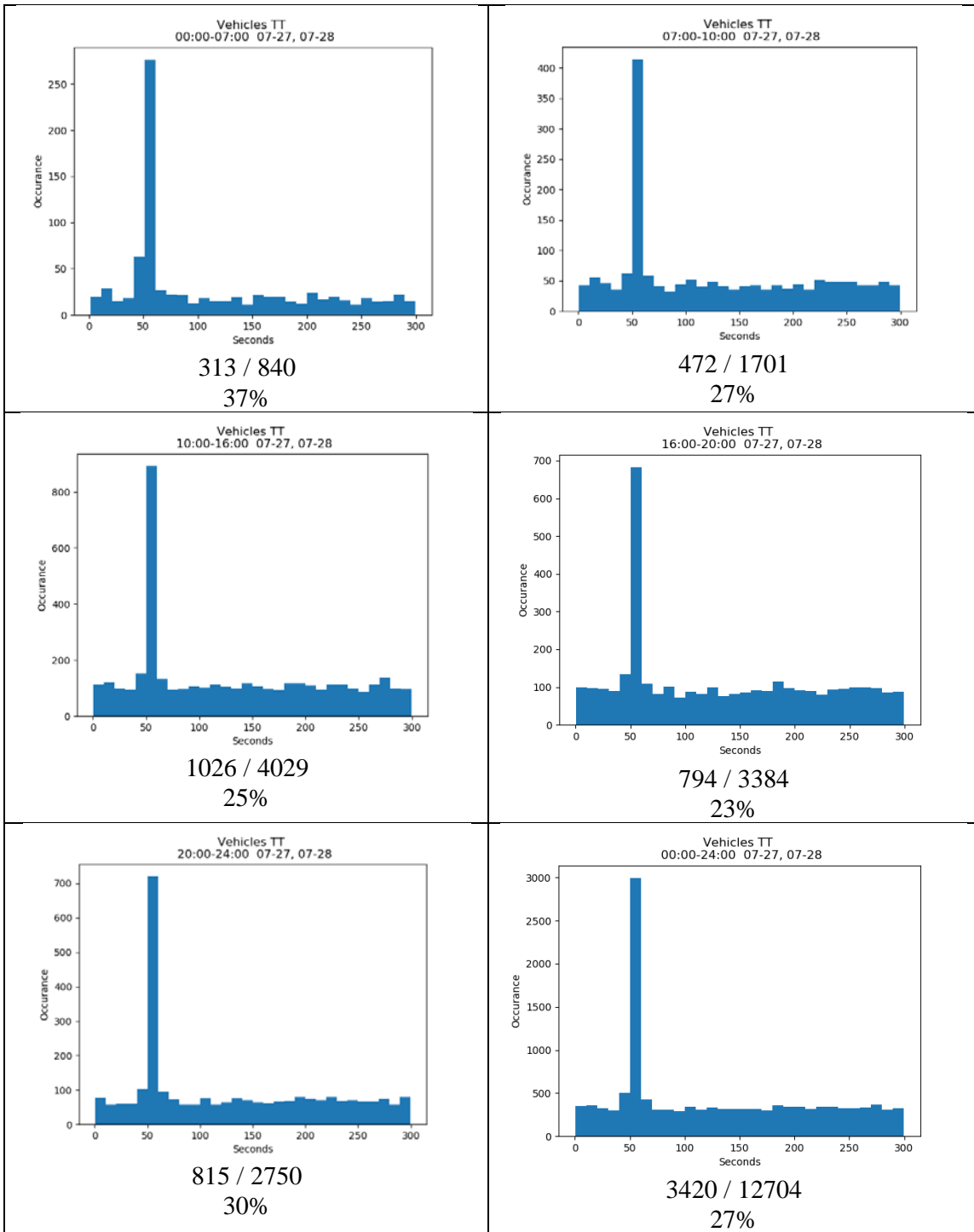
Figure 3-34 Travel Time Values of ILD Traffic Monitoring System During Weekend.

TT using data spike detection algorithm. Correlated signatures contained a significant amount of noisy data, where 27% provided the correct TT and 73% experienced error values. Computing overall mean of correlated signatures resulted in a TT value longer than expected. To illuminate the noise, spike detection algorithms where applied. TT values were binned into 10-second groups, and a spike was selected for estimating TT given that half of the samples inside the spike were greater than the number of samples in other binned groups. Subsequent to detecting spike data, TT can be estimated as the mean value of all samples inside the spike.

- Spike detection is calculated as:

$$\frac{Size_{group\ x}}{2} = Size_{group\ i}\ ; i \in [1,n]; i \neq x \qquad \textbf{Eq. 3-8}$$

- TT estimation is represented by:

$$TT = mean\left(TT_{spike\ group}\right) \qquad \textbf{Eq. 3-9}$$
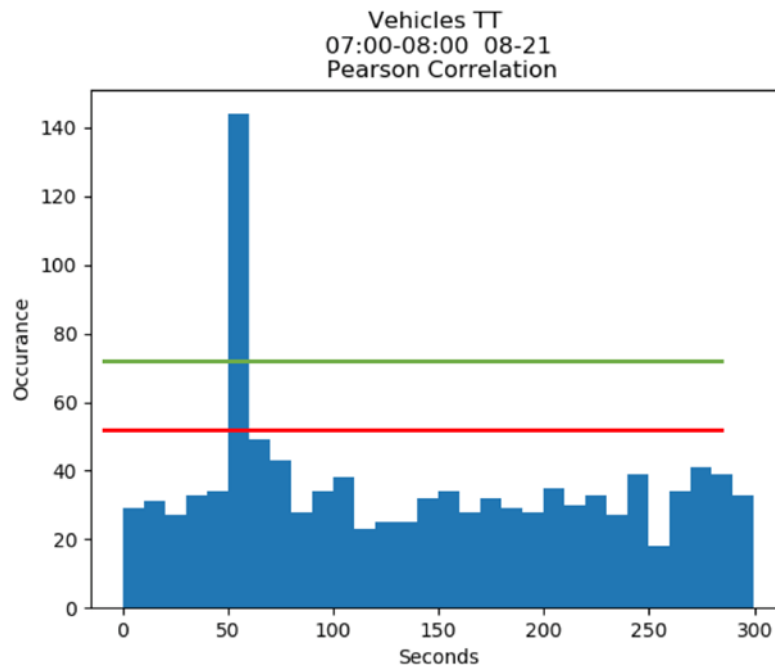
Figure 3-35 Travel Time Data Spike.

Figure 3-35 shows a sample of TT values for a single hour, in which the search window was 300 seconds. Data spike was considered for estimating TT value. Figure 3-36 illustrates estimated TT values for a single day wherein TT values were grouped into 20-minute segments. Total number of segments was 72. Unfortunately, the algorithm was not able to function well during morning rush hour (7:20 to 9 a.m.) and evening rush hour (3:20 to 6 p.m.). For 17 segments, the algorithm wasn't able to detect

a data spike or estimate TT. Figure 3-37 illustrates examples in which the algorithm was unable to detect data spikes.

Several methods have been investigated to improve real-time TT accuracy (e.g., reducing correlation search window from 5 minutes to 2:30 minutes for 1-mile distance). The 5-minute search window proved more accurate than the shorter period, primarily because it aided in flattening error values. See Figure 3-38.
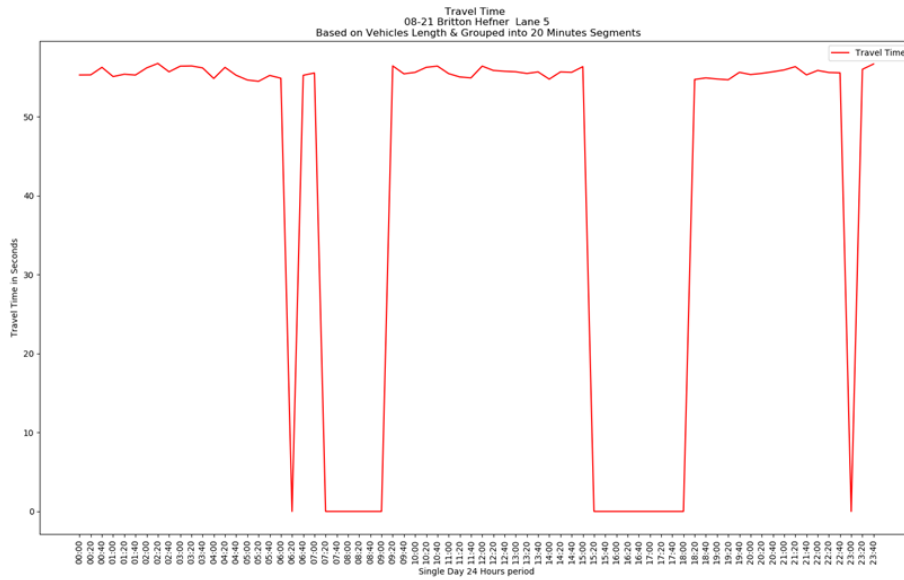
Figure 3-36 Estimated TT Values for 1-mile distance.
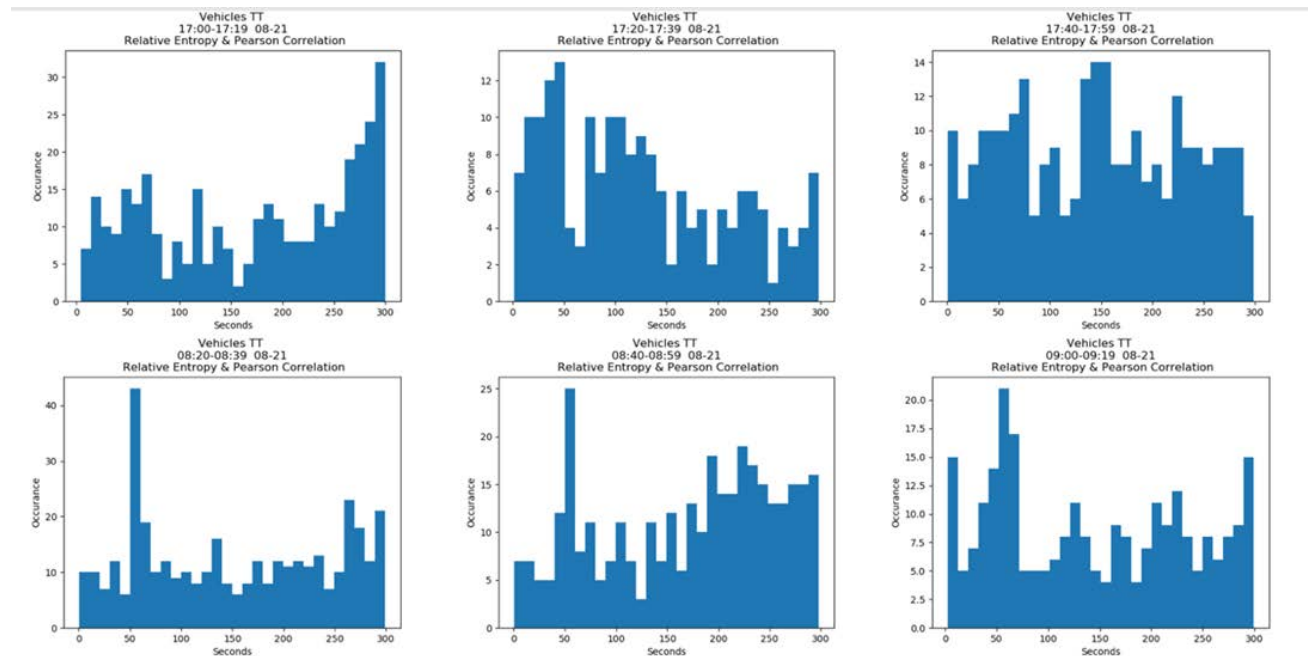
Figure 3-37 Data Spikes During Rush Hour.

61
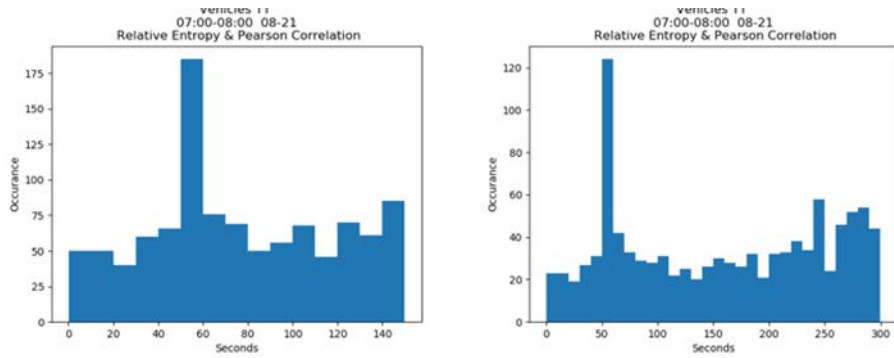
Figure 3-38 TT for a 2:30-minute vs. 5-minute Search Window.

Improving TT accuracy based on vehicle length. Longer vehicles have more unique signatures, which, in turn, provide improved accuracy in signature correlation and TT estimation (See Figure 3-39 and Figure 3-40). Sedan passenger cars are the most common vehicle type with the majority characterized by the same signature shape. Hence, sedans prove to be the primary cause for error when estimating TT (See Figure 3-41). The optimized algorithm uses only long vehicles for replacing missing TT values with estimates. Figure 3-42 illustrates the way in which applying the length-based TT estimation enhancement reduced the number of segments missing TT from 17 to 13.
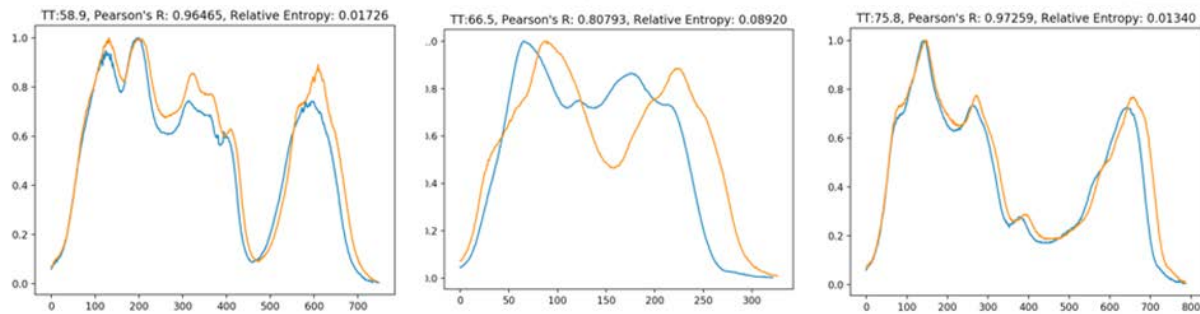
Figure 3-39 Correlated Signatures for Long Vehicles.
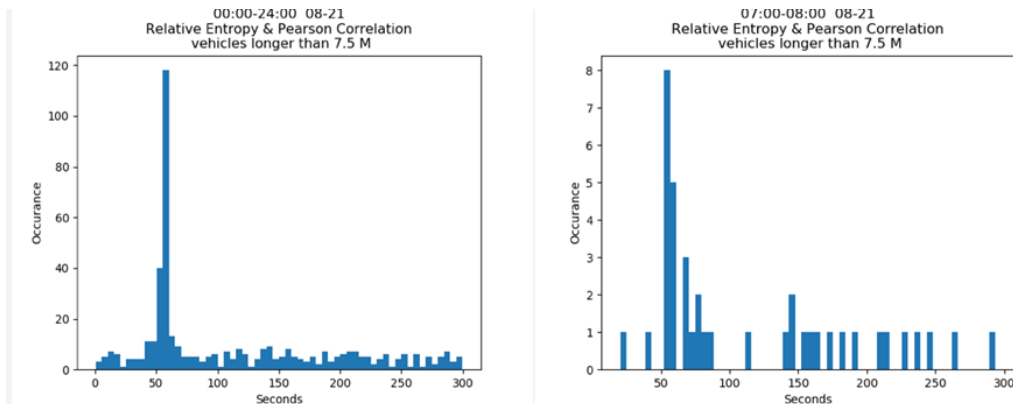
Figure 3-40 TT for Long Vehicles.

62
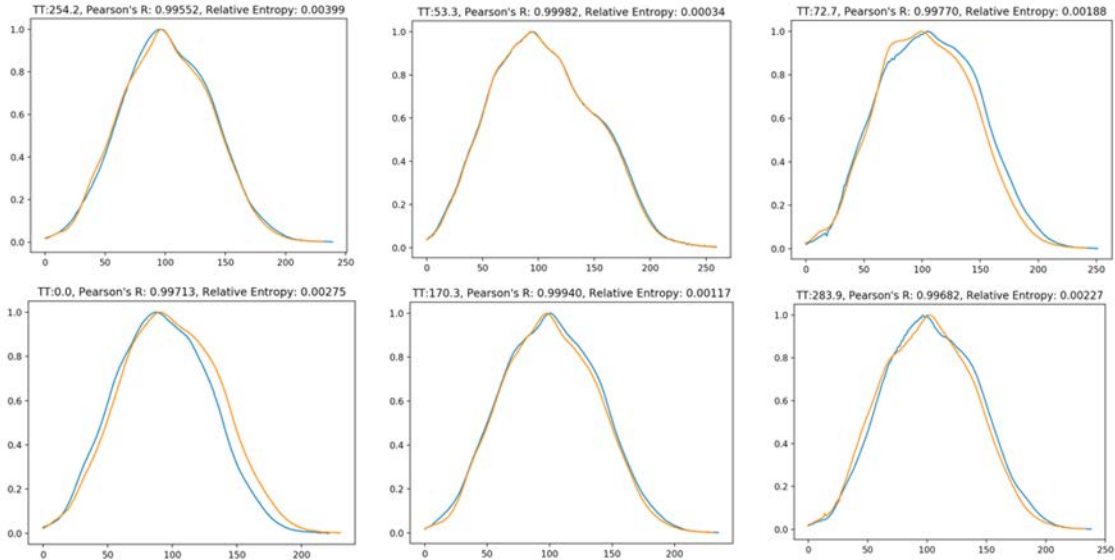
Figure 3-41 Correlated Signatures for Sedan Vehicles.
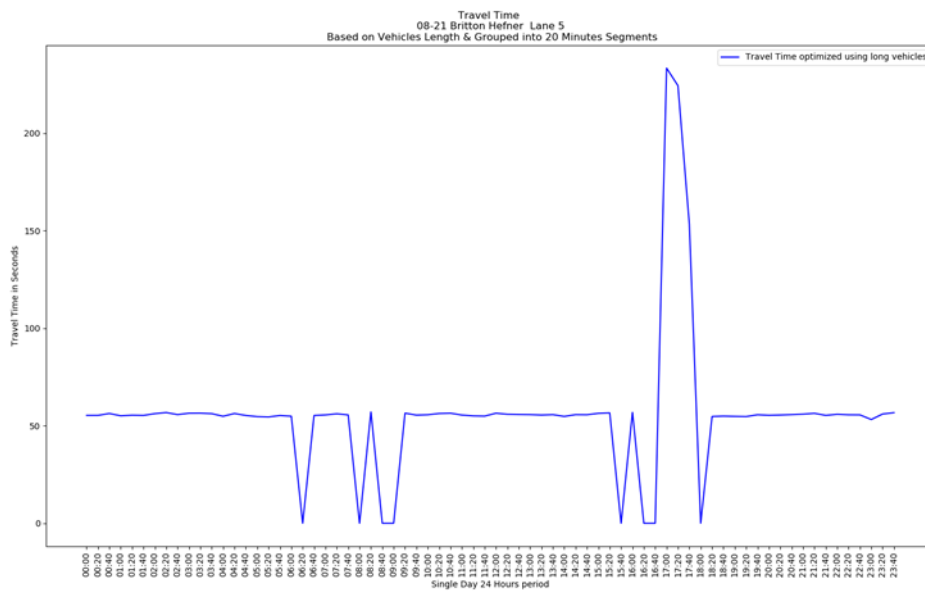
Figure 3-42 TT Estimation Using Vehicle Length Enhancement.

Another enhancement in the algorithm also aided in increasing system reliability. When searching for a data spike, the algorithm compares neighboring data groups to the group with the maximum number of vehicles. Given that a neighboring group has a vehicle number with more than half vehicles characterized with a maximum vehicle number, both data groups will be combined as a single data spike. These will then be compared with all other groups for estimating TT based on average of TT values inside the new data group. Figure 3-43 illustrates the way in which this final optimization reduced the number of segments with missing TT from 13 to only 4 of 72 segments.

63

Such optimization enables the system to estimate TT up to 9% of the time and to update TT estimation every 20 minutes.
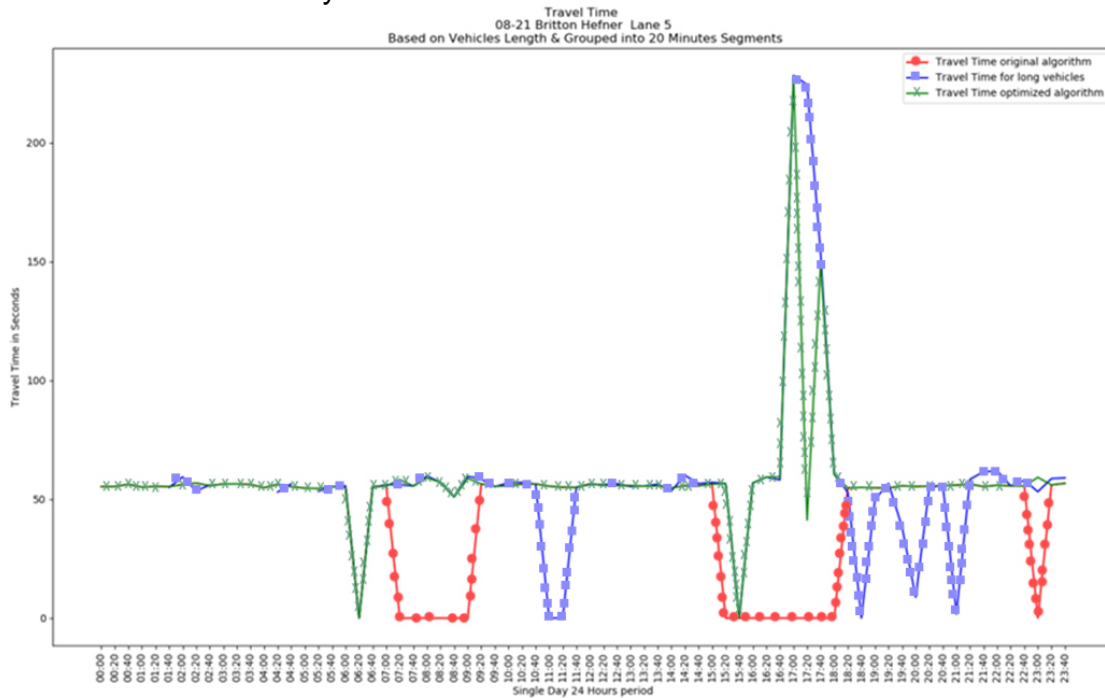
Figure 3-43 TT Estimation Using Optimized Spike Detection Algorithm.

	Bluetooth System	ILD System
Number of detected vehicles		
Travel Time Estimation		
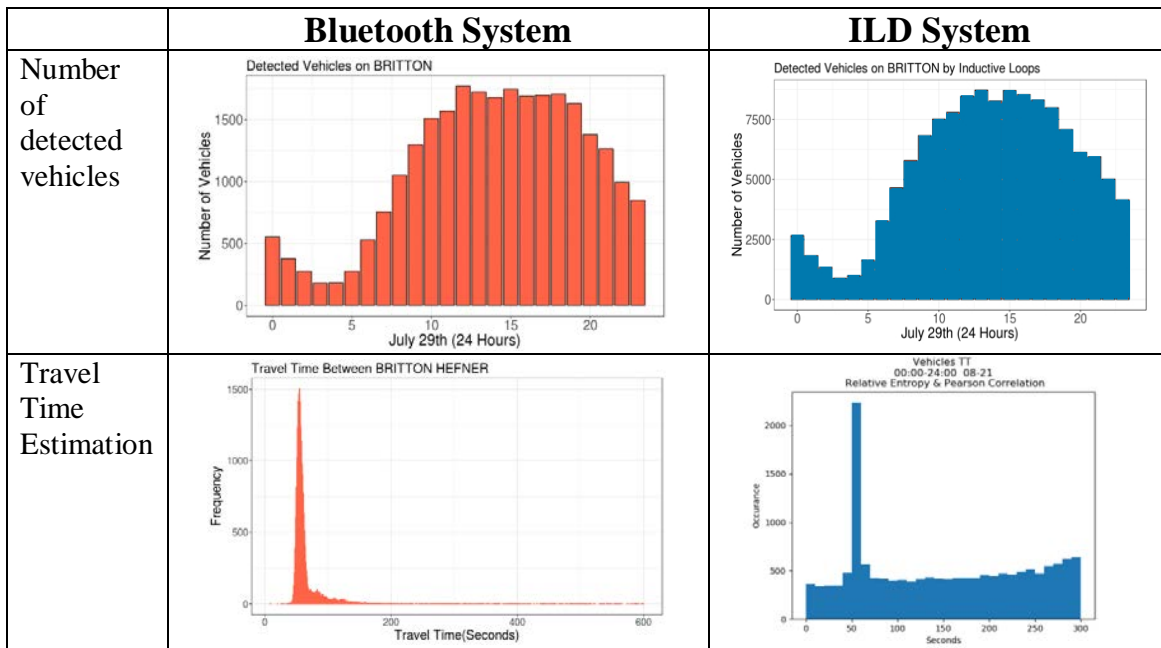
Figure 3-44 Comparison Between ILD and Bluetooth Traffic Monitoring Systems.

Comparison between ILD and Bluetooth signatures (See Figure 3-44):

- The ILD system demonstrated higher penetration than the Bluetooth system, although both were characterized by the same distribution. Only 20% penetration was achieved using Bluetooth sniffer with external directional antenna.

- Both systems detected TT and facilitated TT estimation. However, the ILD system experienced more noise—only 27% of the data were within the correct TT. Thus, the ILD system requires advanced processing to filter out noise and estimate TT.

- Both systems proved reliable for estimating TT. While the Bluetooth system provided instant, accurate TT 99.9% of the time, the ILD system provided correct TT estimates 94% of the time and updated TT measures every 20 minutes.

- The Bluetooth system was considered a real-time system since it instantly provided TT measures. However, data was measured for a combination of all traffic lanes. Although data was reported only every 20 minutes, the ILD system estimated and provided more precise TT measures, as estimates were provided on a per lane basis.

- The ILD system is a rich information system, reporting measures for vehicle length, class, and vehicle speed on a single site, as well as TT per lane, while the Bluetooth system provided only TT.

- Many factors affect ILD system accuracy (e.g., vehicles changing lanes, vehicles changing speed while crossing the loops, congestion, distance between two sites, and other environmental factors that cause electrical noise). Bluetooth systems have fewer factors that affect performance (e.g., type of the antenna, distance between sniffer and the roadway).

4. TRAVEL TIME DATA COLLECTION ALGORITHMS

The accuracy of the method described in Chapter 2 proved inadequate for TT calculation and analysis. Hence, a separate dataset was chosen for developing TT models. This new dataset (i.e., National Performance Management Research Dataset (NPRMDS) contains TT for all NHS roadways, including those in the state of Oklahoma. The following section provides information necessary to understand the framework for processing the dataset, including limitations and challenges associated with utilizing the NPMRDS.

4.1 Data Acquisition

NPMRDS is a vehicle probe-based TT data set acquired by the Federal Highway Administration (FHWA) to support its Freight Performance Measures (FPM) and Urban Congestion Report (UCR) programs. The dataset reports average TT records observed for the entire NHS. Data is collected 24 hours-a-day in 5-minute intervals for freight truck vehicles and passenger vehicles. An all-vehicle record combines totals for both passenger vehicles and freight trucks.

Following are proposed uses for NPMRDS:

- Measure TT on road segments (i.e., Traffic Message Channel Codes [TMCs]), routes, corridors

- Decipher travel patterns throughout the day, week, month, and season

- Identify peak TT

- Compare TT across passenger and freight vehicles

- Analyze urban vs rural conditions

- Analyze special occurrence days (i.e., days affected by accidents, lane blockages, weather)

- Identify congested areas

NPMRDS components include two sets of information files:

1. Monthly average TT data files:

   • TMC code

   • Date (MMDDYYYY)

   • EPOCH (5 minute increments, in the range 0-287)

   • TT–all vehicles (seconds)

- TT–passenger vehicles (seconds)

- TT–freight vehicles (seconds)

2. TMC static data files

- TMC code

- Country

- State

- County

- Distance (length of TMC in miles)

- Road number

- Road name

- Latitude

- Longitude

- Road direction (NB, SB, EB, WB)

Passenger vehicle probe data is obtained from several sources, including mobile phones, vehicles, and portable navigation devices. Freight probe data is obtained from the American Transportation Research Institute, which leverages embedded fleet systems. Data records for this project were obtained from ODOT after NPRMDS data files were collected from a shared FHWA repository accessible only by state DOTs and Metro Planning Organization (MPO) agencies. NPRMDS is composed of large TT files that include information recorded per segment on NHS roadways. Figure 4-1 depicts Oklahoma's NHS roadways.
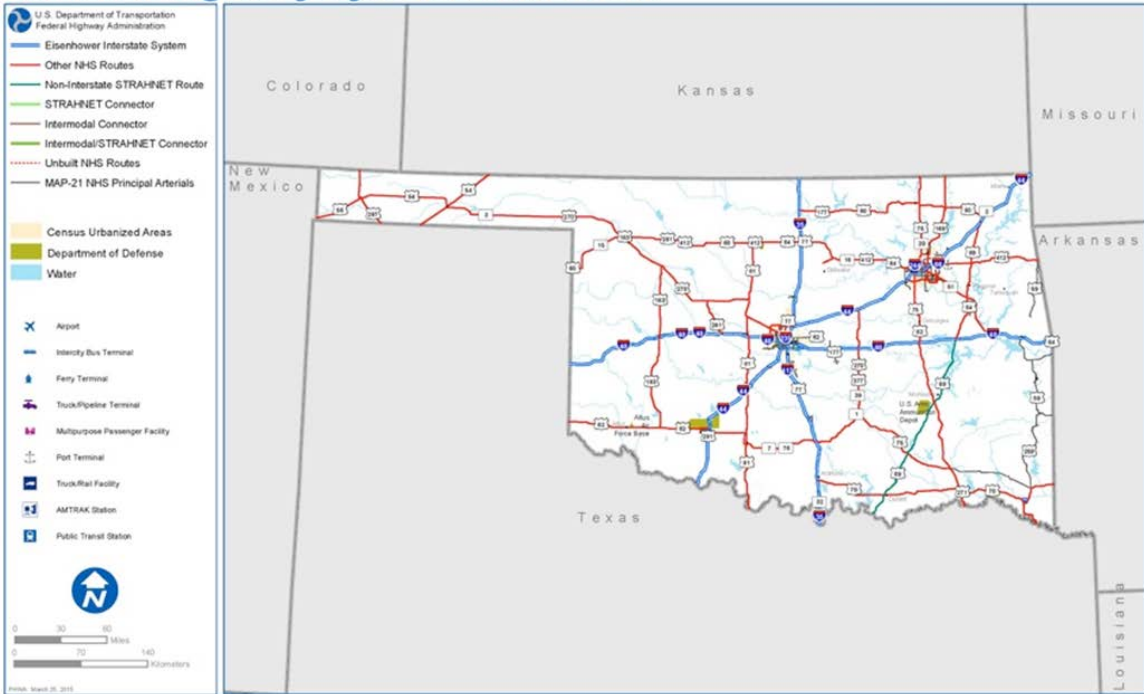
Figure 4-1 NHS Roadways in Oklahoma.
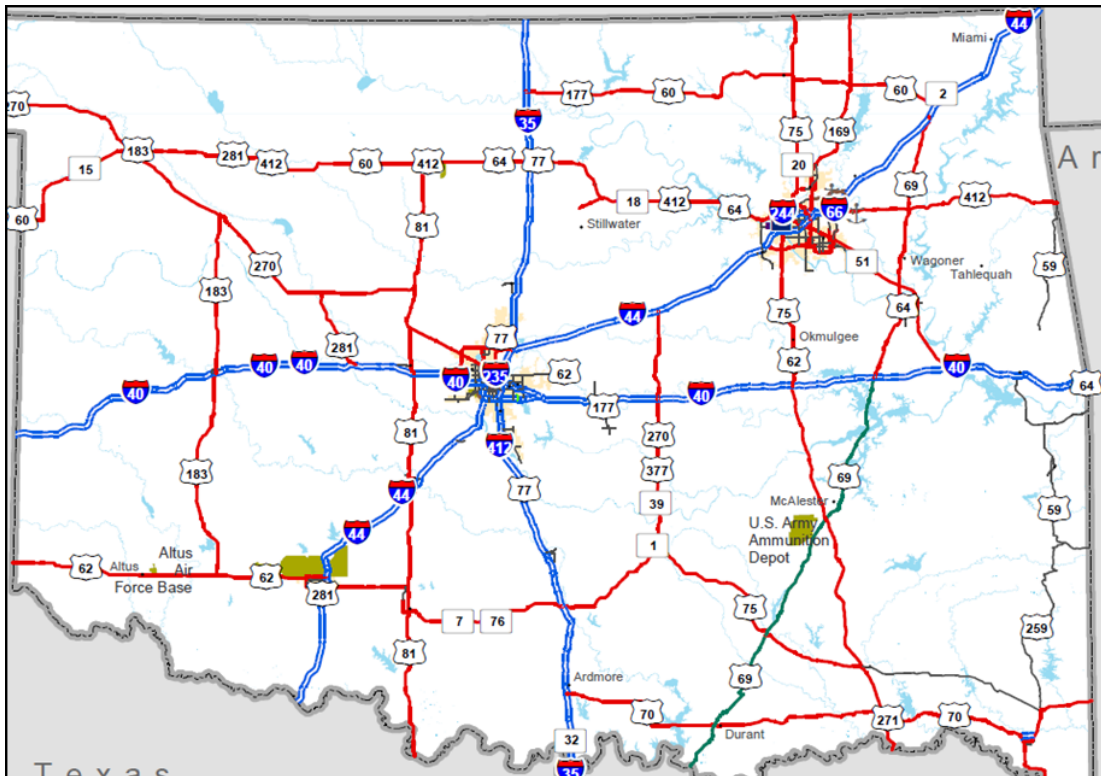
Figure 4-2 NHS Roadways in Oklahoma Magnified.

4.2 Dataset Characteristics: Challenges and Limitations

NPMRDS is based on instantaneous GPS data records obtained from vehicles carrying GPS devices that report location and speed. Combined TT measurements reported in NPMRDS are computed as a weighted average of both recorded passenger vehicle and freight truck TT according to the number of available probes for each. Actual volume for each vehicle type is not reported. Understanding the nature of NPMRDS is key for effective data post processing (e.g., anomaly and outlier detection, as well as measures for their removal). Challenges and limitations are enumerated below:

4.2.1 Data Quality

The amount of data in the monthly NPMRDS is sizeable. Moreover, the number of records generated per segment for each highway renders conventional tools, such as Microsoft Excel, ineffective for post processing. For example, any given typical month can generate data in the order of 30 to 40 million records. This number far exceeds the one million record capability of Excel. As such, working with NPMRDS data requires database and scripting expertise [3, 23].

4.2.2 High Spatial-Temporal Probe and Record Data Variability

NPMRDS probe data is based on a variable number of probes and, therefore, results in a variable number of records generated at any segment location. Data fluctuates considerably depending on time-of-day and day-of-week. Furthermore, variability is dependent upon the number of probes per vehicle type at the same location and the same time (i.e., passenger vehicle vs. freight truck probes). Figure 4-3 shows TMC segment (111N04920) located south of Oklahoma City.
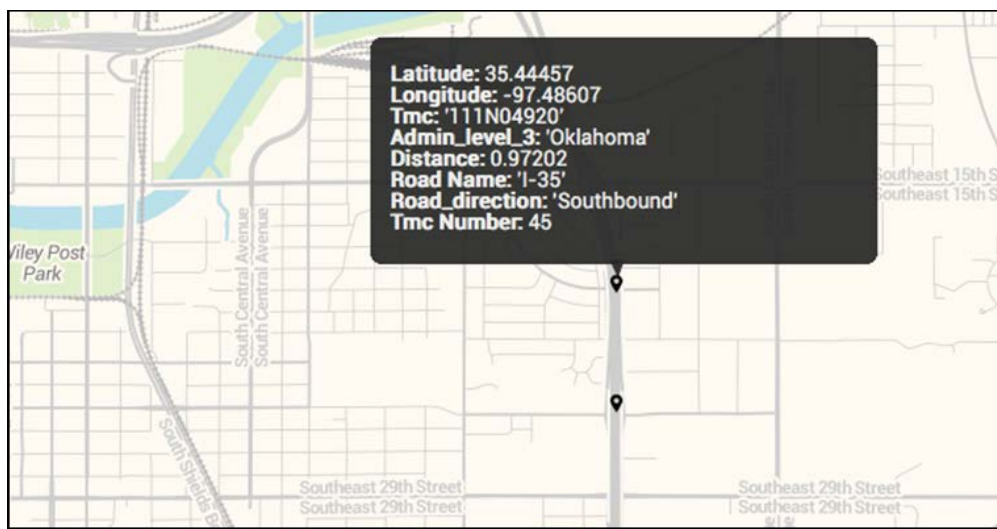
Figure 4-3 TMC "111N04920" Located South of Oklahoma City.

Figure 4-4 shows a bar plot for the total number of epochs recorded on TMC 45 segment (111N04920) per day for 31 days during the month of January 2015. Mean value of recorded epochs was 219.5806, and Standard Deviation (STD) was 20.0678. This figure clearly demonstrates the number of epochs for the same segment fluctuates daily.
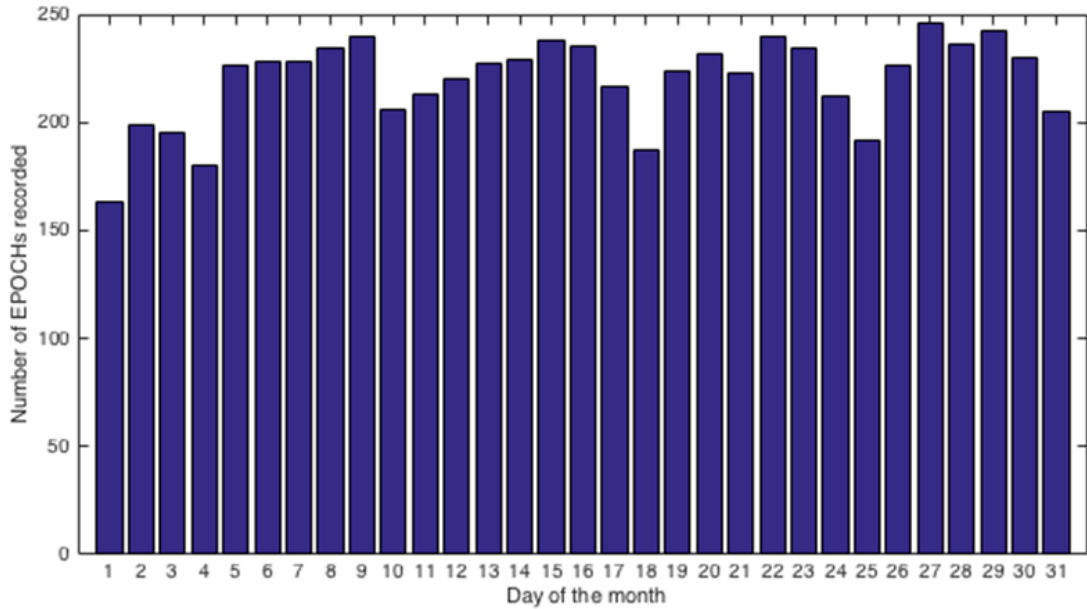
Figure 4-4 Daily Bar Plot of Epochs Recorded for TMC 45 During Jan 2015.

Figure 4-5 details the difference in epoch count per day for two bordering segments—TMC 45 and TMC 46. For TMC 46, mean was 184.0968 epochs and STD was 24.2918. Epoch count variance is considerable.
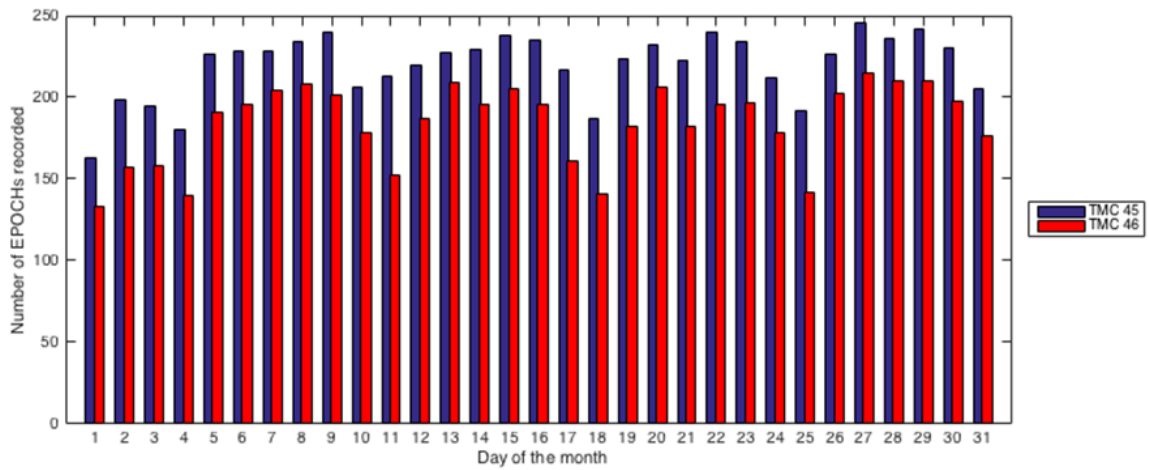
Figure 4-5 Bar Plot of Epochs Recorded for Segments 45 and 46 During Jan 2015.

Variance per day relative to three time-groupings for segment TMC 45 is shown in Table 4-1. Group 1 is indicated by morning hours from 12 a.m. to 8 a.m.; Group 2 indicates afternoon hours between 8 a.m. and 4 p.m.; and Group 3 represents evening hours from 4 p.m. to 12 a.m. Group 2 (i.e., afternoon) generated the greatest number of epochs; the least number of epochs were generated during Group 3 (i.e., evening).

Table 4-1 Probe Epochs Available Per Time of Day for Segment 45.

Group	Group (1): 12am – 8am	Group (2): 8am – 4pm	Group (3): 4pm – 12am
Mean	56.3508%	93.9180%	78.4610%
STD	8.8708	6.0338	6.8185

When inspecting the number of epochs recorded per vehicle type per day, a difference between probe types was evident. As count per probe type varies, combined TT computed as the weighted average is highly influenced. Table 4-2 shows the mean percentage of epochs per probe type, as well as the percentage of combined TT mean.

Table 4-2 Mean Number of Epochs Per Probe Type for Segment 45.

Group	Combined	Passenger Vehicles	Trucks
Mean	76.2433%	57.1909%	56.5076%
STD	20.0678	30.4961	19.5703

Averages across all segments of OK I-35 demonstrate similar results, as shown in Table 4-3 and Table 4-4.

Table 4-3 Probe Epochs Available Per Time of Day for OK I-35 (98 Segments).

Group	Group (1): 12am – 8am	Group (2): 8am – 4pm	Group (3): 4pm – 12am
Mean	58.1135%	87.8185%	76.6424%
STD	8.6746	4.4879	5.8671

Table 4-4 Mean Number of Epochs per Probe Type for OK I-35 (98 Segments).

Group	Combined	Passenger Vehicles	Trucks
Mean	74.1915%	49.8046%	60.9439%
STD	16.4836	25.1715	16.4760

4.2.3 Missing Data

Missing data was evident on rural NHS roadways in Oklahoma when average probe number was very low and only a small number of epochs and missing records were captured. Large data gaps for several hours made characterizing TT for a particular segment highly skewed. This problem was found to a lesser extent, as well, on interstate highways and large arterial roadways where the number of probes is higher on average. A comparison between the number of epochs generated on I-35 during January 2014 and January 2015 is provided in Table 4-5. Clearly, the number of probes increased for both types of vehicles, particularly for freight trucks, however. This phenomenon resulted in an increase in combined TT epochs, from approximately 54% to 73%, as shown in Table 4-6.

Table 4-5 Number of Epochs Recorded per Probe Type.

Group	Combined	Passenger Vehicles	Trucks
January 2014	481338	388040	234403
January 2015	649134	435762	533225

Table 4-6 Percentage of Total Epochs per Probe Type.

Group	Combined	Passenger Vehicles	Trucks
January 2014	53.913306%	43.463262%	26.254816%
January 2015	72.707661%	48.808468%	59.725022%

4.2.4 Bias Toward Lower Speeds

TT data in NPMRDS is composed of probe data based on GPS records that are reported at fixed rates of time. Hence, the slower the probe vehicle speed, the larger the number of samples generated as a vehicle travels the length of the roadway segment. Consequently, a slow vehicle will report more records than a fast vehicle. Since TT reported for a segment is the average of all probe TT calculated during a fixed time period and since slow moving vehicles report a higher number of records, average TT is biased toward slower moving vehicle speeds. This limitation can be overcome by implementing a weighted average, wherein each vehicle is weighted according to the number of samples generated prior to computing TT average of the segment. Doing so increases data collection complexity, but also eliminates the effect of bias toward slower moving vehicles.

4.2.5 Variability of Segment Lengths

TMC segments defined for use in NHS roadways vary considerably in length. This variability entails several effects on TT reliability and measurement accuracy. In general, shorter segments produce a smaller number of samples. Figure 4-6 illustrates Oklahoma I-35 southbound between the Kansas and Texas borders, per segment, per day. Several factors are at play, one being that the shorter the length of the segment, the less the density of vehicles contained during any unit of time. Moreover, because probe vehicles traverse the length of a short segment faster than they do a long segment, a smaller number of samples is generated in the shorter segment. In some cases, it is possible for probe vehicles to pass through an entire segment without reporting any data, especially if sample time for instantaneous data being reported is longer than the time required for the vehicle to traverse the segment.
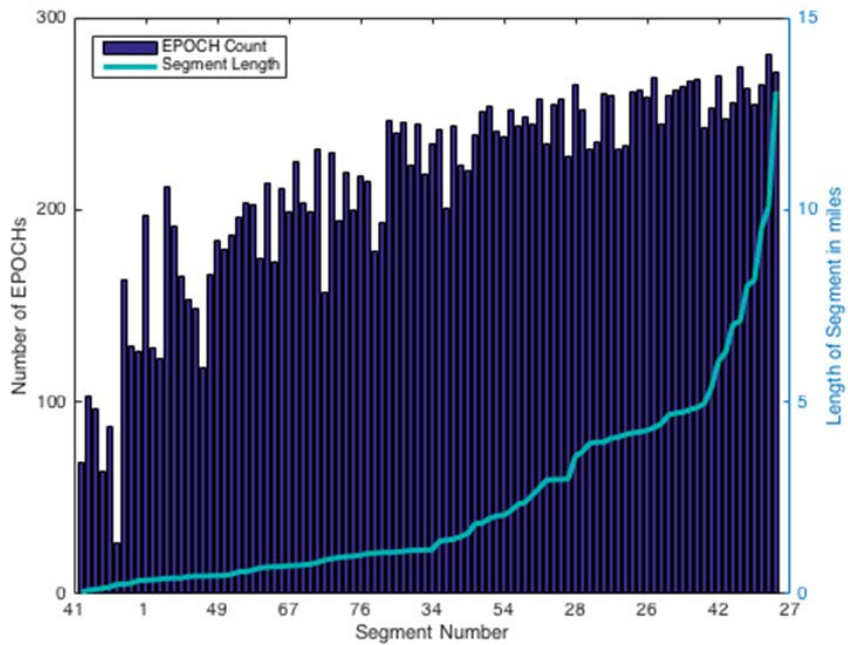
Figure 4-6 Trend Plot for Number of Epochs Recorded Versus Length of Segment.

Consequently, the number of samples recorded per segment for any roadway is affected. Figure 4-7 illustrates the variability of average number of epochs recorded per day for Oklahoma I-35 southbound during January. Long segments could detect different TT across different parts of the segment, rendering average TT an inaccurate representation of actual TT across the entire segment.
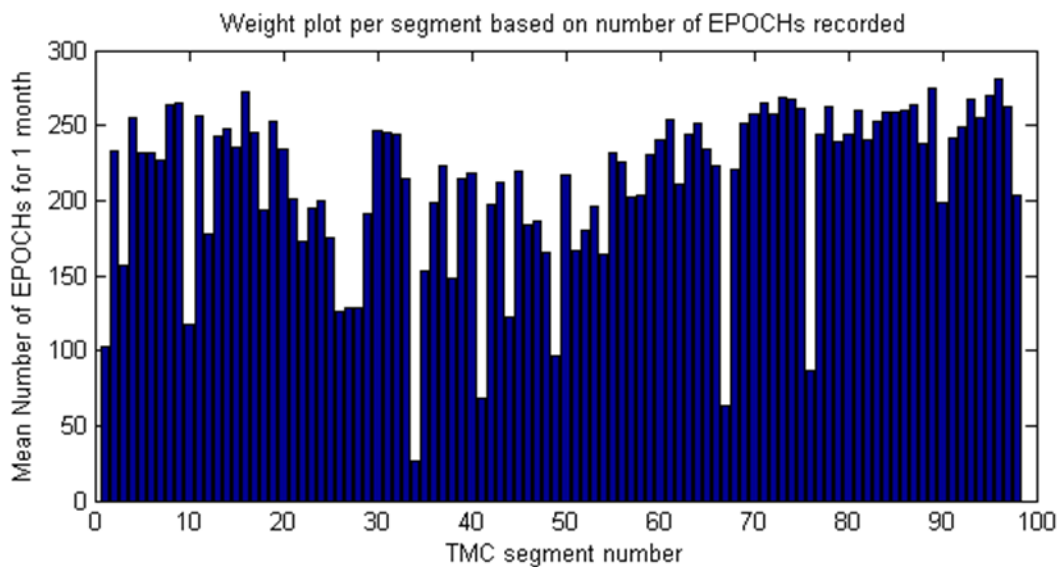
Figure 4-7 Average Number of Epochs Recorded Per Day Reported Per Segment.

74

4.2.6 Vehicle Performance and Roadway Geometry Effect

In particular cases, freight truck-reported TTs were higher than passenger vehicle-reported TT. Inversely, this means that freight trucks traveling those particular segments were moving slower on average than passenger vehicles. Freight truck-reported TT are prone to what is known as the Power-to-Weight ratio model, which adversely affects freight truck speed. Trucks with heavier cargo tend to slow their speed for precautionary measures. In addition, traversing steep or elevated roads could also cause freight trucks to reduce their speeds. In such cases, reported TT would model vehicle performance or roadway geometry characteristics rather than traffic conditions.

4.2.7 Instantaneous Speed Reporting Increases Variability

Given a small number of probes, average speed for all vehicles on the roadway might not be accurately represented by the average of probe samples. Moreover, because TT is derived from instantaneous speeds reported by GPS devices, captured TT values could project higher variability than might actually be occurring on the roadway. Because vehicles maintain an average speed when traversing a roadway during these periods, it is possible that vehicles might continually increase and/or decrease at speeds above and below the average. Reporting instantaneous speeds results in TT variation that might indicate variation that is different from that which is actually occurring on the roadway. Figure 4-8 illustrates the variation in speed for TMC 45 for one entire, non-congested day. Clearly, there is significant variation between each consecutive epoch.
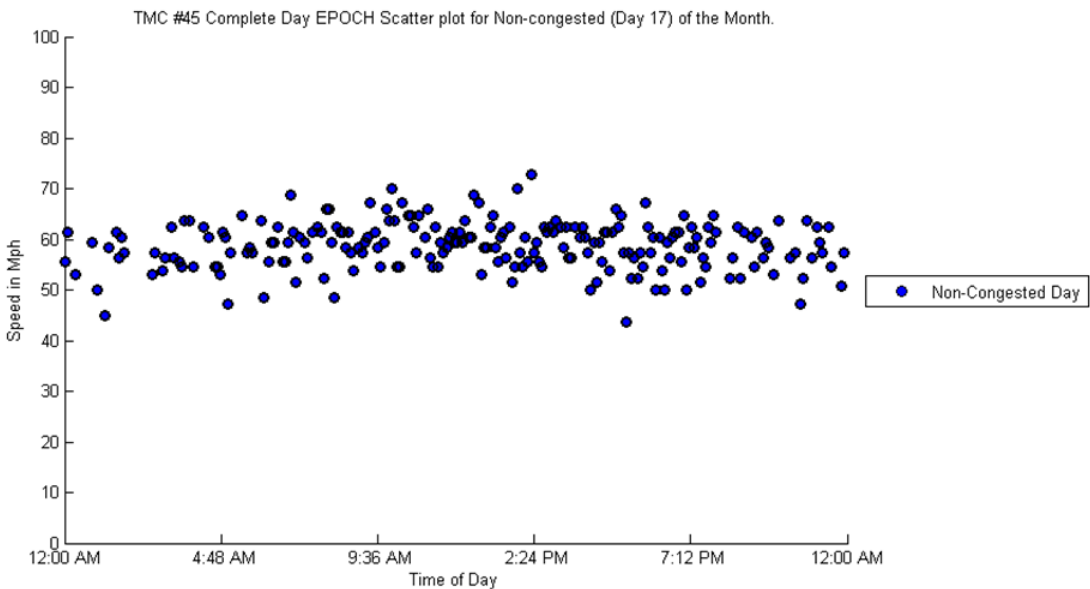
Figure 4-8 TMC 45 Complete Day Epoch Scatter Plot for Non-Congested Day of January.

4.2.8 GPS inaccuracy

In some cases, GPS coordinates of NHS roadways could match coordinates of non-NHS roadways. For example, bridges, tunnels, and parallel roadways cause NHS and non-NHS roadways to be located at the same geographical coordinate. Consequently, vehicles traveling on non-NHS roadways could be mistakenly accounted as those traveling on NHS roads and, as a result, distort collected TT measurements. For example, if vehicle directionality is not provided or if the accuracy of GPS positioning is not precise, a vehicle can easily be mistaken on an NHS roadway, even though it is actually traveling a non-NHS roadway that is near the NHS road. At an intersection, GPS location is associated with directionality, thus the error can be detected. Ultimately, the result of miscounted data is an increase in the variability of road TT.

Figure 4-9 shows TMC 47 characterized by 0.5m of roadway crossing major arterial SE Grand Blvd. The satellite view depicted in Figure 4-10 shows that the NHS passes under the roadway. If directionality was not reported as a function of GPS measurement, vehicles on SE Grand Blvd. could be miscounted as traveling on I-35. Figure 4-10 also shows two parallel non-NHS roadways adjacent to I-35 southbound and northbound. If GPS positioning is not completely accurate, an erroneous count is possible as a result of vehicles traveling on either road.
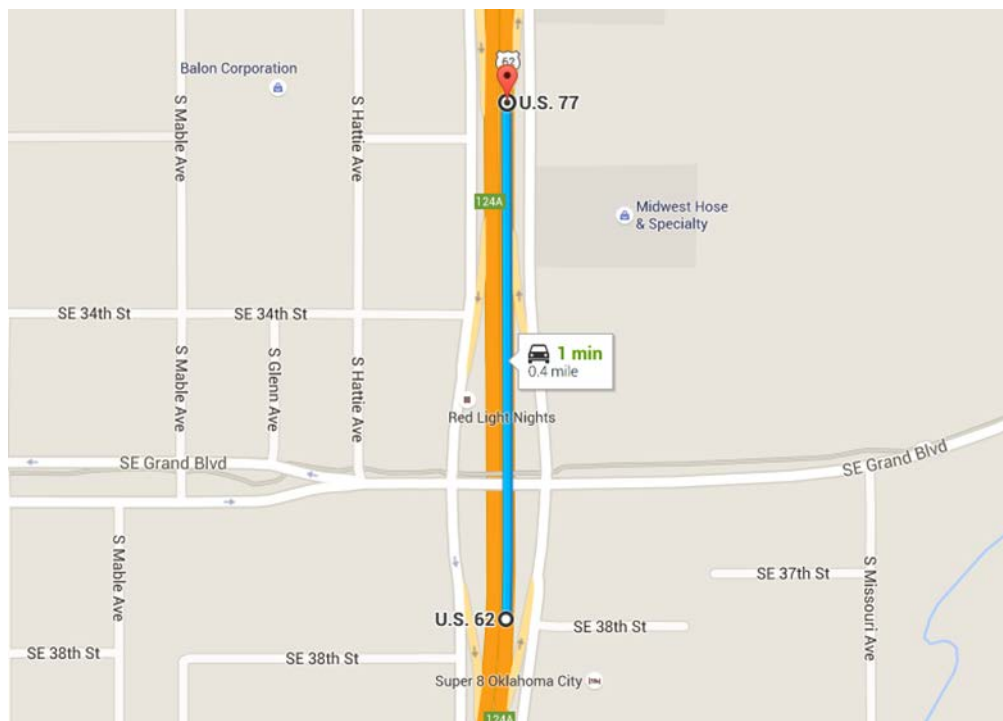
Figure 4-9 Map View of TMC 47 Crossroads with A Major Arterial.

76
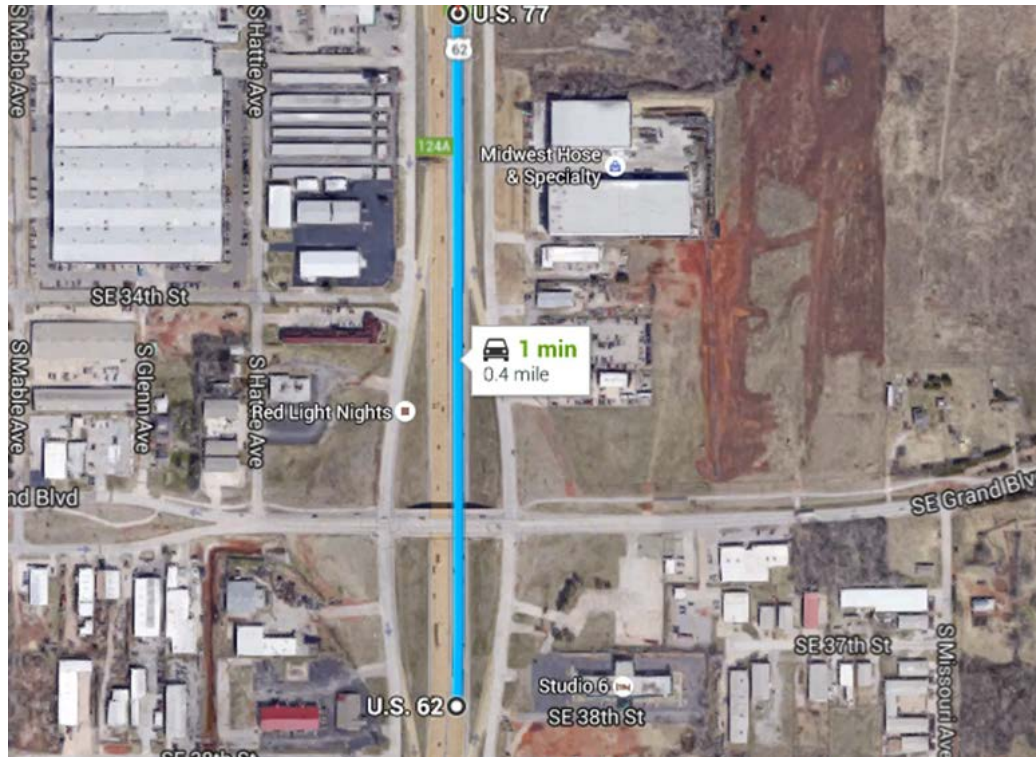
Figure 4-10 Satellite View of TMC 47 Crossroads with A Major Arterial.

4.3 NPMRDS Database Design

The OU research group employed PostgreSQL to develop the database for housing NPMRDS data. The following considerations were taken into account for improving query execution time and responsiveness for multi-user access.

1. Optimizing data type assignments: Utilize the smallest data type size possible for importing into the developed schema. Doing so had a significant impact on performance and improved query response time, especially for large scale queries of multiple data types.

2. Generating Integer Keys: Map Segments Identifiers to Integer Keys to facilitate faster queries.

3. Separating "Date" and "Time" entries: For "Datetime" fields, a separate "Time" and "Date" column were introduced to facilitate faster processing of queries without specific time requirements. This functionality leverages the smaller type size the word "Date" has over the word "Datetime."

4. Improving queries: Write efficient and optimized queries to minimize response time (e.g., avoiding "select *" queries, using "select (required_columns_list)") for improved performance.

5. Normalization: Optimize performance and prevent excessive repetition of data.

4.4 NPMRDS Tools

Based on database design, a series of tools were developed for users to access and utilize NPMRDS for aforementioned use cases. Web tools are available at URL https://speed.tulsa.ou.edu/. The "Login Form" depicted in Figure 4-11 greets new users visiting the website.
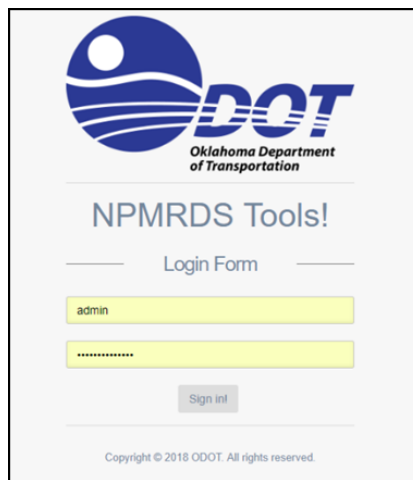
Figure 4-11 NPMRDS Login Form.

Upon signing in, access to NPMRDS v.1 (HERE) and NPMRDS v.2 (INRIX) is available, as shown in Figure 4-12.
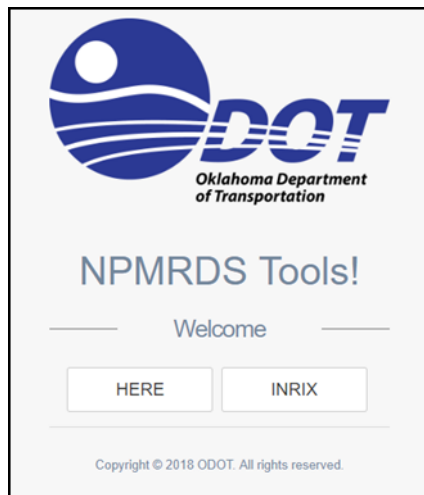
Figure 4-12 Option to Select HERE or INRIX Datasets.

4.4.1 Dashboard

The dashboard tool, shown in Figure 4-13, is the first tool developed for NPMRDS that allows fast and easy access to dataset contents in a simple and intuitive manner. The tool enables end users to quickly search and download segment data for different queries through a wide variety of filtering tools, which are described below.
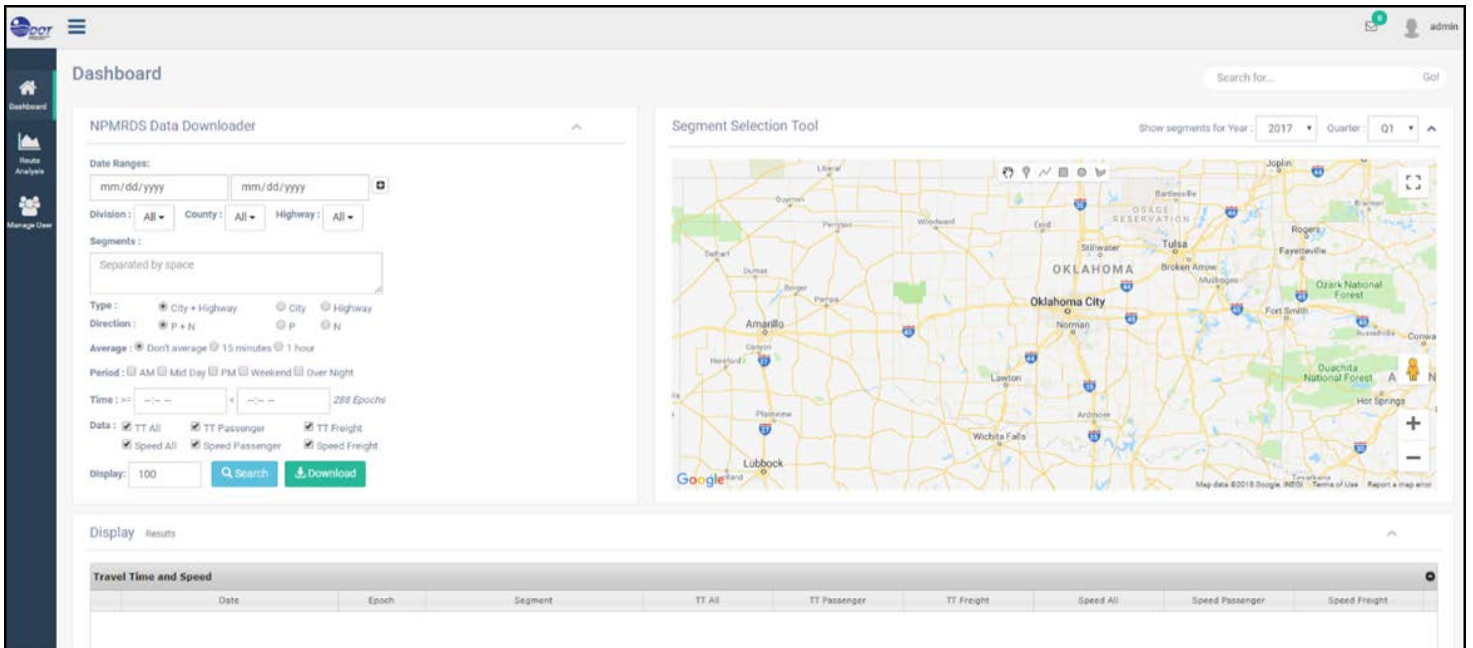
Figure 4-13 NPMRDS Dashboard Tool.

4.4.2 Graphical search

Graphical segment search is enabled through the segment selection tool located on the right side of the webpage, as shown in Figure 4-14. By setting the year and quarter dropdown selectors to the intended search criteria, a user can quickly locate all segments in a given geographic region.
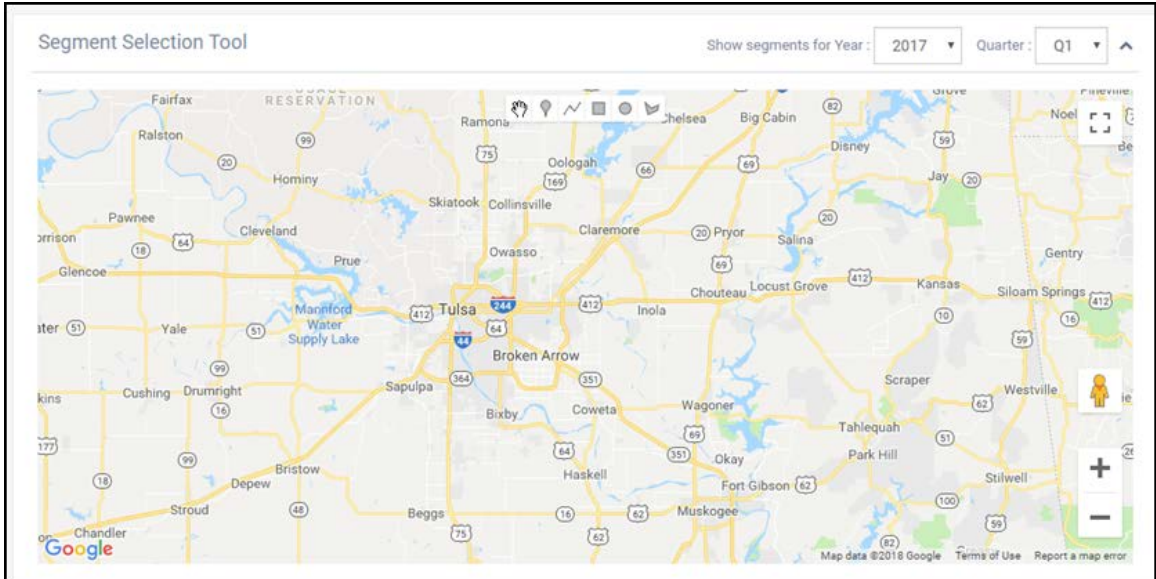
Figure 4-14 Segment Selection Tool.

The stop drawing selector (i.e., glove selector) disables all other selectors, allowing a user to freely move individual markers, points, or drawings on the map.

The location marker selector enables a user to mark points on the map for plotting and capturing segment data on a specific route (See Figure 4-15).
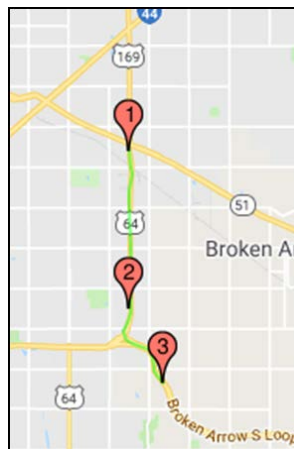
Figure 4-15 Example of Marker Point Route Selection.

The shape selectors (i.e., box, circle, polygram) enables a user to draw custom shapes to cover a specific region (See Figure 4-16).

Notably, the graphical user interface (GUI) has auto-retrieval enabled for all selection and filtering criteria, meaning an implicit query returns segment information to

the GUI map and populates segment fields upon mouse-click-release of any of the aforementioned selectors (See Figure 4-17).
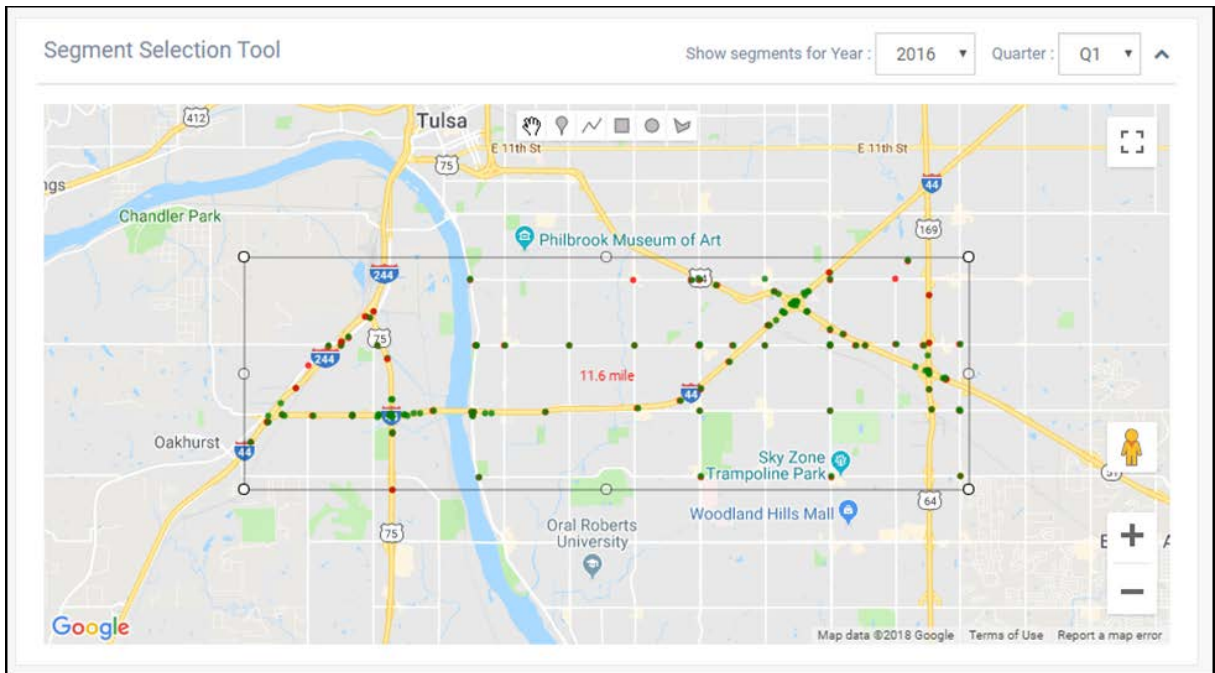
Figure 4-16 Example of Rectangle Drawing Selection.
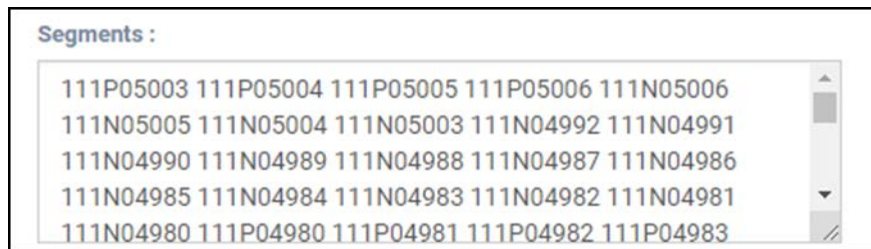
Figure 4-17 Segment Fields Populated with Auto-retrieval.
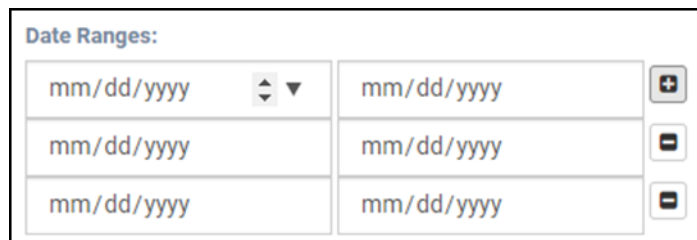
Figure 4-18 Date Range Filter.

Segments selected through a graphical search can be further refined to fit a more detailed criteria. The date range filter shown in Figure 4-18 allows the user to specify data retrieval periods, including one long time period or a range of specific dates. This feature is enabled when a user selects more than one date range by clicking on the plus

sign located to the right side of the filter box. When activated, this filter will take precedence over the year and quarter selectors found in the segment selection tool.

Additional filters include:

- A Type filter for selecting highway, intra city, or all segments in NPMRDS.

- A PN filter for selecting positive or negative direction traffic flows.

- An Average filter for adjusting reported data retrieved according to a 15-minute or 1-hour interval.

- A Period filter for indicating custom time frames for data retrieval, including AM (06:00 AM < 10:00 AM), Mid-Day (10:00 AM < 04:00 PM), PM (04:00 PM < 08:00 PM), or Weekend and Over Night periods. Moreover, specific time periods can be combined to form a larger selection of specific times (e.g., selecting AM and Mid-Day will report data from 06:00 AM < 04:00 PM).

- A Time filter for choosing specific times —other than the popular Period time filters listed above— for a query search. It is important to note that the default selection is all times (i.e., 288 epochs).

- A Data filter for selecting a specific type of data records, including TT or speed records for passenger vehicles, freight trucks, or the combined all category, as previously explained.

4.4.3 Division, county, highway and segment search

Custom filters allow an ODOT user to instantly limit results to segments located in a specific division, county, highway, or segment. Subset groups can also be generated. For instance, a user might be interested in segments pertaining to Division 3, which are located only in Hughes, Johnston, and Lincoln counties and which belong only to I-44. Figure 4-19 and Figure 4-20 show query results.

Figure 4-19 Custom Query Example Segment Result.

Figure 4-20 Custom Division, Country, Highway Query Example.

4.4.4 Route Analysis

The Route Analysis tool enables quick route and segment data analysis. Users can use this filter to obtain summary statistics for average TT and average speed over a specified time period. Employing the marker point selector, a user can leverage the graphical route search map to achieve analysis similar to that performed using the dashboard tool. Alternatively, segments can be entered individually in the segment form and filtered according to desired criteria, including direction, average duration, and time of interest. Individual or multiple highways can be selected for rapid analysis. Finally, the Route Analysis tool allows a user to set custom thresholds for identifying and coloring output results.

Figure 4-21 through Figure 4-26 illustrate examples of analyzing I-35 for 31 days using the Route Analysis tool. Results in some cases are shown for August 2015, and others for August 2016.
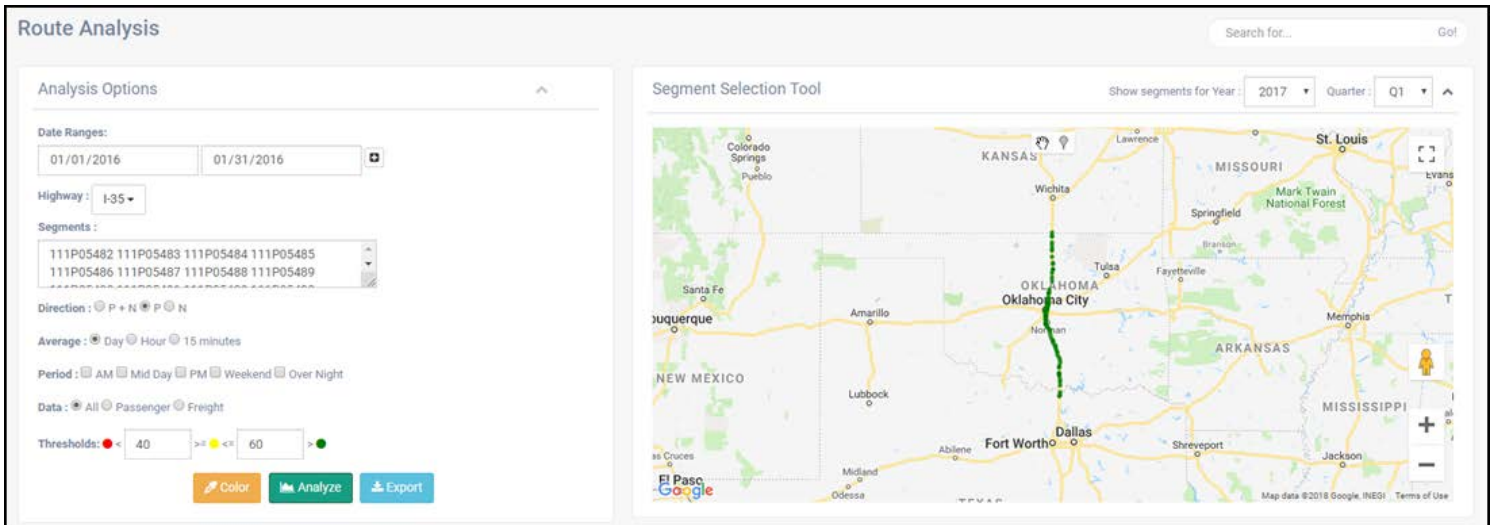
Figure 4-21 Route Analysis (I-35 P Aug. 2016).
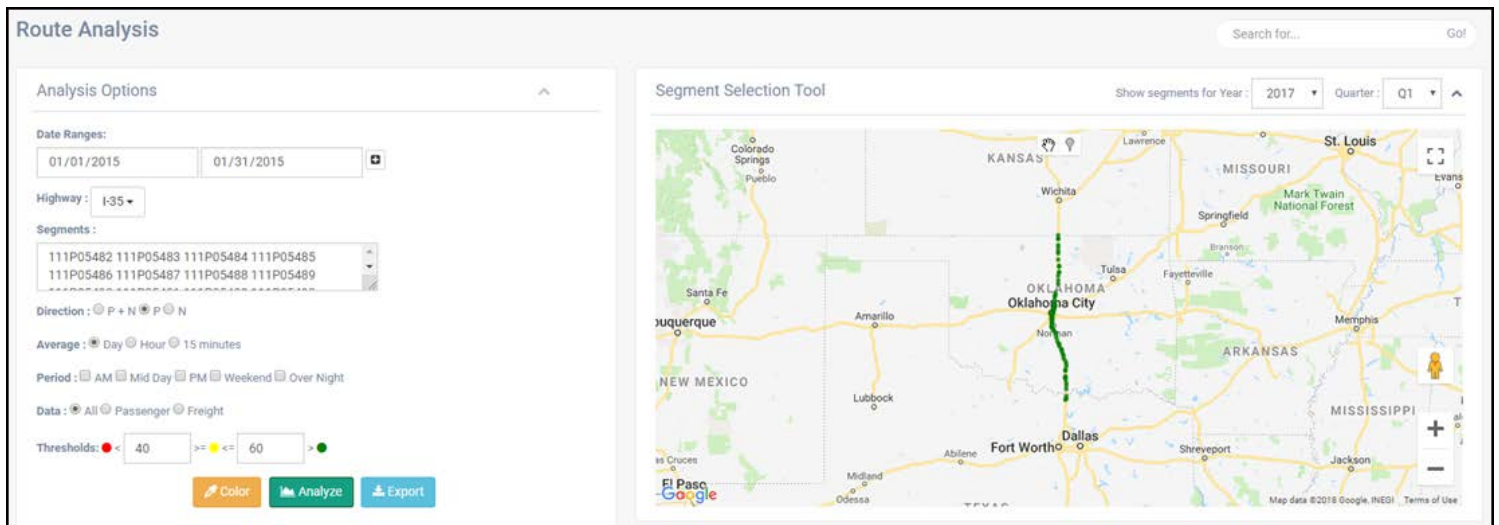
Figure 4-22 Route Analysis (I-35 P Aug. 2015).
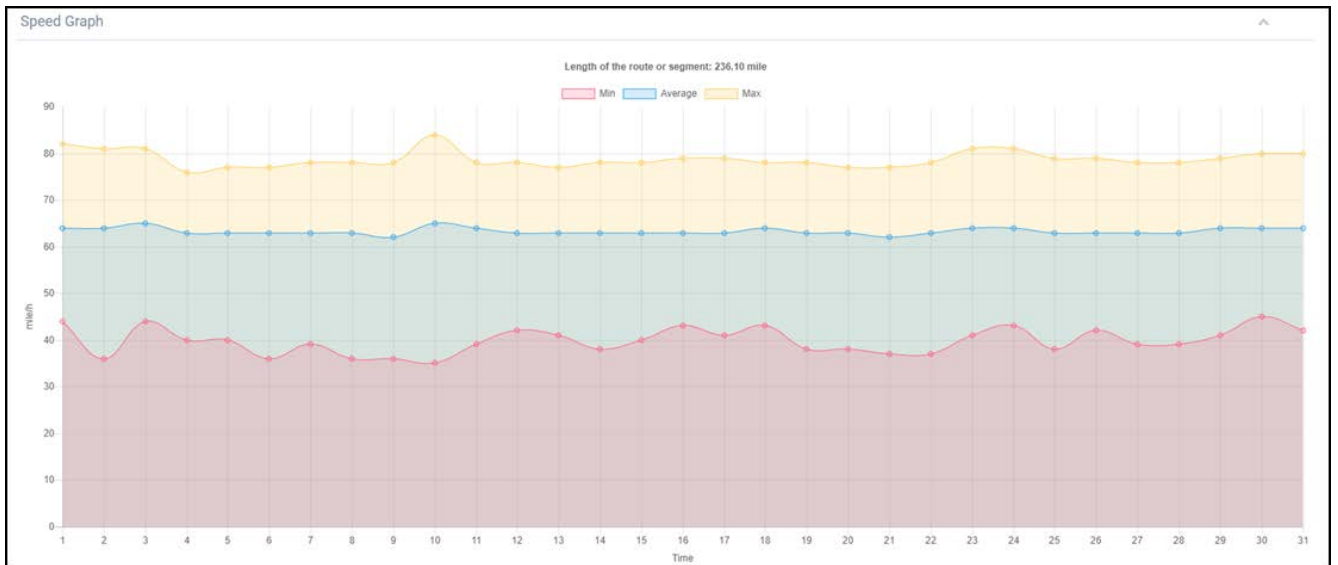
Figure 4-23 Average Speed (I-35 P Aug. 2016).
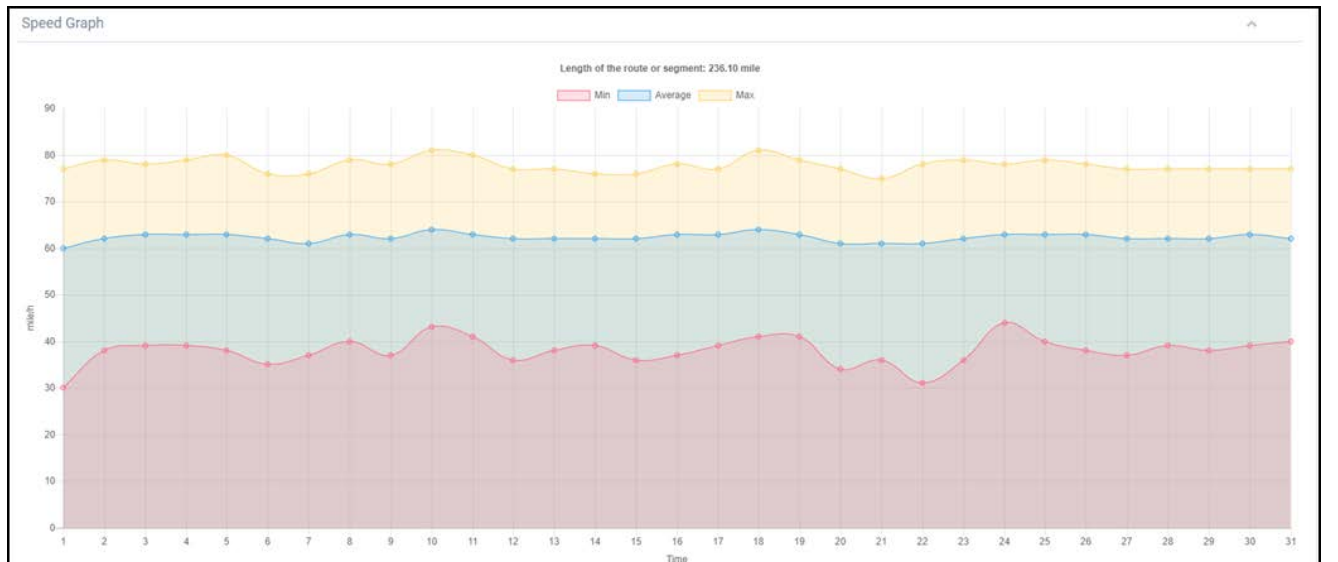
Figure 4-24 Average Speed (I-35 P Aug. 2015).
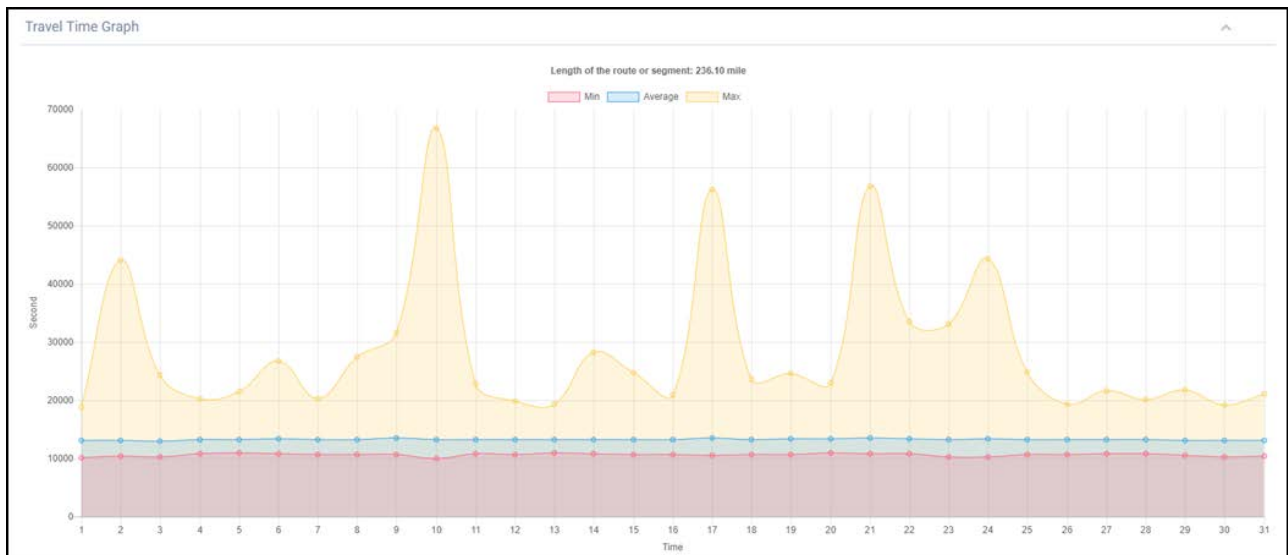
Figure 4-25 Average Travel Time (I-35 P Aug. 2016).
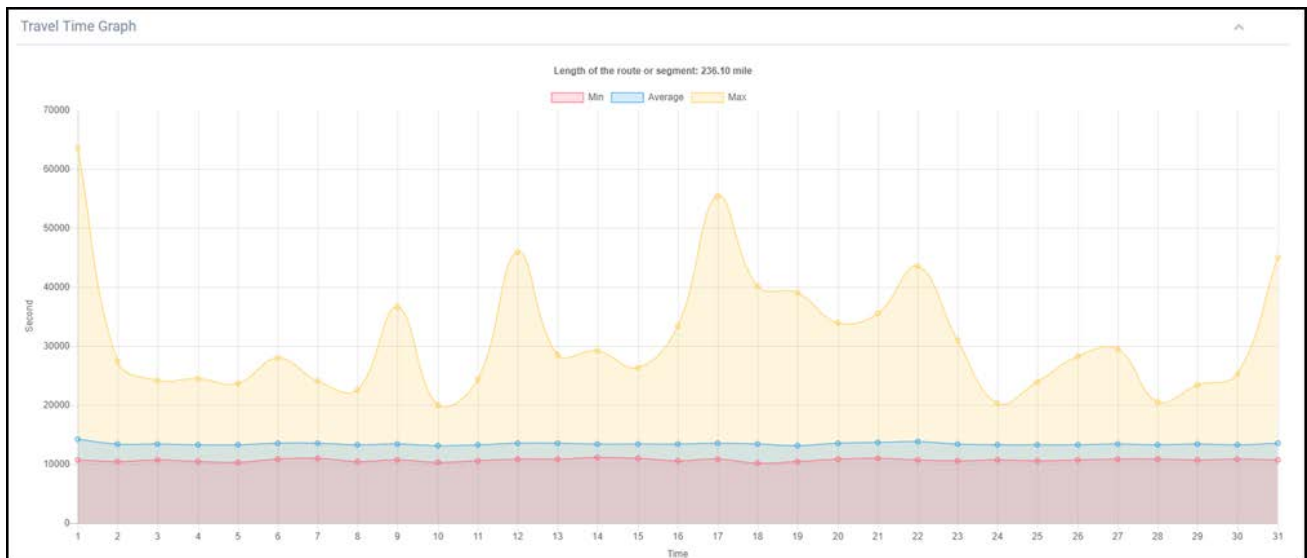
Figure 4-26 Average Travel Time (I-35 P Aug. 2015).

86

5. DATA CONDITIONING AND FUSION ALGORITHMS

Despite the limitations and challenges discussed in Chapter 4, the NPMRDS dataset has important advantages, making it a valuable tool for crafting traffic performance measures. For example, because NPRMDS is a probe data set, TT can be easily collected from different geographic regions. Compared to traditional fixed location detectors, NPRMDS data has higher granularity without the confines of location or forced infrastructural physical constraints. Moreover, NPRMDS data is continuously generated, enabling DOT agencies to look beyond separate periodic surveys of unusual highway conditions. Capturing this information requires developing tools for extracting, manipulating, and processing NPRMDS data. A thorough understanding of domain characteristics is necessary for accurate and effective statistical processing. Limitations enumerated previously serve as guidelines for further anomaly detection and outlier removal procedures. The following processes were developed and published in [3] and [23]. For the sake of completeness for our readers, the highlights are included in this document.

5.1 Data Outliers

Congestion on segmented roadways is a function of both time and space. In space, a shock wave starts at the observed segment and then ripples to subsequent segments lagging behind the observed segment. The result is an increase in reported TT. With regard to time, the aforementioned shockwave manifests at the observed segment with increased TT for a recorded epoch, and then expands to later epochs of the same segment as congestion continues. At a certain point of time—given that the duration of congestion is long enough—spillover to epochs of segments behind the observed segment occurs and expands congestion in space. Consequently, congestion can first be detected in time in the observed segment, and then stretch in space to adjacent segments. Given the observed segment is short in length, time and space can expand nearly simultaneously, meaning epoch TT duration simultaneously increases in the observed and lagging segments when sampling time is long enough to allow congestion spillover to adjacent segments. In light of this understanding, we proceed to analyze outliers and formulate procedures for removing them from NPMRDS.

5.2 Effect of High Spatial-temporal Variance

As aforementioned, there is a high spatial-temporal variance in the number of epoch records in NPMRDS for NHS roadway segments. The chief cause for this variance is the fluctuating number of probe vehicles present on any segment at any moment in time. One particular case occurs when sample size is very low, which could result in outliers being non-representative of actual TT for vehicles traveling on the segment. These outliers can either be high or low valued points. Cases where sampled

data points exhibit extremely unrealistic values could also be caused by a system-related error during data acquisition or conditioning. Detecting these outliers is possible by evaluating the dataset for data points that are too extreme to be realistic. In this work, average speed above 3 mean SDs from the speed limit (e.g., speed equal to 20.8 mph) is considered an outlier. This equates to approximately 90 mph on a roadway with a speed limit of 70 mph. Reported speed represents averages. Thus, it is unrealistic for all cars traveling on the roadway to be averaging 90 mph or above. If such findings were to occur, results could be indicative of a very small sample size. Values for OK Highway I-35 southbound were first thresholded above 90 mph. Results were plotted per segment in ascending order for combined (i.e., passenger car and freight truck) TT, as shown in Figure 5-1. Figure 5-2 shows results for passenger car TT, and Figure 5-3 shows the same for freight truck TT.
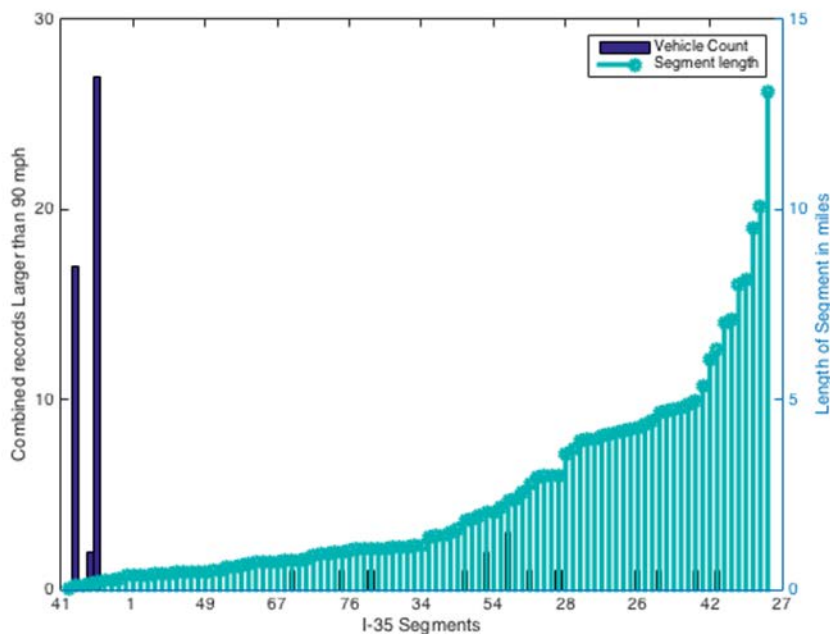
Figure 5-1 Combined Vehicle Count Plot for Number of Epochs with Speeds

Greater Than 90 Mph for OK I-35 Southbound Segments.

Two phenomena can be observed:

1. Shorter segments have smaller densities, which in turn affects sample size. Thus, a fast traveling vehicle might be the only sample present at a particular moment in time, making its speed not representative of average vehicle speed. Nevertheless, if the high speed is considered an accurate value of vehicle speed, one could surmise that vehicles can travel at free flow speed with no obstruction or congestion regardless of actual free flow speed. If the outlier were to remain in

88

the dataset, it would cause problems when performance metrics were calculated. For statistical analysis integrity, the outlier must be removed.

2. Speed quantization error related to the variability of segment length.

For the sake of congestion analysis, we set all such points to the speed limit, as they are merely indicative that no congestion is present and that vehicles have the ability to travel at free flow.
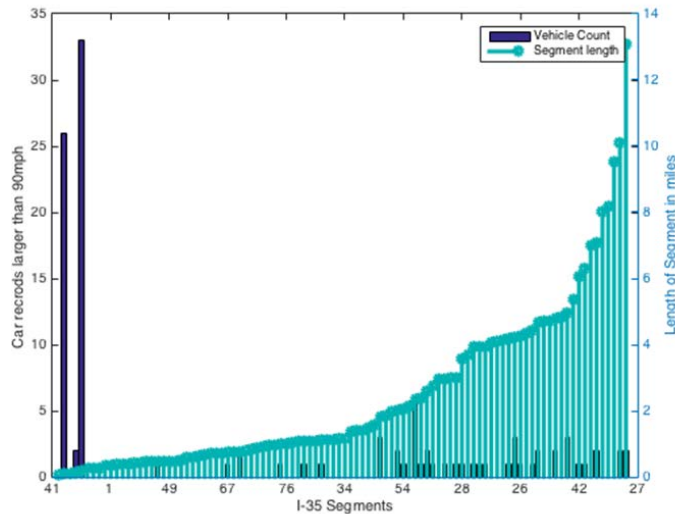
Figure 5-2 Passenger Vehicle Count Plot for Number of Epochs with Speeds Greater Than 90 Mph for OK I-35 Southbound Segments.
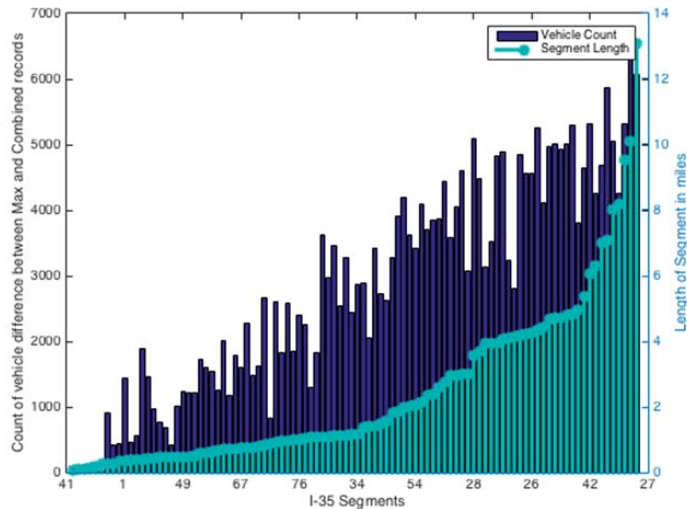
Figure 5-3 Truck vehicle count plot for number of epochs with speeds greater than 90 mph for OK I-35 southbound segments.

89

5.3 Vehicle Specific Performance Data Points (Power-to-Weight)

To detect outliers that might be caused by vehicle-specific characteristics on the road—as explained in the power-weight phenomena occurring in heavier vehicles, we build on the assumption that freight trucks recording slow speeds in correlation with passenger cars recording faster speeds is indicative that the latter represents a better approximation of true speed on the roadway. Slower freight truck speeds represent characteristics of a truck itself, or what is termed as vehicle specific performance data. Accordingly, a combined (i.e., passenger car and freight truck) speed data matrix is set to the speed of the fastest passenger car or freight truck, and the outlier is removed. Thus, detection is accomplished by correlating freight truck and passenger car vehicle speed for the same epoch and segment so that outliers are removed by replacing speed entries with the higher of the two speeds.
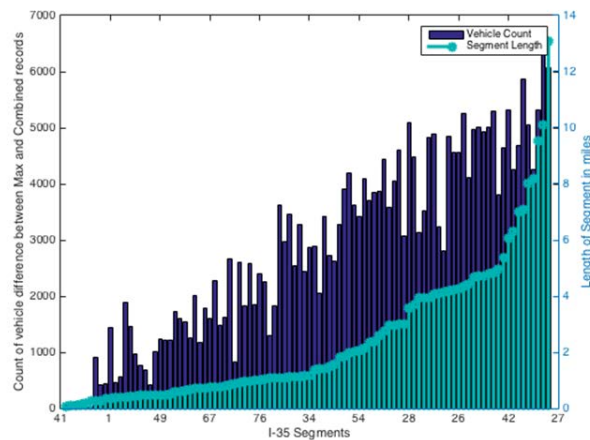
Figure 5-4 Epoch Record Count for Difference of Max (Truck, Car) Matrix to Combined Matrix.
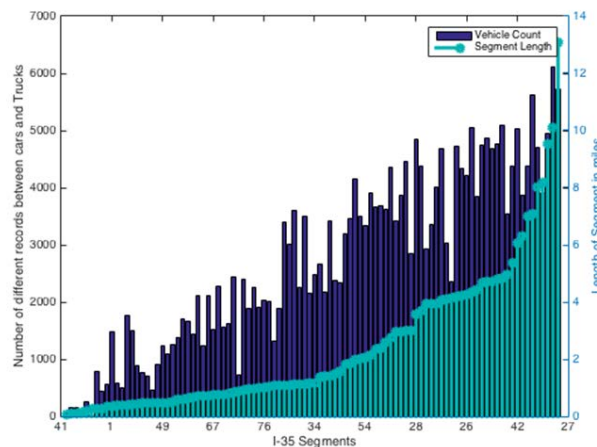
Figure 5-5 Epoch Record Count for Difference Between Car and Truck Matrices.

Figure 5-4 shows a plot of the maximum speed matrix subtracted from NPMRDS combined all-vehicles matrix. Figure 5-5 shows a plot of the number of epochs when passenger car speeds were faster than freight truck speeds. Both figures are nearly identical, indicating that the majority of slower speeds were caused by freight trucks slowing for vehicle-specific reasons rather than for roadway conditions affecting all traffic. Figure 5-5 demonstrates that as segment length increases, the number of effected epochs averages down from maximum value increases, as well. This phenomenon was confirmed when examining the percentage of down-shifted epochs relative to the total number of epochs available per segment. Results indicate that an outlier would have a more profound effect on results due to the fact that fewer samples decrease the probability of correction when an outlier is part of the dataset.

Figure 5-6 and Figure 5-7 show the mean and the standard deviation, respectively, of the speed difference between maximum and combined vehicle speeds. Average difference for most segments is approximately 5 mph, with standard deviation of approximately 2 to 3 mph. As segment length decreases, mean increases. Reported combined speeds in NPMRDS show on average a 5 mph reduction in speed compared to actual roadway speed, likely as a result of slower freight trucks.
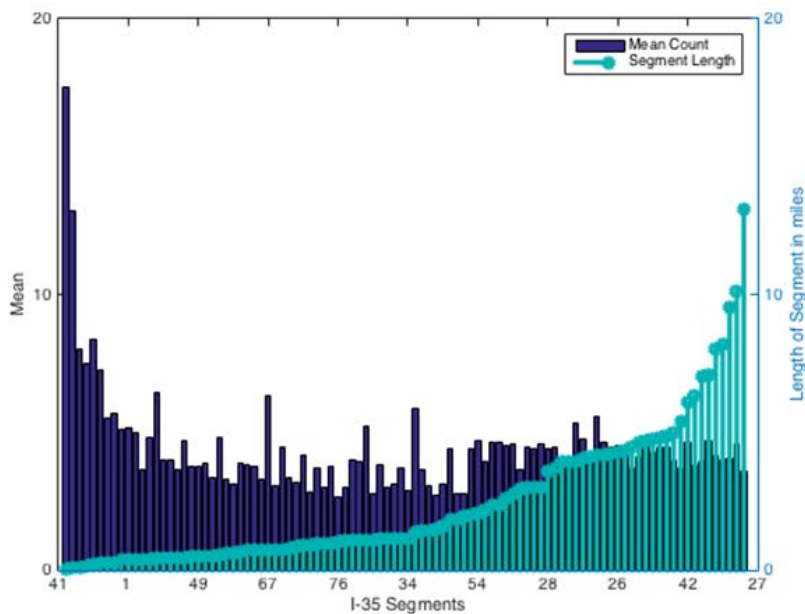
Figure 5-6 Mean Speed Difference Between Max Passenger and Combined Speeds.
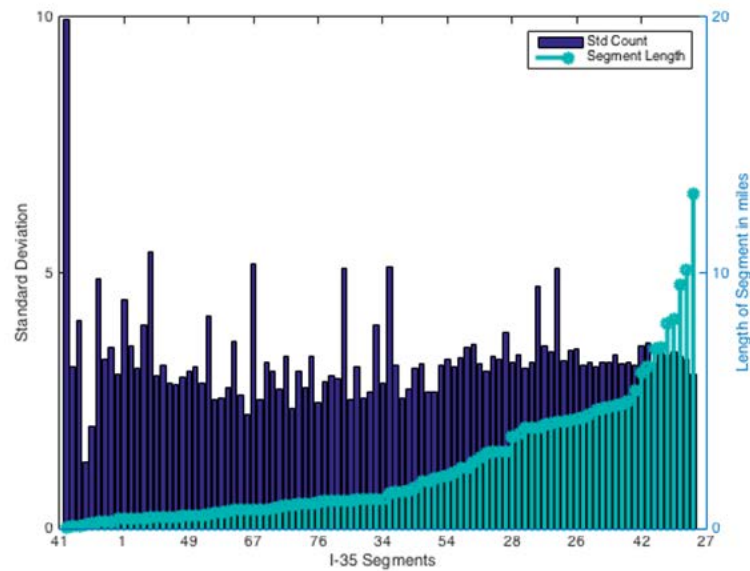
Figure 5-7 Standard Deviation of Speed Difference Between Max Passenger and Combined Speeds.

5.4 Roadway Geometry

When roadway geometry affected TT, segments consistently reported slow TT compared with roadway speed limit. This phenomenon builds on the assumption that slower TT is a result of highway topography caused by the nature of the road itself, which forces vehicles to slow down. Given that roadway conditions might affect larger freight truck speeds far more than passenger car speeds, the power-weight ratio law would not consistently be cause for slowing down traffic. Accordingly, when slow freight trucks were differentiated based on passenger vehicles traveling at free flow speeds, changes were not made to the dataset. Instead, such cases were marked for post check in the graphical information system (GIS). These cases are of interest to DOT agencies, as they show locations where segments could possibly undergo optimization for freight truck TT.

To investigate roadway segments, mean freight truck speeds were collectively monitored vis-a-vis speed limit during a one-month time period. Figure 5-8 shows results for OK I-35 southbound. Average freight truck speed in January 2015 was somewhat below the speed limit. Plots of the highest mean day speed per segment is shown for freight trucks and passenger cars in Figure 5-9 and Figure 5-10, respectively. For most segments, average freight truck speed was recorded below the roadway speed limit. Notably, some segments recorded average passenger car speed below the speed limit, as well. TMC 44 in particular stands out for having speeds significantly

below the speed limit throughout the month of January 2015. This result was consistent for both freight trucks and passenger cars.
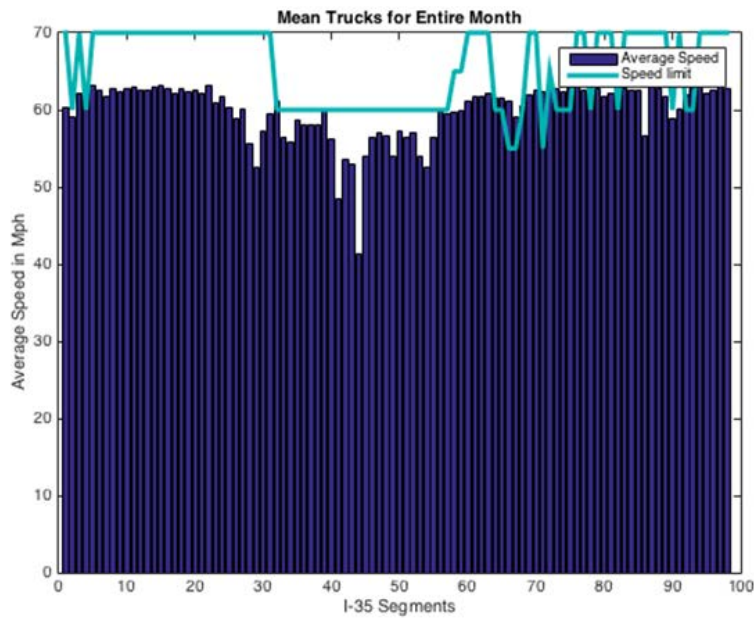
Figure 5-8 Average Epoch Truck Speed Per Segment for January 2015.
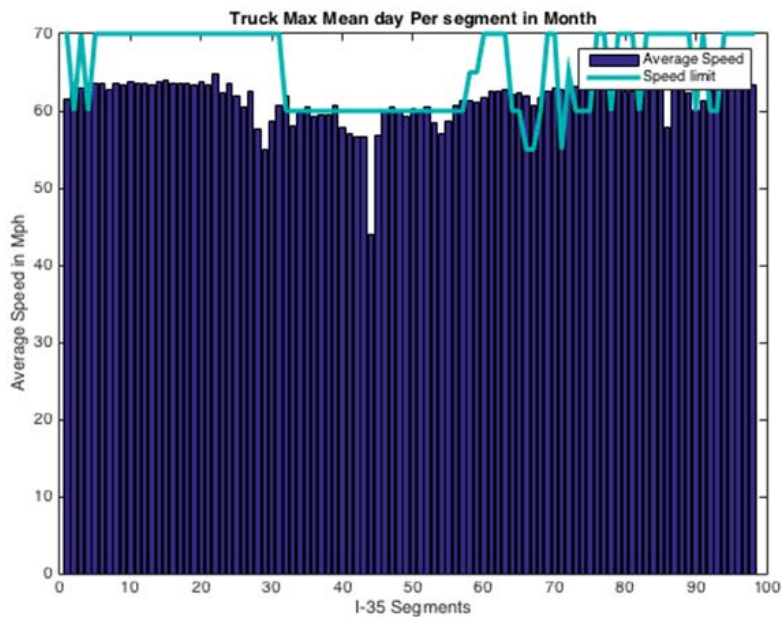
Figure 5-9 Max Day Mean Epoch Truck Speed for January 2015.
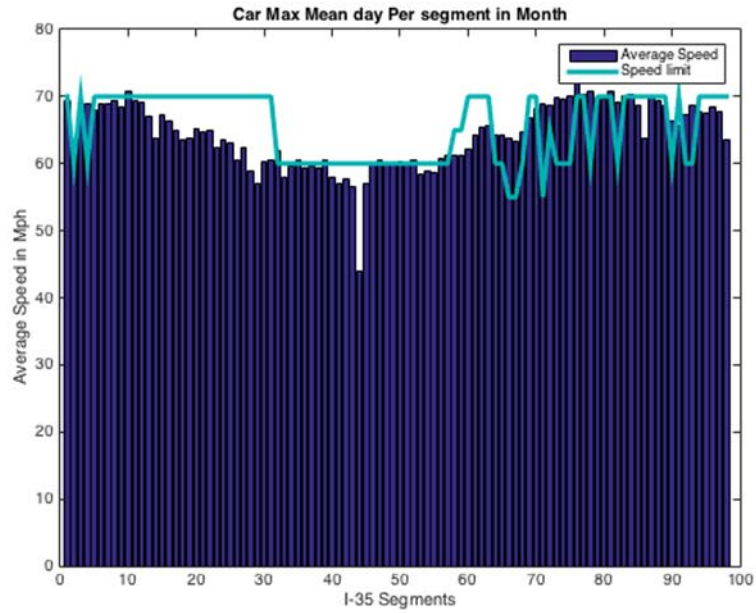
Figure 5-10 Max Day Mean Epoch Car Speed for January 2015.

Coordinates for TMC 44 were extracted and are shown on the Google map satellite image in Figure 5-11 and Figure 5-12.

Figure 5-11 Segment 45 I-35 Intersect with The Centennial Expressway HW 235.

TMC 44 begins at the intersection of OK I-35 and Centennial Expressway Highway 235. The one lane on-ramp causes traffic slowdown for passenger cars and freight trucks alike, as evidenced in NPMRDS.

Figure 5-12 Close View of Segment 44 I-35 Intersect with The Centennial Express Way HW 235.

5.5 GPS Inaccuracy (Non-NHS Roadway Data Points)

Faulty GPS units or insufficient positioning accuracy result in inclusion of data points that are not part of NHS roadways. As mentioned earlier, data records could actually belong to roadways adjacent to the NHS. When sample size is large, outlier effect is minimal. When the sample size is small, however, outlier effect is possibly measurable. Recall that detection relies on the assumption that there is a speed difference between NHS roadways and adjacent non-NHS roadways. Thus, any record mistakenly reported due to GPS inaccuracy would be different from lagging and leading epochs for any segment under study. Another indicator occurs when passenger car speeds are slower than freight truck speeds by one or more SD in the same segment. By extracting all cases where trucks are faster than cars and removing all cases where cars are slower than trucks by less than the maximum SD (e.g.,15 mph for OK I-35 southbound), all cases with noteworthy speed difference between passenger vehicles and freight trucks can be identified, as shown in Figure 5-13(a) and (b). Although such cases could be indicative of non-NHS roadways, differences could also be the result of a small sample size for passenger vehicles in which reported outliers were not representative of average speed per segment. Accordingly, threshold results were based on number of occurrences. Empirically, 20 occurrences were chosen, assuming the higher occurrence was indicative of GPS inaccuracies.
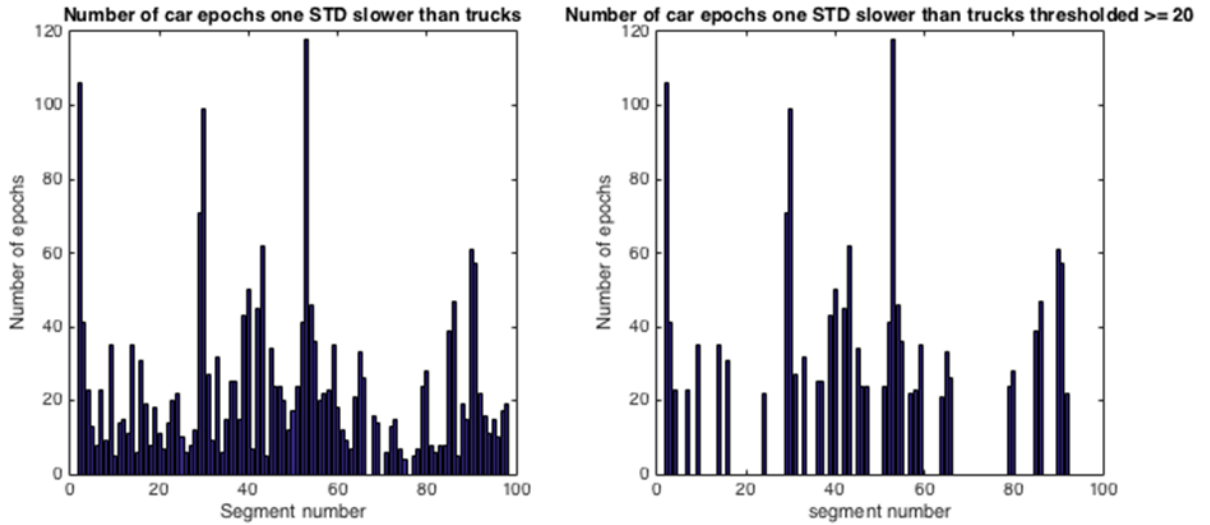
Figure 5-13 (a). Cars One Standard Deviation Less Than Trucks. (b). Threshold Result for Count >= 20.

Coordinates of a random sample of segments were extracted, and Google maps were used for validation. Figure 5-14 shows that TMC 53 had the highest peak and was found to be adjacent to the OK I-35 southbound service road. Similarly, TMC 30, which proved to be the segment with the third highest error count, is positioned adjacent to the OK I-35 northbound service road (See Figure 5-15).
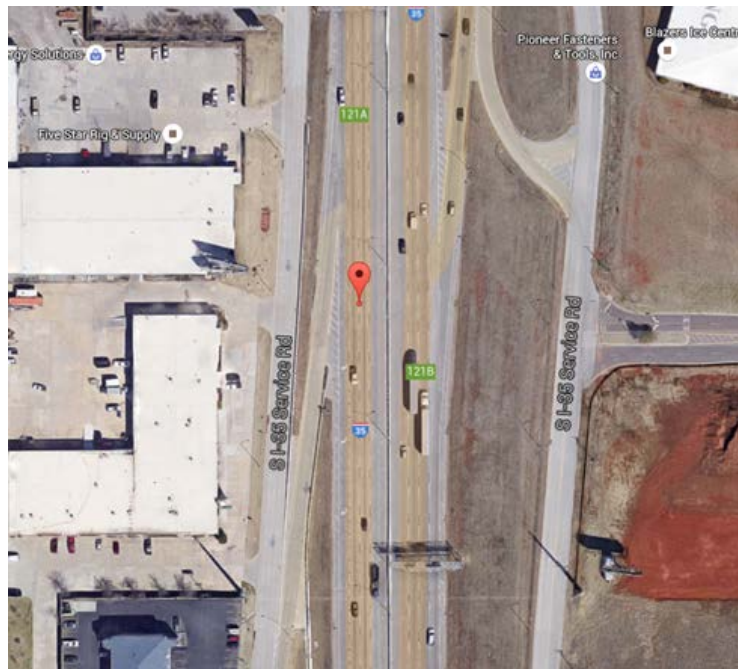
Figure 5-14 Segment 53 Adjacent to S I-35 Service Road.

Figure 5-15 Segment 30 Adjacent To N-I35 Service Road.

To identify and remove the remaining outliers, the following two procedures were performed:

1. A new output speed matrix was generated and consisted of the maximum speed record reported for both passenger cars and freight trucks given epoch. The matrix alleviated non-NHS outliers when both car and truck speeds were available.
2. Building on the notion of congestion described earlier in this chapter, a mask filter was constructed to scan the entire database to identify remaining outliers and then remove them.

Figure 5-16 illustrates the mask used to scan the speed database. The mask filter identified three types of congestion: 1) New congestion evident in future epochs; 2) Present congestion evident in past epochs; and 3) Propagating congestion evident in adjacent segment epochs. Figure 5-17 provides a flow chart for the process used to remove outliers from the database. The process commences with thresholding a current segment epoch based on a modified congestion detection approach. Once an epoch has been identified as likely congestion, all gray marked entries in the mask are thoroughly inspected for likely congestion. If speed value of a grey entry is indicative of congestion, a flag is raised for the particular corresponding entry. If a check flag is detected at the end of the process, the current segment epoch is not altered. Given there is no flag, the current segment epoch is reset to the speed limit. A 20-minute detection range was chosen for NPMRDS, primarily because some missing epochs (i.e., epoch holes) were evident for consecutive records in particular segments in the dataset.
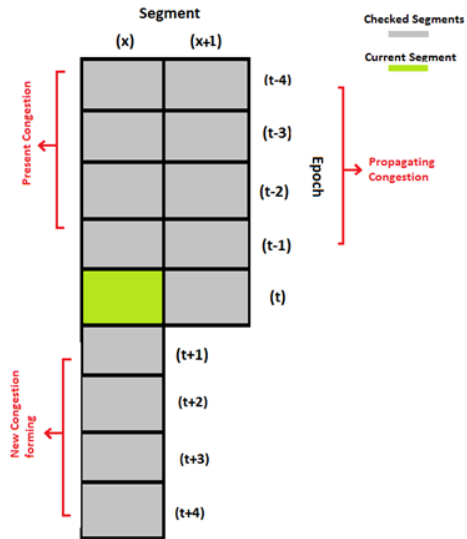
Figure 5-16 Mask Filter To Scan for Outliers.
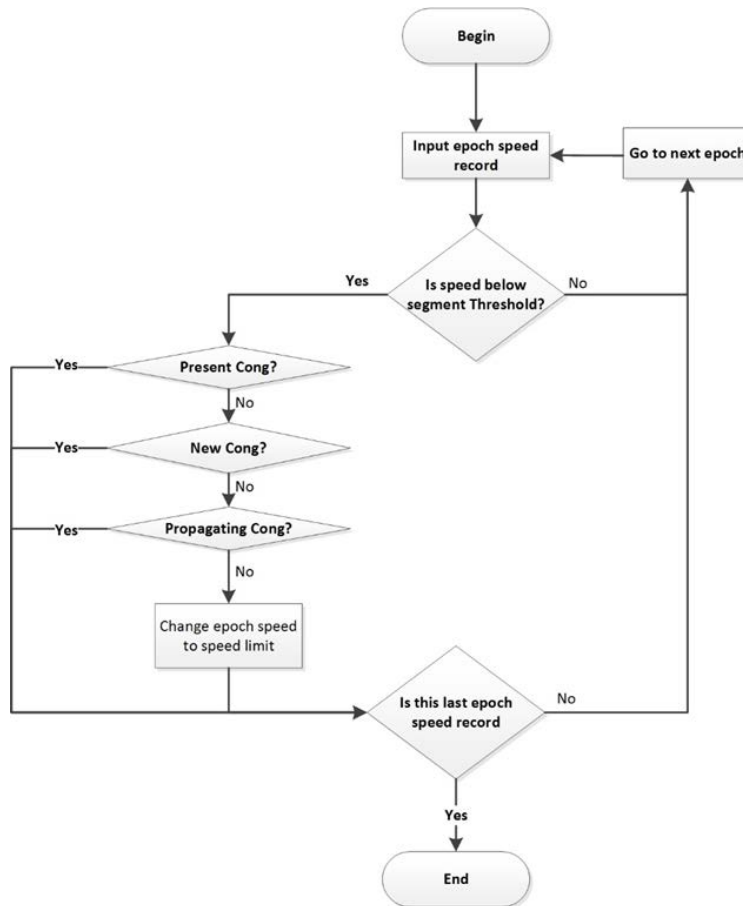
Figure 5-17 Flow Chart for Scanning Outliers Using Mask Filter.

5.6 Cleansed Dataset

After applying the methods and processes described above, a cleansed dataset was generated. Table 5-1 shows a database example for TMC 97 with outlier speed reported. Epoch 1818 speed of 34.6485 mph is considerably lower than previous, consecutive, and adjacent recorded epoch speeds. As such, the value was considered an outlier and was reset, accordingly, to the speed limit for the segment.

Table 5-1 Database Outlier for TMC 97 in Raw Database.

	97
1805	61.6913
1806	62.1969
1807	62.4529
1808	62.711
1809	77.8259
1810	62.9712
1811	64.034
1812	65.9828
1813	62.9712
1814	62.4529
1815	64.8549
1816	67.1507
1817	60.7042
1818	34.6485
1819	64.034
1820	61.4415
1821	65.6972
1822	64.5789
1823	63.2335

Figure 5-18 and Figure 5-19 illustrate plots for segment 97 and segment 69 speed records, respectively, in January 2015. These were composed of both raw speed data obtained from the TT measurements without processing and the cleansed dataset following anomaly and outlier detection/removal procedures.
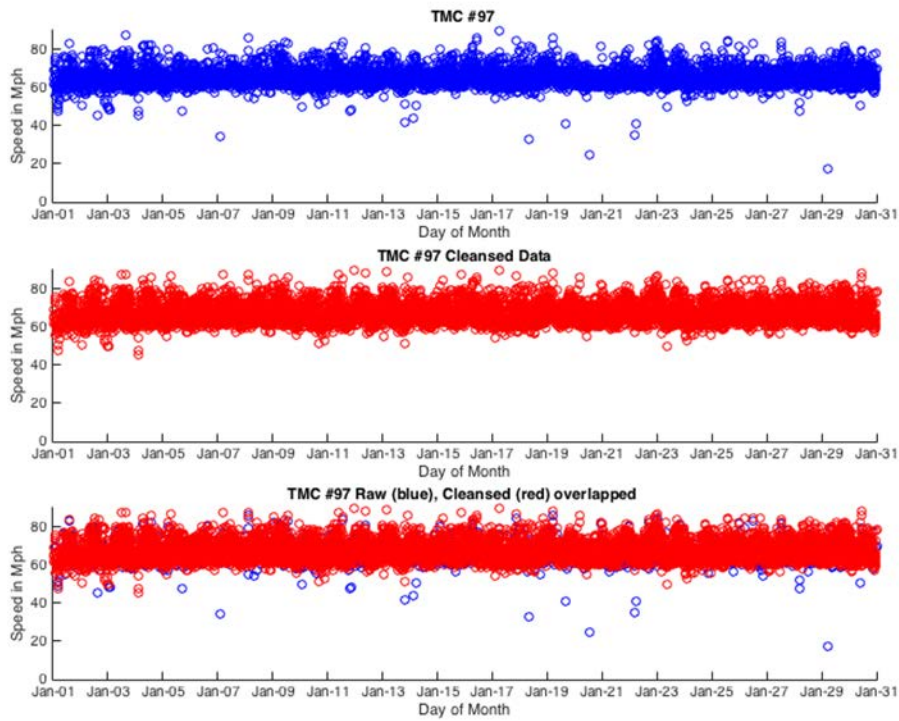
Figure 5-18 Comparison for TMC 97 Speed Records, Raw Vs. Cleansed Data, for January 2015.
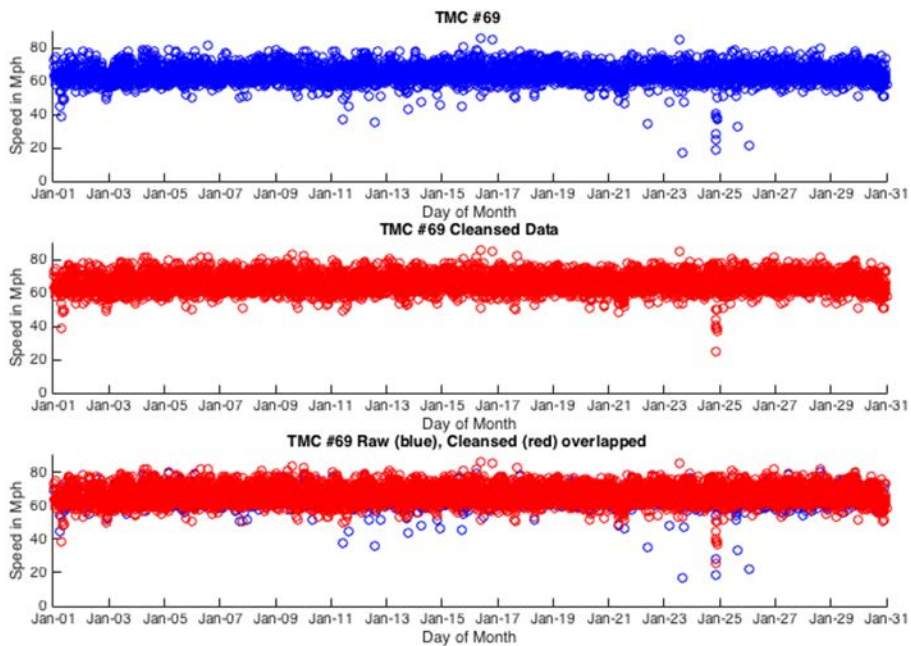
Figure 5-19 Comparison for TMC 69 Speed Records, Raw Vs. Cleansed Data, for January 2015.

6. TRAVEL TIME ANALYSIS ALGORITHMS

The FHWA published a Notice of Proposed Rulemaking (NPRM) in the Federal Register, which formed a series of related rules establishing a set of performance measures for state DOT agencies and MPOs to use, as required by the Moving Ahead for Progress in the 21st Century Act (MAP-21) and by the Fixing America's Surface Transportation (FAST) Act. This following section details the use of NPMRDS to compute required performance measures, as defined in 23 CFR Part 490 of Federal Register, vol. 82, no. 11.

6.1 Assessing Performance of the National Highway

Two TT reliability measures were established in the related rules, which pertained to the third iteration of the FHWA defined performance measures [3]:

1. Percent of reliable person-miles traveled on the Interstate (i.e., Interstate TTR measure)
2. Percent of reliable person-miles traveled on the non-Interstate NHS (i.e., Non-Interstate TTR measure).

The following definitions are described for completeness [3]:

1. Level of TTR is a comparison—expressed as a ratio—of the 80th percentile TT of a reporting segment with the "normal" (i.e., 50th percentile) TT of a reporting segment that occurs throughout a full calendar year.
2. Normal TT (or 50th percentile TT) is the TT to traverse the full extent of a reporting segment, which is greater than the time for 50 percent of the travel in a calendar year for traversing the same reporting segment.
3. TT cumulative probability distribution is a representation of all TT for a road segment during a defined reporting period (e.g., annually) presented in a percentile ranked order, as provided in the TT data set. The normal (i.e., 50th percentile) and 80th percentile TT used to compute TTR measures may be identified by the TT cumulative probability distribution.

NPMRDS is used to calculate performance metrics defined by the FHWA. State DOTs are advised to refrain from replacing missing TT when data are not available in the TT data set (i.e., data not reported or reported as "0"/null). Average Annual Daily Traffic (AADT) will be used as reported to the Highway Performance Monitoring System (HPMS) in June of the reporting year. Annual Volume (AV) for each segment is calculated as:

$$\text{Annual Volume}_{\text{segemnt}} = \text{AADT}_{\text{segment}} \times 365 \text{ days} \qquad \textbf{Eq. 6-1}$$

Average Occupancy Factor (AOF) is obtained from data published by the FHWA.

6.1.1 Metric Calculation [3]

Two performance metrics are required for the NHS Performance measures.

1. Level of Travel Time Reliability (LOTTR) for TTR measures, which can be calculated according to the following procedures:
   - Conflation between NPMRDS and HPMS should be performed.
   - Four new datasets should be created—according to time intervals highlighted below—for each reporting segment in a ranked list of average TT for all traffic (i.e., "all vehicles" in NPMRDS nomenclature), and then reported to the nearest second for 15-minute periods.
     - "AM Peak": TT occurring between 6 and 10 a.m. for weekdays (Monday thru Friday) from January 1st through December 31st of the same year.
     - "Mid Day": TT occurring between 10 a.m. and 4 p.m. for weekdays (Monday thru Friday) from January 1st through December 31st of the same year.
     - "PM Peak": TT occurring between 4 and 8 p.m. for weekdays (Monday thru Friday) from January 1st through December 31st of the same year.
     - "Weekend": TT occurring between 6 a.m. and 8 p.m. for weekend days (Saturday and Sunday) from January 1st through December 31st of the same year.
2. Travel Time Cumulative Probability Distribution (TT-CDF) is computed for the entire year per segment.
   - Normal and 80th percentile TTs are determined from the TT-CDF.
   - Four LOTTR metrics defined as the 80th percentile TT divided by the 50th percentile TT and rounded to the nearest hundredth should be calculated for each reporting segment—one for each data set created according to the second bulleted step above.

6.1.2 Measure Calculation [3]

The specified Interstate TTR measure should be computed to the nearest tenth of a percent, as follows:

$$\text{Percent of the person} - \text{miles traveled on Interstate that are reliable} = 100 \times \frac{\sum_{i=1}^{R} SL_i \times AV_i \times OF_j}{\sum_{i=1}^{T} SL_i \times AV_i \times OF_j} \quad \textbf{Eq. 6-2}$$

where:

R = total number of Interstate NHS reporting segments that exhibit LOTTR below 1.50 during all four time periods identified above,

i = Interstate reporting segment,

SL_i = length, to the nearest thousandth of a mile, of reporting segment "i,"

AV_i = total annual traffic volume to the nearest single vehicle of reporting segment "i,"

J = geographic area in which reporting segment "i" is located, where a unique occupancy factor has been determined,

OF_i = occupancy factor for vehicles travelling on the NHS, and

T = total number of Interstate system reporting segments.

The specified Non-Interstate TTR measure should be computed to the nearest tenth of a percent, as follows:

$$\textbf{Percent of the person} - \textbf{miles traveled on Non} - \textbf{Interstate that are reliable} = \textbf{100} \times \frac{\sum_{i=1}^{R} SL_i \times AV_i \times OF_j}{\sum_{i=1}^{T} SL_i \times AV_i \times OF_j} \quad \textbf{Eq. 6-3}$$

where:

R = total number of non-Interstate NHS reporting segments that exhibit LOTTR below 1.50 during all four time periods identified above,
i = non-Interstate reporting segment,
SL_i = length, to the nearest thousandth of a mile, of reporting segment "i,"
AV_i = total annual traffic volume to the nearest single vehicle of reporting segment "i,"
J = geographic area in which reporting segment "i" is located, where a unique occupancy factor has been determined,
OF_i = occupancy factor for vehicles travelling on the NHS, and
T = total number of non-Interstate system reporting segments.

6.1.3 Measure Results

Figure 6-1 illustrates results obtained using NPMRDS and calculating measures for the state of Oklahoma in 2017.
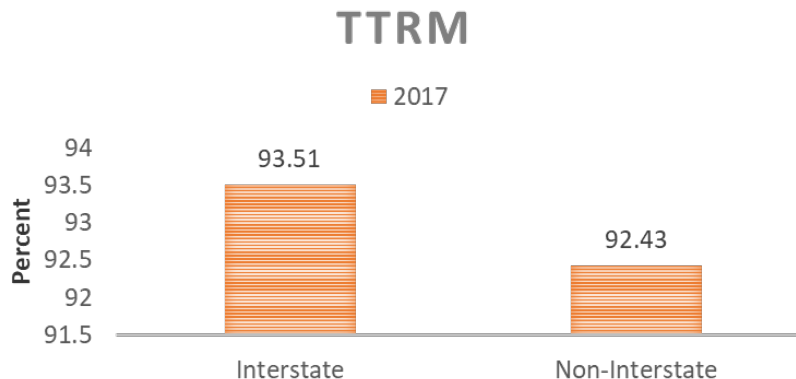
Figure 6-1 TTRM Results for Oklahoma.

6.2 Assessing Freight Movement on the Interstate System

The Truck Travel Time Reliability (TTTR) Index measure was chosen as the reliability metric for assessing freight movement on the interstate system. NPMRDS was used to calculate performance metrics. Given that freight truck TTs were not available in the TT data set (i.e., data not reported or reported as "0"/null) for a given 15-minute interval, missing TT with an observed TT that represented all traffic on the roadway during the same 15-minute interval (i.e., "all vehicles" in NPMRDS nomenclature) was replaced.

6.2.1 Metric Calculation [3]

Truck Travel Time Reliability (TTTR) performance is required for NHS performance measures specified for freight movement assessment. To calculate this metric, five datasets were created—according to time intervals highlighted below—for each reporting segment in a ranked list of average TT for freight truck traffic (i.e., "Freight vehicles" in NPMRDS nomenclature) for 15-minute periods, to the nearest second.

- "AM Peak": TT occurring between 6 and 10 a.m. for weekdays (Monday thru Friday) from January 1st through December 31st of the same year.
- "Mid Day": TT occurring between 10 a.m. and 4 p.m. for weekdays (Monday thru Friday) from January 1st through December 31st of the same year.
- "PM Peak": TT occurring between 4 and 8 p.m. for weekdays (Monday thru Friday) from January 1st through December 31st of the same year.
- "Weekend": TT occurring between 6 a.m. and 8 p.m. for weekend days (Saturday and Sunday) from January 1st through December 31st of the same year.
- "Overnight": TT occurring overnight between 8 p.m. and 6 a.m. Sundays thru Thursdays from January 1st through December 31st of the same year.
  - o Travel Time Cumulative Probability Distribution (TT-CDF) is computed for the entire year per segment.
  - o Normal and 95th percentile TT are determined from the TT-CDF.
  - o Five TTTR metrics defined as 95th percentile TT divided by the 50th percentile TT and rounded to the nearest hundredth should be calculated for each reporting segment—one for each data set created in the first bullet-step mentioned above.

6.2.2 Measure Calculation [3]

Freight Reliability measure was computed to the nearest hundredth:

$$\frac{\sum_{i=1}^{T} SL_i \times maxTTTR_i}{\sum_{i=1}^{T}(SL_i)} \qquad \textbf{Eq. 6-4}$$

where:

SL_i = length of reporting segment "i" rounded to the nearest thousandth of a mile,
T = total number of interstate system reporting segments,
$maxTTTR_i$ = maximum TTTR of five time periods mentioned above to the nearest hundredth of Interstate system reporting segment "I," and
i = Interstate reporting segment.

6.2.3 Measure Results

Figure 6-1 illustrates results obtained for calculating the measure for the state of Oklahoma in 2017 using NPMRDS for both interstate and non-interstate segments.

TTTR
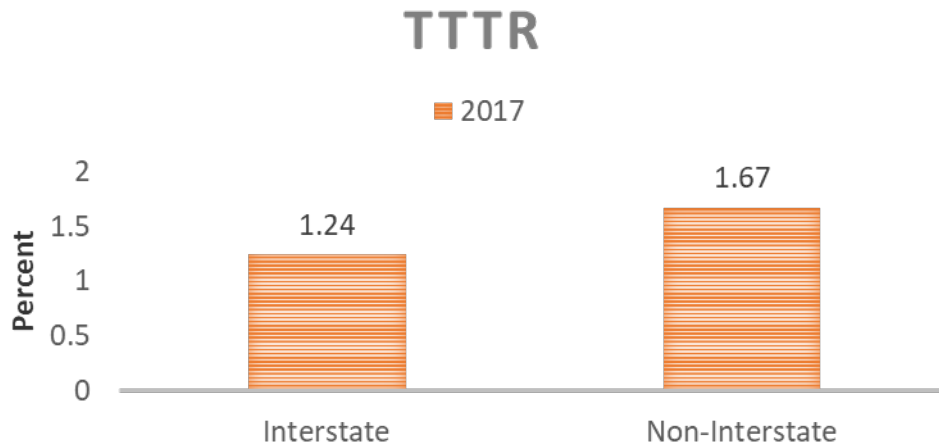
Figure 6-2 Results for Oklahoma.

6.3 Assessing Congestion Mitigation and Air Quality Improvement Program—

Traffic Congestion

The following definitions are described for completeness [3].

- Excessive delay indicates additional time spent in congested conditions as defined by speed thresholds that are lower than a normal delay threshold. (For the purposes of this rule, the speed threshold is 20 mph or 60 percent of the posted speed limit, whichever is greater).
- Peak Period is defined as weekdays from 6 to 10 a.m. and either 3 to 7 p.m. or 4 to 8 p.m., at the discretion of State DOTs and MPOs.

6.3.1 Measures

Two performance measures assess traffic congestion for carrying out the CMAQ program (i.e., collectively referred to as the CMAQ Traffic Congestion measures) [3]:

1. **PHED:** Annual hours of Peak Hour Excessive Delay (PHED) per capita.
2. **Percent Non-SOV Travel:** Non-Single Occupancy Vehicle (SOV) travel measure.

For calculations reported in this paper, the research team focused only on the PHED measure.

Using NPMRDS for calculating PHED per capita, hourly traffic volume data was developed for each reporting segment in the following way:

1. An estimate of hourly traffic volumes for peak periods on each weekday of the reporting year was performed using Annual Average Daily Traffic (AADT) reported to the HPMS;
2. Hourly traffic volumes were assigned by hour to each reporting segment (e.g., between 8 and 8:59 a.m.);
3. Annual vehicle classification data was used for each reporting segment using data;
4. ADT reported to HPMS was used to estimate annual percent share of traffic volume for passenger cars, buses, and freight trucks;

where

- Buses = value in HPMS data item "AADT_Single_Unit";
- Freight trucks = value in HPMS data item "AADT_Combination"; and
- Passenger cars = subtract values for buses and trucks from the value in HPMS data item "AADT."

Using data reported to HPMS, data values were separated to represent the appropriate travel direction of the reporting segment.

Annual Average Vehicle Occupancy (AVO) factors for passenger cars, buses, and freight trucks in applicable urbanized areas were estimated from annual vehicle occupancy factors provided by FHWA.

6.3.2 Metric Calculation

The PHED performance metric is required to calculate Total Peak Hour Excessive Delay (i.e., person-hours, referred to as the PHED metric), calculated using the following data.

- TT of all traffic (i.e., "all vehicles" in NPMRDS nomenclature) during each 15-minute interval for all applicable reporting segments in the TT data set during peak periods from January 1st through December 31st of the same year,
- length of each applicable reporting segment,
- Hourly volume estimation for all days and for all reporting segments in which excessive delay is measured,
- Annual vehicle classification data for all days and for all reporting segments when excessive delay is measured, and
- AVO factors for passenger cars, buses, and freight trucks for all days and for all reporting segments where excessive delay is measured.

Excessive delay threshold TT for all applicable TT segments is calculated, as follows [3]:

$$Excessive\ Delay\ Threshold\ Travel\ Time_s = \left(\frac{Travel\ Time\ Segment\ Length_s}{Threshold\ Speed_s}\right) \times 3600$$

Eq.6-5

where

- $Excessive\ Delay\ Threshold\ Travel\ Time_s$ = the time of travel—to the nearest whole second—to traverse the TT segment at which any longer measured TT would result in excessive delay for the TT segment,
- $Travel\ Time\ Segment\ Length_s$ = total length of TT segments to the nearest thousandth of a mile for TT reporting segment, and
- $Threshold\ Speed_s$ = the speed of travel at which any slower measured speeds would result in excessive delay for TT reporting. For example, the speed threshold is 20 mph or 60 percent of the posted speed limit TT reporting segments, whichever is greater.

Excessive delay is determined for each 15-minute bin reporting segment for every hour and every day in a calendar year, as follows.

TT segment delay (RSD) is calculated to the nearest whole second, as follows [3]:

$$RSD_{s,b} = Travel\ time\ (s)_b - Excessive\ Delay\ Threshold\ Travel\ Time_s \qquad \text{Eq. 6-6}$$

and

$$RSD_{s,b} \leq 900\ seconds \qquad \text{Eq. 6-7}$$

where,

- $RSD_{s,b}$ = TT segment delay calculated to the nearest whole second for a 15-minute bin "b" of TT reporting segment "s" for a day in a calendar year; $RSD_{s,b}$ not to exceed 900 seconds,
- $Travel\ time(s)_b$ = measured TT to the nearest second for a 15-minute time bin (b) recorded for TT reporting segment s,
- b = 15-minute bin of a TT reporting segment "s," and
- s = TT reporting segment.

Excessive delay (i.e., the additional amount of time to traverse a TT segment in a 15-minute bin compared to the amount of time needed to traverse the TT segment when traveling at the excessive delay travel speed threshold) was calculated to the nearest thousandths of an hour.

$$Excessive\ Delay_{s,b} = \begin{cases} \dfrac{RSD_{s,b}}{3600} & when\ RSD_{s,b} \geq 0 \\ 0 & when\ RSD_{s,b} < 0 \end{cases} \qquad \text{Eq. 6-8}$$

Hourly traffic volumes for calculating the PHED metric for each reporting segment were as follows:

$$Total\ Excessive\ Delay_s = AVO \times \sum_{d=1}^{TD}\left(\sum_{h=1}^{TH}\left(\sum_{b=1}^{TB}\left(Excessive\ Delay_{s,b,h,d} \times \right.\right.\right.$$
$$\left.\left.\left.\left(\frac{hourly\ volume}{4}\right)_{s,h,d}\right)_b\right)_h\right)_d \qquad \text{Eq. 6-9}$$

where,

- AVO = Average Vehicle Occupancy,
- s = TT reporting segment,
- d = a day of the reporting year,
- TD = total number of days in the reporting year,
- h = single hour interval of the day where the first hour interval is 12 a.m. to 12:59 a.m.,
- TH = total number of hour intervals in day "h,"
- b = 15-minute bin for hour interval "h,"
- TB = total number of 15-minute bins in which TT are recorded in the travel time data set for hour interval "h," and
- d = a day of the reporting year.

$$AVO = (P_C \times AVO_C) + (P_B \times AVO_B) + (P_T \times AVO_T) \qquad \text{Eq. 6-10}$$

where,

- P_C = percent of cars as a share of total AADT on the segment,
- P_B = percent of buses as a share of total AADT on the segment,
- P_T = percent of trucks as a share of total AADT on the segment,
- AVO_C = average vehicle occupancy of passenger cars,
- AVO_B = average vehicle occupancy of buses, and
- AVO_T = average vehicle occupancy of freight trucks.

6.3.3 Measure Calculation

To arrive at PHED (i.e., Annual Hours of Peak Hour Excessive Delay Per Capita), performance measure for CMAQ traffic congestion was computed to the nearest tenth by summing PHED metrics of all reporting segments in each of the urbanized area, and then dividing the result by the population of the urbanized area:

$$Annual\ Hours\ of\ Peak\ Hour\ Excessive\ Delay\ per\ Capita = \frac{\sum_{b=1}^{T} Total\ Excessive\ Delay_s}{Total\ Population}$$

<div align="right">**Eq.6-11**</div>

6.3.4 Measure Results

Figure 6-3 illustrates results from calculating PHED for the state of Oklahoma in 2017 using NPMRDS. Oklahoma City serves as the largest contributor to excessive delay.
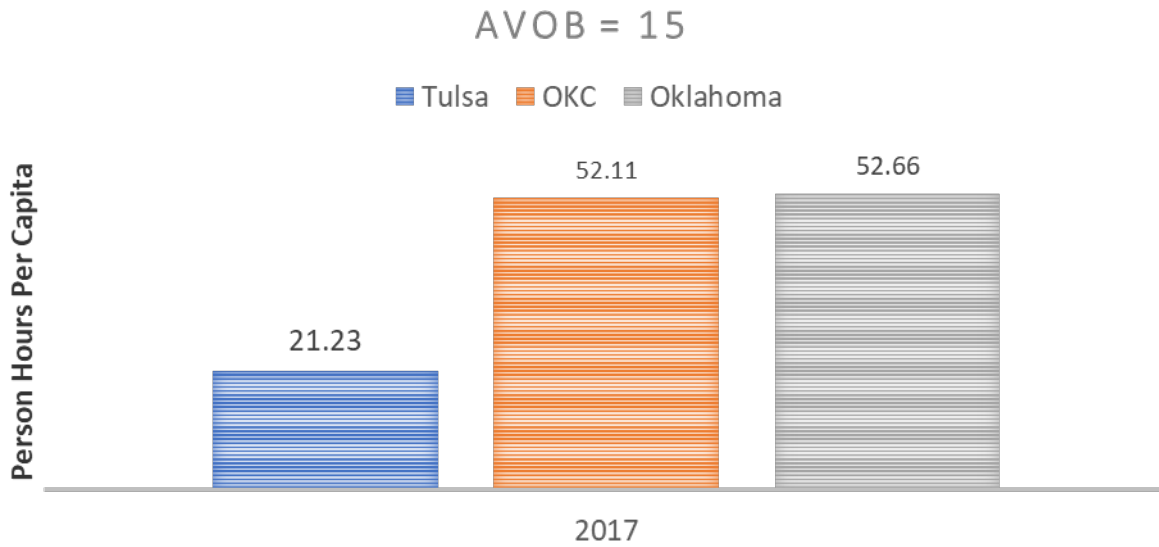
Figure 6-3 PHED Result for Oklahoma.

7. PROBABILISTIC MODELING

7.1 Secondary Incident Detection

Highways are the most frequently used means of transportation and the leading source of travel mishaps. Crashes or incidents on highways—both primary and secondary—constrain highway capacity, threaten passenger safety, and increase TT, resulting in delays and wasted traffic management resources. This report aimed to expand field knowledge about the detection of secondary incidents by analyzing primary incidents and their spatiotemporal influence on traffic.

Analytical and statistical methods, including logit, probit, and artificial neural network (ANN) models, were designed for automating incident classification by processing vehicle count, weather conditions, and traffic flow, among other parameters. The logit and probit model showed similar performance with an accuracy of 67% in the former and 66% in the latter. Identical precision was 48%. The contribution of each independent feature was gauged using odds ratio. ANN out-performed the logit and probit model. A simple three-layer ANN was used for incident classification, reporting 91% accuracy and 89% precision. ANN's superior performance can be attributed to its ability to learn complex relations.

A novel connection-weight algorithm was used to determine the importance of various features on the dependent variable, as well as how each factor affected the model. Results were encapsulated in a GUI for facilitating data collection and analysis.

7.2 Data Acquisition/Preparation for Analysis

Data records of various state highways in Oklahoma were obtained from ODOT databases. Two divisions—Traffic Engineering Division, for their Accident database, and Intelligent Transportation System (ITS) Division, for their Incident database—were instrumental in providing the data. The Accident database was composed of all incidents occurring in the state of Oklahoma and was accessible via an online portal. Individual or query-related records functionality allowed easy access to incident records reported by county or city. The present study was based on 65,000 incident records from 2014 in the city of Tulsa, OK.

The Incident database was composed of 3,026 records collected between 2014 and 2015 from a variety of highways throughout the state and included incident duration, number of lanes closed, and directionality of lane closure. Although the Accident database is more comprehensive than the Incident database, a combination of databases provided a comprehensive view of incidents that occurred throughout the state of Oklahoma.

7.3 Defining Spatiotemporal Boundaries of Primary Incidents

The spatiotemporal area of influence of primary incidents was defined using the following parameters:

- Queuing: ways in which vehicle drivers respond to highway incidents and how vehicles form queues on highways following incidents
- Lane blockage and its effects: primary incident impact on highway capacity
- Time distribution of traffic flow: effect of traffic intensity at different times during a day and how intensity affects vehicle movement on roads
- Lane changing behavior: driver behaviors as the travel from one lane to another
- Spatiotemporal effect: distance and time boundaries with respect to a primary incident

Such parameters can be used to generate average vehicle wait time and queue length for the highway network system. A definition of each parameter is defined in sub-steps in Figure 7-1.
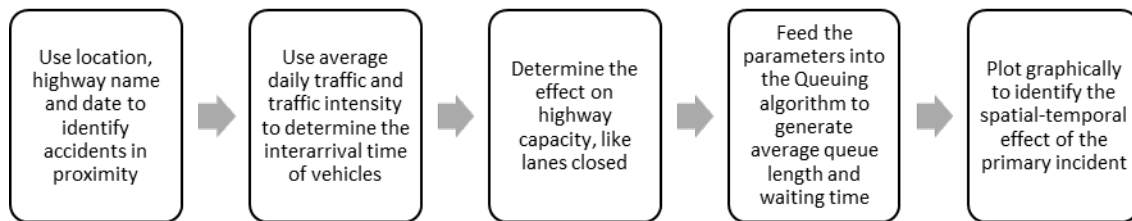
Figure 7-1 Process Definition of Spatiotemporal Area of Influence.

7.4 Queuing

Capturing vehicle movement on the roadway is important for increasing algorithm effectiveness and can be accomplished by simulating the inter-arrival times of vehicles in a real-world situation. A memoryless queueing model was leveraged to capture vehicle movement on roadways/highways. In this study, vehicle arrival rate on highways resembled a memoryless model (M/M/n), wherein the number of servers equals the number of highway lanes and each lane is an independent queue. The memoryless model of queuing used in the algorithm defines a memoryless interarrival rate for vehicles in the system and a memoryless servicing time. This method of queuing was achieved using the CIW library in Python.

Highway vehicles move in a pattern similar to a truncated Poisson process. At any given point in the day, arrival rate of subsequent vehicles is not dependent on the arrival rate of the present vehicles. However, inter-arrival time is generally bound by an upper and lower limit, hence the name truncated Poisson. The plot in Figure 7-2 shows the

distribution of vehicle inter-arrival times used in simulations. These ranged from 4 to 5 seconds for incoming vehicles. This feature aided in simulating a real-world vehicle arrival pattern.
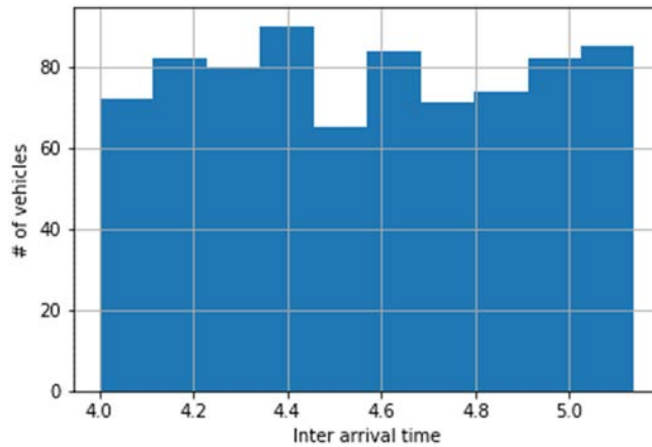
Figure 7-2 Inter-Arrival Times Vs. Number of Vehicles.

7.5 Defining Lane Blockage During Primary Incidents

The Accident database was unable to provide information concerning the effect of a primary incident on highway capacity or lane blockages. The Incident database, however, could do so, although data was limited to 623 instances in Tulsa County. Information garnered from the Incident database lacked the comprehensiveness of that in the Accident database. As such, it was necessary to fetch time and location parameters from both databases to identify a total of 42 incidents that were common in both sets.

To establish a correlation between various features specific by ODOT (e.g., number of vehicles involved in an incident, number of highway lanes, number of lanes blocked, and extent of vehicle damage), an association analysis that considered rear-end and side-swipe incidents was used. Table 7-1 was formed using rules provided by association analysis, which were then used with the algorithm to understand the number of lanes potentially blocked in the event of a primary incident.

Table 7-1 Probabilities of Number of Lanes Closed.

No. vehicles	lanes_closed_1	lanes_closed_2	lanes_closed_3	lanes_closed_4
1	0.98	0.02	0	0
2	0.45	0.54	0.01	0
3	0.31	0.49	0.19	0.01
4 or more	0.01	0.6	0.3	0.09

7.6 Understanding Traffic Intensity, Distribution of Traffic Over Time

Traffic intensity refers to the number of vehicles travelling a highway at a given time of day. Traffic intensity is described in Eq. 7-1, and the inter-arrival rate is described in Eq. 7-2. Measuring traffic intensity at different times of the day, as seen in Figure 7-3, aids the algorithm in determining inter-arrival rate limits for vehicles at given times of the day. The effect of traffic intensity on highway capacity indicates that when traffic intensity is high, inter-arrival times decrease. Hence, an accident with merely low damage extent could potentially result in long queue times, effectively increasing the time spent by a vehicle on the highway network system or a vehicle waiting to be serviced. During peak night hours, inter-arrival time for vehicles increases, resulting in shorter queues and reduced waiting times. Results in this study were obtained utilizing data from a project conducted by the Washington State Transportation Center in which an urban area was considered for observing and recording traffic distribution for 24 hours during a weekday.
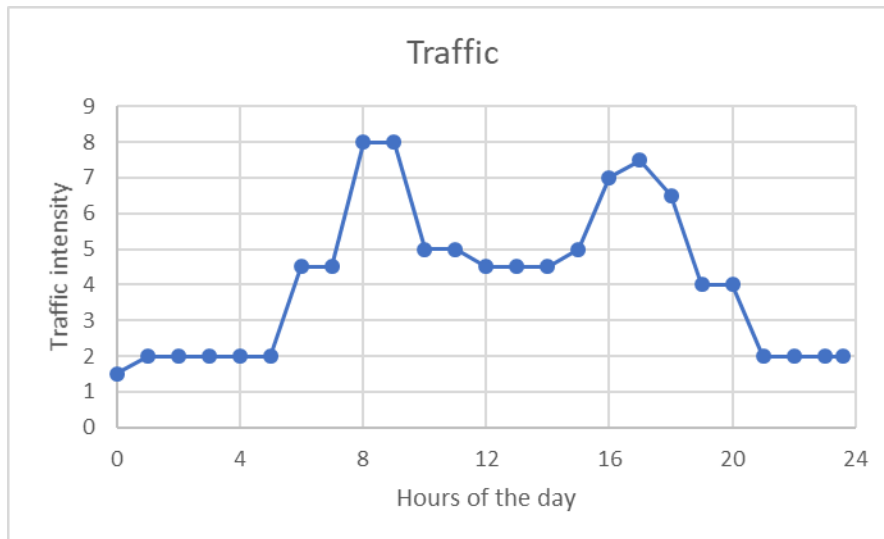
Figure 7-3 Traffic Intensity at Different Times of The Day.

$$Traffic\ per\ hour\ = Average\ traffic\ (24\ hour) * Traffic\ intensity \qquad \text{Eq. 7-1}$$

$$Inter - arrival\ rate = \frac{3600}{Traffic\ per\ hour}\ seconds/car \qquad \text{Eq. 7-2}$$

7.7 Changing-lanes Behavior of Vehicles during an Incident

Figure 7-4 shows vehicle driving patterns during an incident. To simulate this factor in the algorithm, a custom arrival node was created in the CIW library [22] written in Python wherein vehicles are randomly pushed from the affected lane to an adjacent lane, thus effectively keeping traffic in motion. A threshold of a single car was set for research purposes. For example, once an incident and the blocked lane has more than

113

one car in queue, the systems begin to move incoming cars from the blocked lane(s) to lanes still in service.
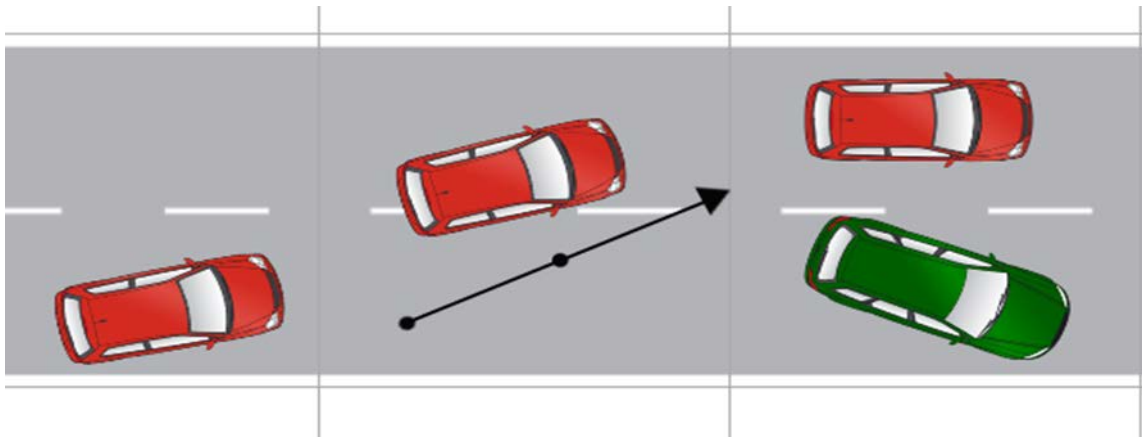
Figure 7-4 Movement of Cars in Case of an Incident.

Pseudocode in Figure 7-5 shows that if an incident occurs in a two-lane highway and lane 1 is blocked, incoming vehicles in lane 1 are directed to move to lane 2 in an effort to keep traffic moving.

```
# lanes = 2 and blocked lanes = 1
class CustomArrivalNode21(ciw.ArrivalNode):
    def send_individual(self, next_node, next_individual):
       self.number_accepted_individuals += 1
       if ((Q.nodes[1].number_of_individuals) <= -1):
          Q.nodes[1].accept(next_individual, self.next_event_date)
       else:
          self.simulation.nodes[2].accept(next_individual,
self.next_event_date)
```

Figure 7-5 Pseudocode for Lane Change Behavior.

The act of lane change can be fed into the algorithm with the aforementioned parameters to define the area of the spatiotemporal boundaries of a primary incident.

7.8 Spatial and Temporal Influence of the Incident

An algorithm was created using the process highlighted in Figure 7-6. The culmination of all factors provides the spatiotemporal influence of the primary incident. In Figure 7-6, incident '300224431' was considered the primary incident. The shaded area represents the spatiotemporal area-of-influence of the primary incident, and other incidents in the shaded area are considered secondary incidents. The primary incident occurring on OK I-44 was a rear-end car crash involving two vehicles, and the extent of damage was graded a 3. The incident resulted in one out-of-service lane for

114

approximately 70 minutes, which caused vehicle service time to increase. A queue build-up increased the time vehicles spent on the highway network.
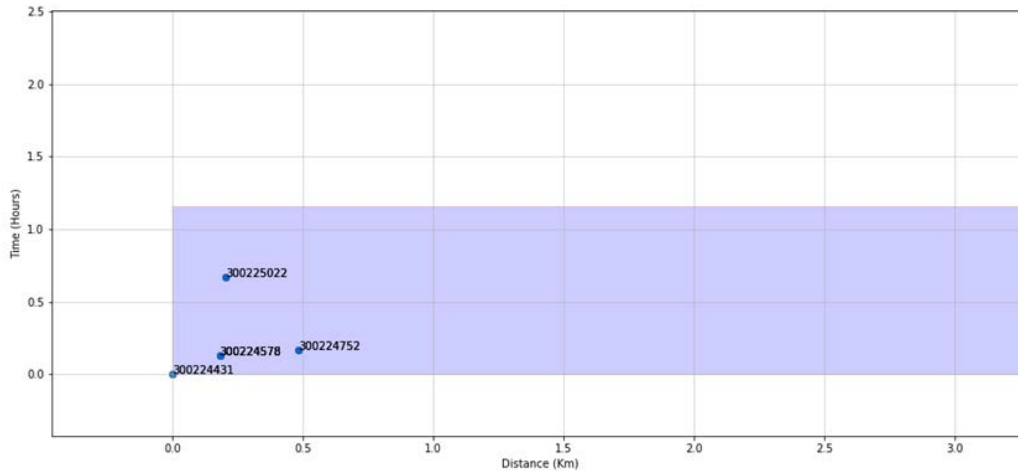
Figure 7-6 Spatiotemporal Influence of a Primary Incident.

7.9 Integrating Google Maps to Detect Direction of Travel and Highway Sections

Although this type of graphical representation provides adequate information about the spatiotemporal effect of an incident, it does not depict the direction of vehicle travel and the affected highway sections. This problem was solved using the Gm-Plot library in Python in conjunction with Google Maps API. Latitude and longitude coordinates contained in the Accident database were utilized for plotting the incident location on a Google Map (See Figure 7-7). Coordinates were calculated up to the fifth decimal place, making them accurate up to 1.1 meter. Using this method for studying the location of incidents provides insight about the highway section affected by the incident, as well as the direction of vehicle flow.
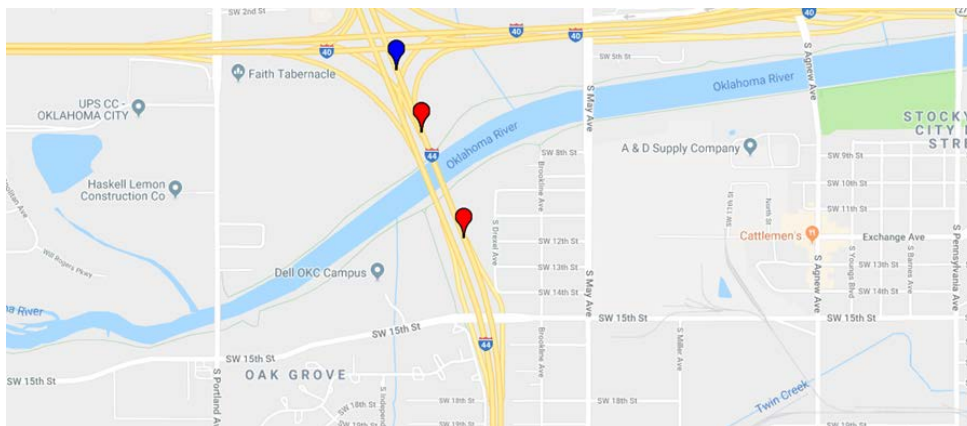
Figure 7-7 Primary and Secondary Incidents Plotted in Google Maps (Primary-Blue, Secondary-Red).

115

7.10 Creating Analytical Models for Prediction of Secondary Incidents

An algorithm was designed using statistical and neural network models for processing incident databases and classifying them as primary or secondary. This type of automated classification aids in assessing a large number of incidents and determining which factors can be used to identify such incidents.

7.10.1 Choosing Features for Analytical and Artificial Neural Network Models

The Accident database provided by the ODOT Traffic Engineering Division was used to create statistical and neural network models. The dataset housed therein was characterized by an array of features related to different aspects of an incident. Figure 7-8 shows the correlation matrix for various features in the dataset. Features selected for analytical and artificial neural network modelling are listed in Table 7-2.

Only two major types of crashes, namely rear-end collisions" and "side-swipe collisions," were considered for statistical and neural network models. After data processing, incident classification based on the factors listed in Table 7-2 became binary. To address this, logit and probit statistical models were selected to provide a starting point for classification and to serve as a benchmark for the ANN modeling.
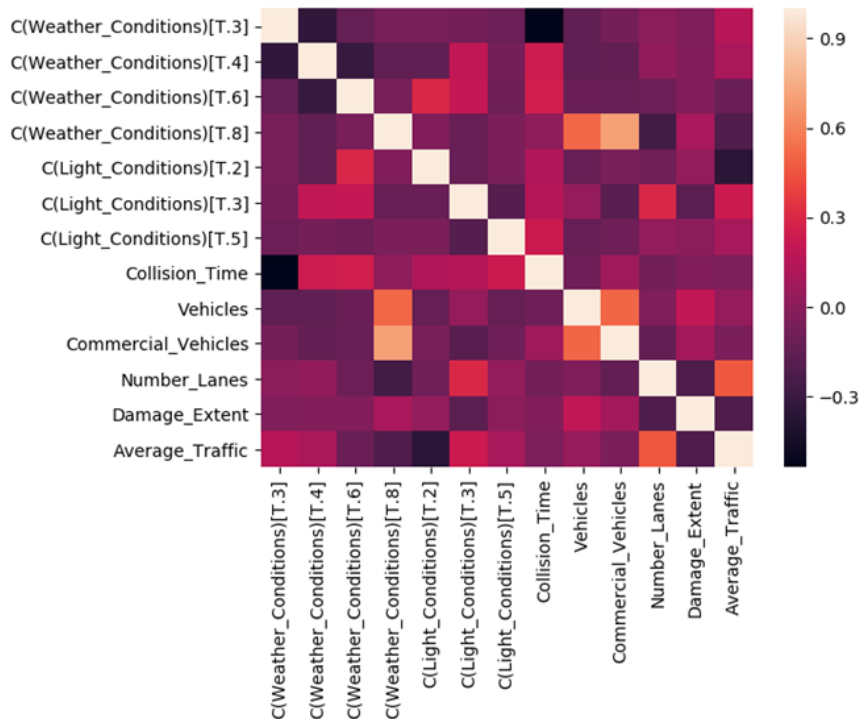
Figure 7-8 Correlation Matrix for Various Features in the Dataset.

Table 7-2 Features Selected for Analytical and Artificial Neural Network Modeling.

Collision Time	Rush Hour Non-rush hour
Number of vehicles involved	The number of vehicles involved in the incident
Commercial vehicles involved	Indicates the presence of commercial vehicles involved in the incident
Number of lanes	Indicates the number of lanes on one side of the highway
Damage extent to the vehicle	01 - None 02 - Minor 03 - Functional 04 - Disabling 09 - Unknown
Average traffic	Indicates the average number of vehicles present on a highway in a day
Weather conditions	01 - Clear 02 - Fog/Smog/Smoke 03 - Cloudy 04 - Rain 05 - Snow 06 - Sleet/Hail (Freezing Rain/Drizzle) 07 - Severe Crosswind 08 - Blowing Snow 09 - Blowing Sand, Soil, Dirt 10 - Other
Light Conditions	01 - Daylight 02 - Dark / Unlighted 03 - Dark / Lighted 04 - Dawn 05 - Dusk 06 - Dark / Unknown Lighting

7.10.2 Creating Logit Model for Secondary Incident Detection

The logit model is a statistical model employing a logistic link function to bound output between 0 and 1. The logistic model was created in Python leveraging the Statsmodels library. Data was divided into training and testing datasets with a split of 70-30, respectively. The model was then trained with the former dataset. Results derived from the logit model are detailed in Table 7-3. The ROC for logit model is shown in Figure 7-9.

Table 7-3 Results and Coefficients from the Logit Model.

	coef	OddsRatio	P>|z|
Intercept	-1.3411	0.1913744	0.322
C(Weather_Conditions)[T.3L]	0.6222	2.111998	0.26
C(Weather_Conditions)[T.4L]	0.9132	3.286169	0.027
C(Weather_Conditions)[T.6L]	1.1729	2.811445	0.044
C(Weather_Conditions)[T.8L]	20.8792	4.35728E+12	1
C(Light_Conditions)[T.2L]	-0.5897	2.995745	0.564
C(Light_Conditions)[T.3L]	0.1713	1.259635	0.631
C(Light_Conditions)[T.5L]	1.9051	15.69422	0.014
Collision_Time	0.0129	1.017518	0.796
Vehicles	0.4181	1.73322	0.017
Commercial_Vehicles	0.7481	1.634679	0.092
Number_Lanes	-0.4668	0.5377444	0.039
Damage_Extent	0.0632	0.9575034	0.697
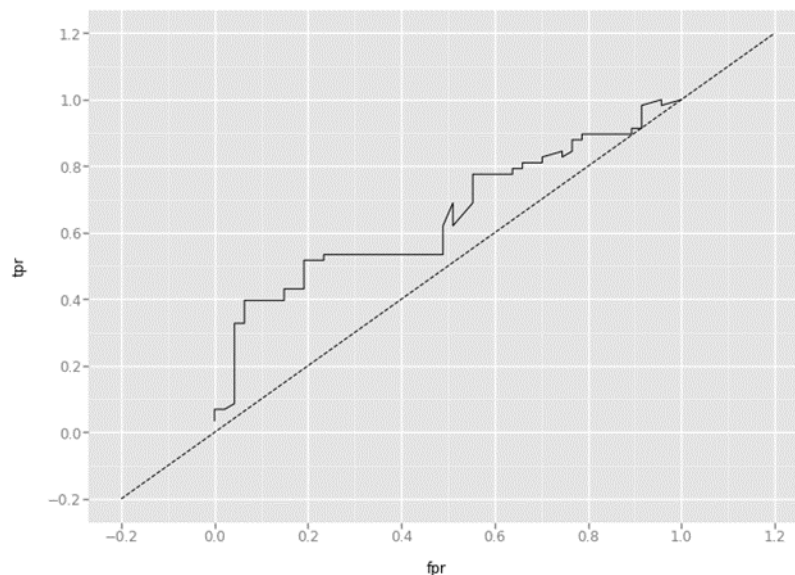
Figure 7-9 ROC for the Logit Model.

118

7.10.3 Creating Probit Model for Secondary Incident Detection

The probit model uses the cumulative distribution of the standard normal distribution to bound output between 0 and 1. Like the logit model, p-values in the probit model provide insight to the uniqueness of the data in the dataset. Table 7-4 shows results obtained after executing the probit model using the training dataset.

Table 7-4 Coefficients and Results from Probit Model.

	coef	OddsRatio	P>|z|
Intercept	-0.7949	0.451621	0.332
C(Weather_Conditions)[T.3L]	0.3369	1.400595	0.31
C(Weather_Conditions)[T.4L]	0.4982	1.645807	0.037
C(Weather_Conditions)[T.6L]	0.6641	1.942813	0.057
C(Weather_Conditions)[T.8L]	7.5359	1.345443	1
C(Light_Conditions)[T.2L]	-0.3857	0.679976	0.529
C(Light_Conditions)[T.3L]	0.1041	1.109763	0.635
C(Light_Conditions)[T.5L]	0.9966	2.709062	0.013
Collision_Time	0.0102	1.010238	0.735
Vehicles	0.2492	1.282982	0.018
Commercial_Vehicles	0.4607	1.58515	0.094
Number_Lanes	-0.2821	0.754233	0.036
Damage_Extent	0.0327	1.033282	0.729
Average_Traffic	4.58E-06	1.000005	0.177

The probit model performed with 66% accuracy and 48% precision. The area under the ROC curve for the probit model, which is shown in Figure 7-10, was less than that of the logit model; this demonstrates a decrease in accuracy. Notably, the probit model performed with similar precision to the logit model.
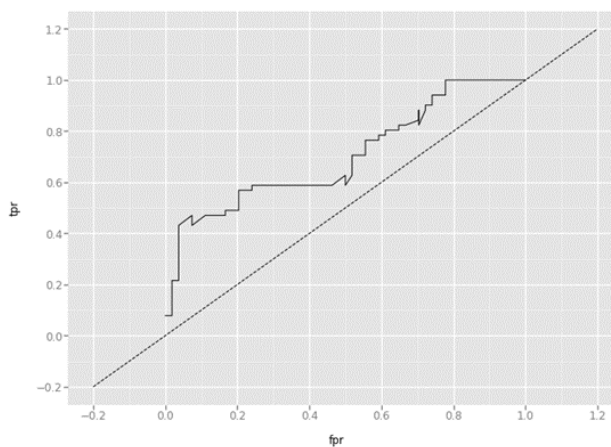
Figure 7-10 ROC for Probit Model.

7.11 Creating Neural Network Models for Secondary Incident Detection

ANNs have proven acceptable for both accuracy and precision in classification solutions and have also been used as classifier for many problems. Figure 7-11 illustrates a simple ANN architecture. In this experiment, the ANN has 13 input nodes, seven hidden nodes, and a single output node. The ANN model uses the same data as the statistical model, with a 70-30 divide between training and testing datasets.
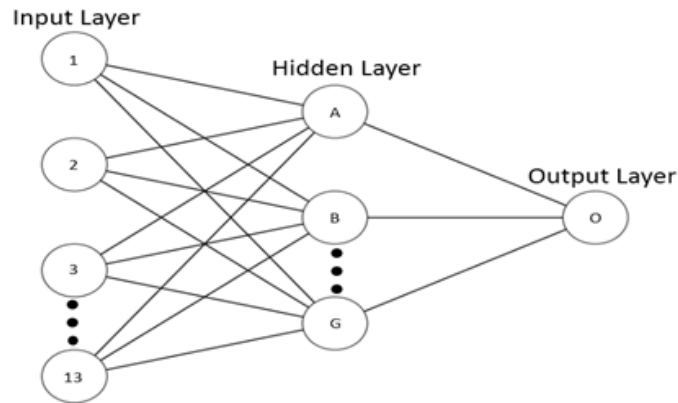
Figure 7-11 Simple Artificial Neural Network.
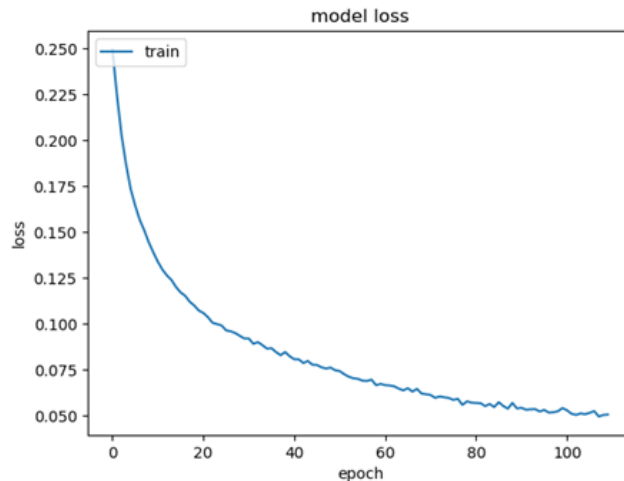
Figure 7-12 Loss vs. Epoch Plot.

Neural network training was performed for 110 epochs. Figure 7-12 shows the loss vs. epoch plot. Accuracy vs. epoch plot, which is shown in Figure 7-13, commences forming a flat tail when training approaches 110 epochs. Figure 7-14 illustrates the point at which training should cease.

An overview of accuracy and precision scores for the various tested models is shown in Table 7-5. ANN clearly outperformed statistical models for both accuracy and precision.
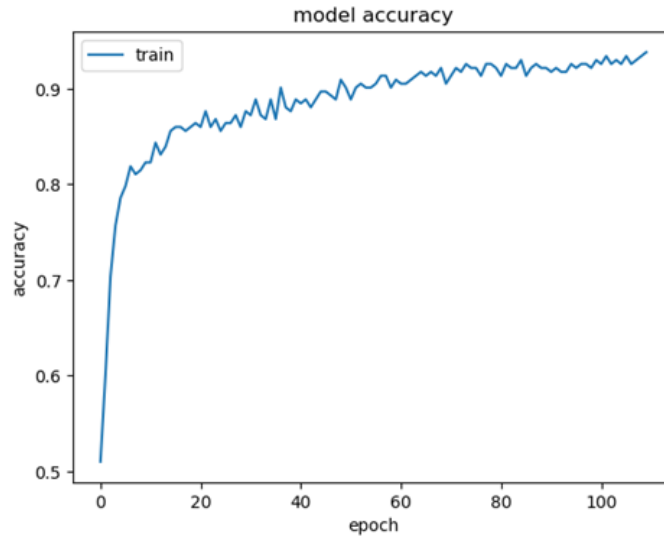
Figure 7-13 Accuracy vs. Epoch Plot.
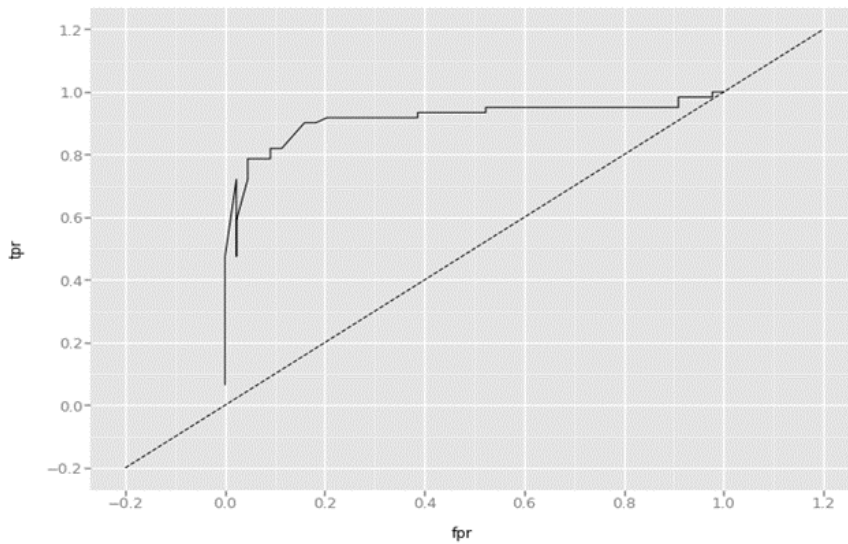
Figure 7-14 ROC for Neural Network.

Table 7-5 Comparative Analysis of Different Models.

	Logit	Probit	ANN
AUC	0.669981188	0.665143779	0.91104182
Precision	0.48	0.48	0.890909091

7.11.1 Determining Feature Importance Using Connection Weight Algorithm

The connection weight algorithm is the preferred method for accessing variable importance in simple feed-forward neural networks. Characteristics of such neural networks can be described as having an input layer and a hidden layer, as well as being fully connected and trained when using the back-propagation algorithm. For this research, the said method was used to gauge feature importance. The effect of variable influence on secondary incident classification was calculated and can be seen in Figure 7-15. Legends for weather and light conditions are shown in Table 7-6 and Table 7-7, respectively. Results from executing the connection weight algorithm demonstrated that features like collision time, number of vehicles, and presence of commercial vehicles heavily contributed to the model for accurately detecting secondary incidents. Similarly, weather related conditions (e.g., normal or light fog) did not affect the system as much as snow or icy conditions.
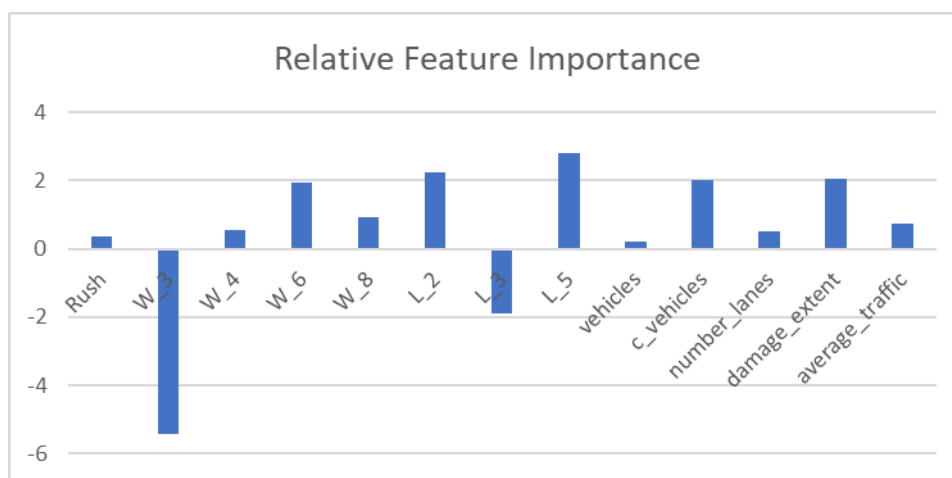
Figure 7-15 Independent Variable Influence for Secondary Incident Detection.

Table 7-6 Legend for Weather Conditions.

W_1	Clear
W_2	Fog/Smog
W_3	Cloudy
W_4	Rainy
W_5	Snow
W_6	Sleet/Hail
W_7	Severe Crosswind
W_8	Blowing Snow

Table 7-7 Legend for Light Conditions.

L_1	Daylight
L_2	Dark-Not Lighted
L_3	Dark-Lighted
L_4	Dawn
L_5	Dusk

7.12   Identification using Bayesian Probability

Various non-recurrent conditions characterize the manner in which vehicle speed is affected on road segments and routes. These conditions correspond to a variety of characteristic models, the impact of which is clearly visible and identifiable on the baseline distribution. Thus, distinguishable statistical models can be used to reveal assorted information for each condition. By combining distribution models with Bayesian probability, an approach can be determined for identifying the underlining condition occurring in both offline and real-time speed analysis. The work reported herein proposes a Bayesian engine for congestion identification. The engine utilizes statistical models derived from observed data records per condition, and then estimates a posterior credibility for each hypothesis. The model was developed to identify three situations: incident (e.g., cash and collision), weather (e.g., snow) and free-flow traffic. Histogram distributions of speeds are used to create distribution density models from TT data.
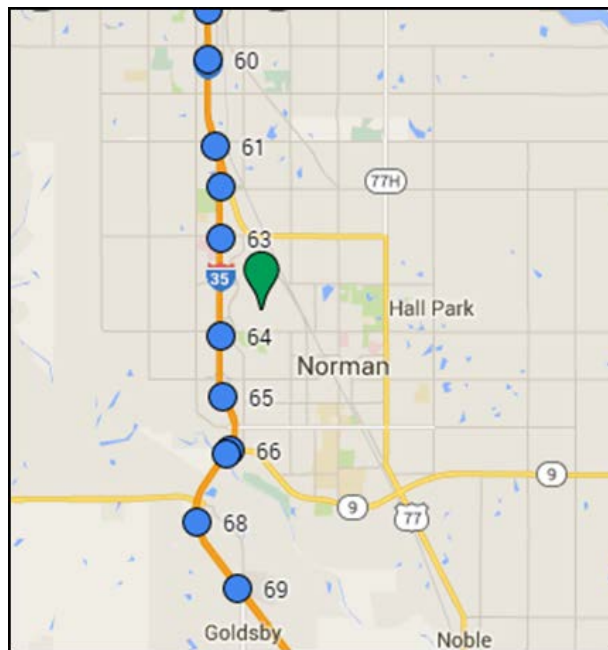
Figure 7-16 Segment 64 on I-35.

7.12.1 Implementation of Bayesian Congestion Identification

Models pertaining to the three distinct conditions mentioned above, namely incident, weather, and free-flow, were constructed. Using NPMRDS, a particular segment on OK I-35 was chosen to derive distribution models. This information was subsequently used to evaluate the proposed Bayesian identification approach on additional segments for three non-recurrent conditions events. TMC 64 west of Norman on OK I-35 (See Figure 7-16) is located proximate to a dedicated weather sensor known to gather accurate historical weather data. A historic incident (crash) event occurred on TMC 64 on March 13, 2015. On that same segment, a snow fall event had occurred on March 4. Free-flow traffic was observed on March 2. Figure 7-17 illustrates the monthly epoch plot for TMC 64 during March 2015.
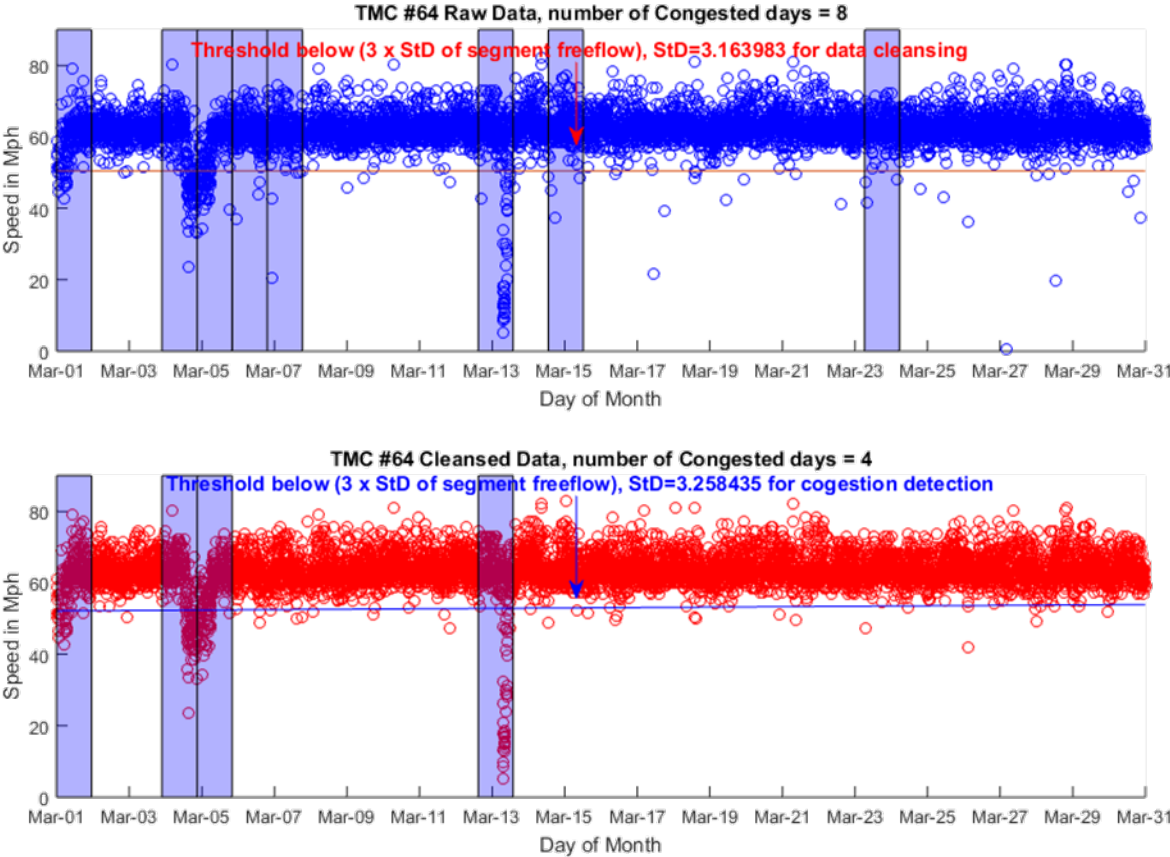
Figure 7-17 Epoch Speed Plot for TMC 64 During the Month of March 2015.

Snow travel and free-flow travel cases were characterized by mean and SD according to a Gaussian distribution model. Incident case modeling was performed using a non-parametric Kernel density estimate to generate probability density function (PDF). This work adopts a probability approach for analysis similar to [25] and [26], which used a generated PDF to asses vehicle class distribution on the road. The

124

formula for the model is given by a smoothing spline, 3rd degree piecewise polynomial. The resulting formula has 70 parameter coefficients. Figure 7-18 illustrates probability for the three cases overlaying the model. High overlap is shown when the value of free-flow mean speed is near the speed limit. Although fitting of snow showed less goodness-of-fit than normal free-flow traffic relative to normal distribution, Bayesian inference results exhibited robustness in decision making and correct case identification, as evident in subsequent results. Results are indicative of the suitability of Bayesian inference for solving problems when accurate, closed-form models are not possible. Figure 7-19 depicts a probability plot showing various probability values for each model relative to various speed measurements on the highway. Three distinct regions are visible. Lower speeds of 0 to 30 mph result in higher probability of incident occurrence. As speeds increase to between 30 and 60 mph, the snow model tends to dominate with overall higher probability values. For travel near the speed-limit, the free-flow model dominates probability values in spite of overlap among distribution models in this region.
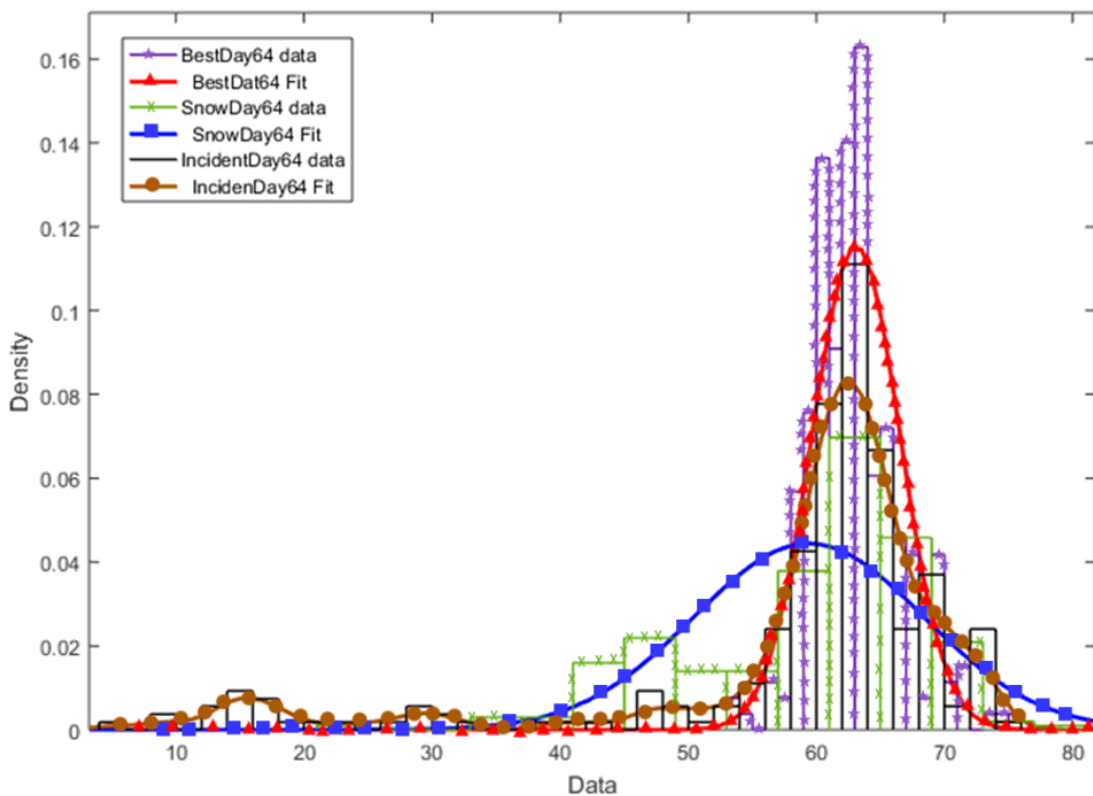
Figure 7-18 Model Fitting for Free-Flow, Snow, and Incident Conditions.
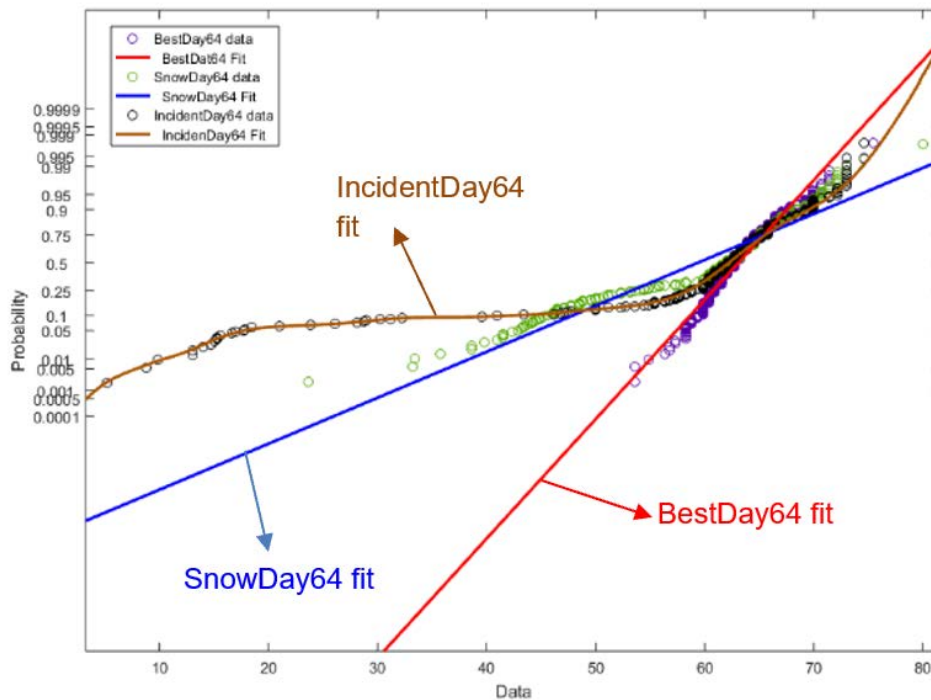
Figure 7-19 Probability for The Three Distribution Models.

7.12.2 Bayesian Updating

Implementing Bayes theorem in a time series input requires updating the posterior. Each of the aforementioned cases occurred over individual time intervals. Snow, for instance, accumulates with time, and the effect on roadways becomes apparent after several hours of continuous snowfall. By contrast, effects of a road incident occur almost instantaneously. Thus, one can intuitively suggest that updating probabilities is related to the duration of the event and the time required for its effects to manifest. As a result, posterior probability was averaged over the course of an hour and a half for incident data and over five hours for the snow event. Free-flow update time was chosen to match the shortest length of time for all cases. Values were chosen based on the duration each event modeled for one day. Prior update time remains an optimization research problem that requires a larger sample size for investigation. Notably, there is a tradeoff between the system's ability to instantly detect an event (i.e., response time) and the stability and accuracy of the system. Decreasing update time results in near instantaneous updating, which causes fast inference decisions. False detection is expected to occur when small values are used, particularly in cases where speed measurements caused by outliers and anomalies are present in the data, or for cases in which there is a high variance between consecutive data samples. On the other hand, increasing update time could result in the system's inability to detect extremely short incident occurrences for durations of 15 or fewer minutes. After taking into account these details, the Bayesian inference engine was coded using Matlab. Inputs of actual

126

speed measurements from NPRMDS—which simulated real-time measurements—were input into the system. System output was a prediction of the type of condition (i.e., event) serving as the source of the input speed measurements given. Results per event are offered below.

7.12.3 Example: Incident

Figure 87 shows a snap shot of the Bayesian inference engine GUI final output after a day of monitoring. The top subplot illustrates speed records arriving in real time. The bottom subplot illustrates the probability of the Bayesian engine pertaining to each of the three defined states: incident, weather (in this case, snow), and free-flow. The right subplot illustrates system output. For this implementation, a threshold of 40% confidence was required for decision-making. The threshold is flexible and can be modified as needed. Figure 7-20 indicates incident detection between 4:23 and 5:20 p.m.
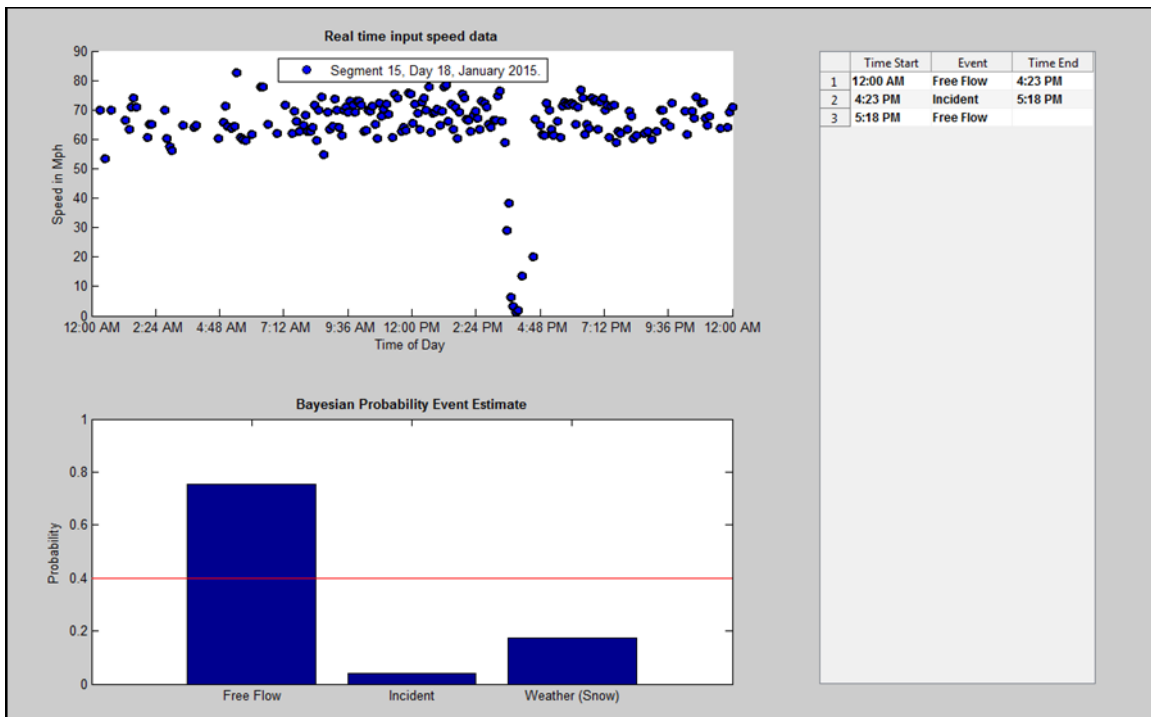
Figure 7-20 Incident Detection Occurring on OK I-35 on 18 January 2015.

8. CONCLUSION

8.1 Research Outcomes

The current ODOT implementation of the Real-Time System Management Information Program (RTSMIP) was analyzed. The research team studied the system's reliability and responsiveness, and then evaluated the system's tolerance to hardware failures. Next, 10 Bluetooth identification devices for monitoring TT were deployed, which have proven accurate given a moderate (7-10%) penetration of Bluetooth-equipped vehicles. Deployed Bluetooth systems were used to evaluate ODOT TT accuracy. System responsiveness, accuracy, and availability were reevaluated for additional TT measurements following Bluetooth identification device installation.

The algorithms for collecting traffic information from various ODOT platforms were developed, and then the data was normalized across time and space for evaluation. Also, the models and algorithms for identifying TT anomalies were developed. The TT anomalies are related to traffic- or weather-related factors, including incidents, work zones, demand fluctuation, special event traffic signals, and weather/road conditions. Furthermore, the models and algorithms for identifying TT errors caused by sensor malfunction or failure were developed.

This fiscal year, the project recorded two significant successful technology transfers: 1) an inexpensive (i.e., $500 versus $5,000 for commercial systems) portable Bluetooth monitoring system that when integrated with the current ODOT network will immediately impact ODOT traffic management programs, and 2) a novel design for developing a TTR and monitoring system composed of multi-sensing technology that leverages empirically developed models for providing accurate information about traffic flow and congestion. This technology is currently prototype to product.

8.2 Future Work Plan

The research team plans the following work during the coming year:

- Continue to field test the developed Bluetooth station for determining: 1) acceptable separation distance between deployment sites while maintaining accurate measurements; and 2) total number and site locations for achieving a comprehensive and accurate overview of traffic flow in a given region.
- Continue to study current ODOT system reliability, responsiveness, and robustness. The research team will analyze and adequately characterize each TT data source (currently, via radar and HERE.COM), including data structure format; TT collection method and calculations; TT spatial resolution per method; and TT temporal resolution per method currently available for ODOT TT system implementation. This objective is critical for data processing, analysis, and fusion.

- Build upon insights obtained from the previous years' objective with an aim to develop algorithms for collecting traffic information from various ODOT platforms and to homogenize data across temporal and spatial domains. Preparing datasets for analyses requires that algorithms perform data conditioning, including detection and removal of TT anomalies, imputation, and interpolation for missing data due to either hardware failure or lack of TT measurements. The research team will construct clean TT datasets for modeling and predicting TT reliability.
- Continue to refine the developed statistical distribution models and prediction models to gain an understanding of the effects of congestion-causing factors, such as traffic incidents and adverse weather conditions on TT measurements. Both an offline and an online (i.e., real-time) computation engine will be developed to utilize historical statistical models representing various operation conditions for predicting and enhancing TT reliability in real time. The team will also incorporate TT measurements obtained at Bluetooth stations currently integrated by ODOT systems for improving overall system responsiveness, accuracy, and availability. Various statistical evaluation metrics will be used to represent system accuracy, including Mean Absolut Error (MAE) as an indicator of expected error from an average reading; Mean Absolute Percent Error (MAPE) as an indicator of a systematic bias to the error such that TT values are consistently high or low; and Root Mean Squared Error (RMSE) as an indicator of mean deviation of TT readings. Divergence between TT probability distributions can be found using Kullback–Leibler Divergence (KLD) measure. Chi-squared and null-hypothesis testing methods will also be used to examine significant differences with respect to performance measures. Statistical metrics will be calculated for each segment at different levels of temporal resolutions, including predefined system, 10-minute response mandated by FHWA Section 1201 [27].

REFERENCES

[1] Texas Transportation Institute. *Travel Time Data Collection Handbook*, Report FHWA-PL-98-035. Federal Highway Administration, Washington, D.C., 1998.

[2] Turner, S. M. "Advanced techniques for travel time data collection," TRR 1551,Transportation Research Board of the National Academies, Washington, D.C., pp. 51-58, 1996.

[3] N. Bitar, "Big Data Analytics in Transportation Networks Using the NPMRDS", The University of Oklahoma, MSc. Thesis, 2016.

[4] Transportation Research Board of the National Academies. *Highway Capacity Manual 2010*. Washington, D.C., 2010.

[5] Shi, Q., and M. Abdel-Aty. "Evaluation of the Impact of Travel Time Reliability on Urban Expressway Traffic Safety," TRR 2582, Transportation Research Board of the National Academies, Washington, D.C., pp. 8-17, 2016.

[6] Lida Y.: Basic Concepts Future Directions of Road Network Reliability Analysis. Journal of Advanced Transportation. 1999, 33(2), pp.125-134 [7] "Truck Safety – Advocates for Highway and Auto Safety." [Online]. Available: http://saferoads.org/issues/truck-safety/. [Accessed: 10-Jan-2016].

[7] Sisiopiku, V. P. and Md Saidul Islam. "A Freeway Travel Time Reliability Study," *International Journal of Engineering Research and Development*, Vol. 3, No. 10, PP. 83-101, 2012.

[8] Elefteriadou, L. "A framework for defining and estimating travel time reliability," 85th Annual Transportation Research Board Annual Meeting, Washington, D.C., 2006.

[9] Texas Transportation Institute. *Possible Reliability Measures*. Texas A&M University System, 2000.

[10] Lomax, T., et al. Quantifying Congestion - Volume 1: Final Report, NCHRP Report 398, Transportation Research Board of the National Academies, Washington, D.C., 1997.

[11] Cambridge Systematics, Inc. Multimodal Corridor and Capacity Analysis Manual, NCHRP Report 399, Transportation Research Board of the National Academies, Washington, D.C.,1998

[12] AASHTO, "Transportation Invest in America, the Bottom Line", American Association of State Highway and Transportation Officials, Washington, D.C., 2000.

[13] TranSystems, Executive Summary, Full-Scale EMT Demonstration, TranSystems Corporation, 2005.

[14] Cambridge Systematics, Inc., Texas A&M Transportation Institute, University of Washington, Dowling Associates, Street Smarts, H. Levinson, and H. Rakha. *Analytical Procedures for Determining the Impacts of Reliability Mitigation Strategies.* SHRP-2 Report S2-L03-RR-1, Transportation Research Board of the National Academies, Washington, D.C., 2013.

[15]   Cambridge Systematics, Inc., and Texas Transportation Institute. *Traffic Congestion and Reliability: Trends and Advanced Strategies for Congestion Mitigation.* Federal Highway Administration, U.S. Department of Transportation, Washington, D.C., 2005.

[16]   Texas Transportation Institute and Cambridge Systematics, Inc. Travel Time Reliability: Making It There on Time, All the Time. Federal Highway Administration, U.S. Department of Transportation, Washington, D.C., 2006.

[17]   Lomax, T., D. Schrank, S. Turner, and R. Margiotta. *Selecting Travel Reliability Measures.* Texas Transportation Institute, Texas A&M University System, Arlington, 2003.

[18]   Margiotta,R., D. McLeod, T. Scorsone, and R. Dowling. *Travel Time Reliability as a Service Measure for Urban Freeways In Florida*, Cambridge Systematics, Florida Department of Transportation and Kittelson Associates, 2013.

[19]   Florida DOT. *The Florida Reliability Method in Florida's Mobility Performance Measures Program.* 2000.

[20]   List, George F., et al., *Guide to Establishing Monitoring Programs for Travel Time Reliability.* SHRP-2 Report S2-L03-RR-2, Transportation Research Board of the National Academies, Washington, D.C., 2014.

[21]   https://github.com/greatscottgadgets/ubertooth/https://github.com/greatscottgadgets/ubertooth/ -

[22]   https://en.wikipedia.org/wiki/WebSocket

[23]   HH Refai, N. Bitar and MS Kaleia, "National Performance Management Research Dataset (NPMRDS) - Speed Validation for Traffic Performance Measures", FHWA-OK-17-02, 2016.

[24]   National Surface Transportation Infrastructure Financing Commission. *Paying Our Way: A New Framework for Transportation Finance.* Washington, D.C., 2009.

[25]   N. Bitar and H. H. Refai, "A Probabilistic Approach to Improve the Accuracy of Axle-Based Automatic Vehicle Classifiers," in IEEE Transactions on Intelligent Transportation Systems, vol. 18, no. 3, pp. 537-544, 2016.

[26]   H. Refai, N. Bitar, J. Schettler, , O. Al Kalaa, The Study of Vehicle Classification Equipment with Solutions to Improve Accuracy in Oklahoma FHWA-OK-14-17, 2014.

[27]   "Safe, Accountable, Flexible, Efficient Transportation Equity Act: A Legacy for Users." FHWA

[28]   Islam M. S. *Travel Time Reliability under Varying Freeway Operating Conditions*, M.S. Thesis, University of Alabama at Birmingham, 2012.

[29]   Kittelson & Associates, Inc. *Evaluating Alternative Operations Strategies to Improve Travel Time Reliability.* SHRP-2 Report S2-11-RR-1, Transportation Research Board of the National Academies, Washington, D.C., 2013

[30]   Kittelson and Associates, Cambridge Systematics, Inc., ITRE, and Texas A&M Research Foundation. *Incorporation of Travel Time Reliability into the*

HCM. SHRP-2 L08, Transportation Research Board of the National Academies, Washington, D.C., 2013.

[31]   Hirschman, I., et al. *Methodology for Estimating the Value of Travel Time Reliability for Truck Freight System Users.* NCHRP Report 824, Transportation Research Board of the National Academies, Washington, D.C., 2016

[32]   Woodard, D., et al. "Predicting Travel Time Reliability using Mobile Phone GPS Data," *Transportation Research Part C: Emerging Technologies*, Vol. 75, pages 30–44, Elsevier Ltd, February 2017.

[33]   Rakha, H., I. El-Shawarby, M. Arafeh, and F. Dion. "Estimating Path Travel-Time Reliability," 2006 Proceedings of the IEEE Intelligent Transportation Systems Conference, Toronto, Canada, pp. 236-241, 2006.

[34]   Margiotta, R., D. McLeod, T. Scorsone, and R. Dowling. *Travel Time Reliability as a Service Measure for Urban Freeways in Florida*, Cambridge Systematics and Kittelson Associates, 2013.

[35]   Haghani, A., Y. Zhang, and M. Hamedi. *Impact of Data Source on Travel Time Reliability Assessment*, Final Report, Department of Civil & Environmental Engineering, University of Maryland, Grant DTRT12-G-UTC03, Mid-Atlantic Universities Transportation Center, 2014.

[36]   Martchouk, M., F. L. Mannering, and L. Singh. *Travel Time Reliability in Indiana, School of Civil Engineering*, Purdue University, p. 87, 2010.

[37]   Tu, H., H. V. Lint, and H. Zuylen. "The Impact of Adverse Weather on Travel Time Variability of Freeway Corridor," 80th Annual Meeting of the Transportation Research Board, Washington D.C., 2007.

[38]   Cambridge Systematics, Inc., Texas A&M Transportation Institute, University of Washington, Dowling Associates, Street Smarts, Herb Levinson and Hesham Rakha. *Analytical Procedures for Determining the Impacts of Reliability Mitigation Strategies*. SHRP-2, Report S2-L03-RR-1, Transportation Research Board of the National Academies, Washington, D.C., 2013.

APPENDIX A: NOTABLE STUDIES OF TRAVEL TIME RELIABILITY

A.1 Evaluation of the Impact of Travel Time Reliability on Urban Expressway Traffic Safety [5]

The objective of this study was to examine whether travel time reliability has an impact on crash frequency on urban expressways. A 20-mi segment of urban expressway SR-408 located in Orlando, in central Florida, was used for the purpose of this study.

Multiple travel time reliability indicators derived from the AVI system on the studied expressway were developed. Percentage of variation, buffer index, and misery index were three major reliability metrics used in the evaluation; the latter two emphasize the late arrivals, while the first indicator gives equal weight to early and late arrivals. Bayesian hierarchical Poisson lognormal models were applied to calibrate the effects of these indicators. To test the necessity of having a reliability indicator, models with only traffic flow parameters and with a latent reliability variable from structural equation models (SEM) were constructed. The majority of t crashes on SR-408 expressway were multivehicle crashes, implying potential differences in crash mechanisms compared with single-vehicle crashes. Therefore, the performances of the multiple reliability indicators were evaluated for total crashes, multivehicle crashes, and single-vehicle crashes.

By comparing the performances of percentage of variation, buffer index, and misery index, both buffer index and misery index proved to have significant effects on total and multivehicle crashes, while percentage of variation could not reflect this effect. This difference between the performances of the three variables suggested that to understand the effects of travel time reliability, early and late arrivals should be differentiated. Reliability issues caused by late arrivals would pose higher risks for motorists.

Both the buffer index and misery index indicated that on urban expressways, lower travel time reliability would cause more multivehicle crashes than would single-vehicle crashes. Multivehicle crashes, especially rear-end and sideswipe crashes, often result from inappropriate lane changing and speed difference between leading and following vehicles. As a result, improving travel time reliability could efficiently reduce unexpected driving behaviors and risky interactions between vehicles, thus achieving more consistent traffic flow and safer roadway environment.

Previous crash frequency models might deduce the effects of travel time reliability according to speed variation (standard deviation of speed and coefficient of variation of

speed). To assess the potential benefits that a direct travel time reliability indicator brings in safety analysis, the models with buffer index and misery index were compared with models with traditional traffic flow parameters and with latent reliability variable built on the SEM. It was also confirmed that to interpret the effects of reliability, direct travel time reliability indicators should be used, instead of speed variation or latent reliability variables.

For traffic agencies, the current study suggests that better travel time reliability would not only improve motorists' experience on their system, but would also have a positive influence on traffic safety, especially on collisions between vehicles. Reduction in reliability caused by delayed trips is worth extra attention from operators, and such a conclusion indirectly encourages efforts to reduce congestion. At present, many toll and turnpike agencies provide travelers with real-time travel time estimation and congestion warning by using dynamic message signs. These signs are beneficial as a way to make road users prepared for current traffic conditions and adjust their driving accordingly. With more consistent traffic flow, better traffic systems pertaining to safety, reliability, and efficiency will eventually be achieved.

A.2 Travel Time Reliability under Varying Freeway Operating Conditions [28]

The objective of this thesis is was to identify measures and methods to evaluate travel time reliability; and apply those methods to study the reliability of travel time along the I-65 corridor in the State of Alabama. The main objectives of this study were:

a) Calculate reliability metrics including standard deviation, % variability, buffer time, buffer time index, travel time index, and planning time index using travel time data collected from INRIX for a study corridor in Alabama;

b) Investigate effect of traffic accidents on travel time reliability, and

c) Compare the field planning time index (PTI) with PTI values calculated using model proposed by SHRP-2 L03 project.

The data used in this study were collected in 2010 using geographic position systems (GPS) technology in freight vehicles and INRIX, a leading provider of traffic information conducted data processing. Traffic incident data were provided by the Alabama Service and Assistance Patrol (ASAP) and were used to analyze the effect of traffic accidents on travel time reliability

The author investigated the travel time reliability of the I-65 corridor by analyzing the variation of reliability indices (planning index and travel time index) by link as well as along the entire corridor as well as four sub-corridors. The effect of accidents on travel time reliability was also investigated by examining the variations in planning time index with and without the events.

Study findings indicate that travel time reliability is closely associated to traffic demand/congestion.

A noticeable increase in PTI values was observed under incident conditions ranging from 14% to over 170%.

A.3 Guide to Establishing Monitoring Programs for Travel Time Reliability [20]

This Guide documents the process of how to develop and use a travel time reliability monitoring system (TTRMS). The information included in the Guide should be useful for system operators in determining what actions they need to take to reduce the variability of travel time and enhance reliability. A companion to the Guide is a brief, stand-alone document "*Handbook for Communicating Travel Time Reliability Through Graphics and Tables*" that provides suggestions for communicating information about time travel reliability.

A TTRMS can help operating agencies monitor system performance, understand the impacts of the various factors that influence travel time, and provide useful information to system users about what travel time reliability to expect. With this information, operating agencies can make better decisions about what actions to take to help improve reliability.

The Guide has two parts. Chapters 1 through 5 describe the process of measuring, characterizing, identifying, and understanding the effects of recurrent congestion and non-recurrent events that affect travel time reliability. The appendices provide more detailed information about the functional specification of a monitoring system, methods, a series of case studies, and a set of use cases that describe how different users of the TTRMS interact with the system.

The Guide describes four key information flow steps that a TTRMS must execute to fulfill its purpose as a decision support tool:

1. Measure segment and route travel times. The Guide includes good discussion on how to measure travel times using available technologies and statistical techniques.

2. Characterize the reliability of a given system. This process entails taking a set of measured travel times and assembling them into probability density functions and cumulative density functions (CDFs) to characterize the performance of a given segment or route, usually specific to a particular operating regime (a combination of congestion level and nonrecurring event).

3. Identify the sources of unreliability and how to improve reliability. The guide follows the causal list used by the Federal Highway Administration (FHWA) to describe why congestion arises: traffic incidents, work zones, demand fluctuations, special events, traffic control devices, weather, and inadequate base capacity. It addresses how to pull in data for these sources and effectively fuse them with travel time data. Identifying the travel times affected by these sources of congestion is required preparation for understanding system reliability.

4. Help operators understand the impact of these sources of unreliability on the system. This step involves both quantitative and qualitative methodologies to transform raw data into actionable decisions.

The process described above is designed to be integrated within an existing traffic management system with a structure like that depicted in Figure A-1. The figure shows the three major modules of a TTRMS: a data manager, a computation engine, and a report generator. The data manager assembles incoming data from traffic sensors and other systems, such as weather data and incident data, and places them in a database that is ready for analysis as "cleaned data." The computation engine works with the cleaned data to prepare indications of the system's reliability (travel time PDFs organized by regimes). Regimes consist of the congestion level and the type of nonrecurring event (including none), such as high congestion and an incident or low congestion and work zone activity. The report generator uses the computation engine to analyze the data and respond to inquiries from system managers or travelers.
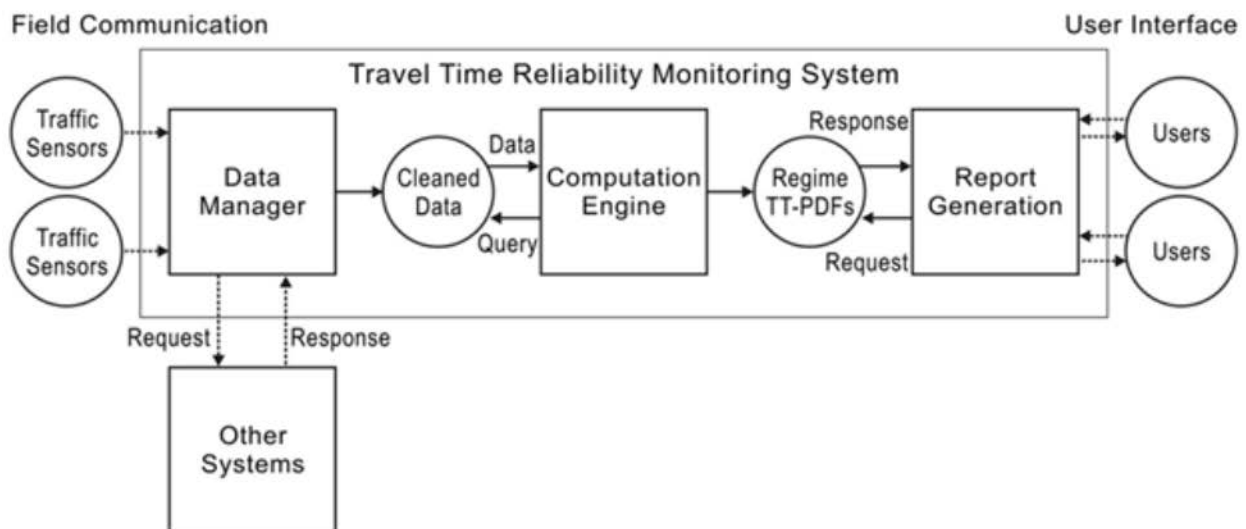
Figure A-1 TTRMS Overview with Boxes for Modules and Circles for Inputs and Outputs [20].

A.4 Evaluating Alternative Operations Strategies to Improve Travel Time

Reliability [29]

The objective of this SHRP-2 project was to identify and evaluate strategies and tactics to improve the travel time reliability of users of the roadway network—travelers and freight shippers in urban and rural areas. The report presents two categories of actions that can be used to respond to the seven sources of congestion: fluctuations in travel demand, special events that cause abnormal levels of demand, bottlenecks, incidents, weather conditions, work zones, and traffic controls.

The first category addresses the demand for travel and includes the use of travel information to influence when, where, how, and how much travel (both personal travel and freight movement) occurs. This category includes the application of pricing mechanisms to influence travel behavior as well as to generate the funds needed for operating, maintaining, and improving the transportation system.

The second category includes actions to increase roadway capacity, such as the following:

- Expansions of highway facilities;

- Application of better operational and technical systems to maximize the performance of existing infrastructure;

- Advances in technology and procedures that more quickly restore capacity following disruptions (incidents, weather conditions, work zones); and

- Optimal use of existing transportation system capacity controlled by other transportation agencies, firms, or individuals. (This can be accomplished by providing incentives for mode shifts from single-occupant vehicles to multi-occupant vehicles and more effective use of alternative rights-of-way.)

Table A-1, Table A-2 and Table A-3 summarize the actions for reliable transportation of persons and freight.   The types of solutions that can address demand and capacity imbalances depend on whether congestion can be anticipated or whether it results from unexpected events.   In the case of recurring congestion, demand management and capacity increases are likely to be effective in improving reliability. In cases in which unexpected disruptions cause the bulk of congestion, techniques that detect disruptions and facilitate rapid recovery from those events are more likely to be effective.

The report presents forecasts of the year 2030 under alternative assumptions that may influence travel time reliability. In addition, the report discusses options related to

technological changes, operational solutions, and organizational actions that have the potential to improve travel time reliability both now and in the future (by the year 2030).

Table A-1 Actions and Consequences of Unreliability for Passenger Travelers [29].

Trip Purpose	Importance of Reliability	Actions to Deal with Unreliability	Consequences of Unreliability
Appointments (e.g., medical, personal services)	High	Schedule appointments in off-peak periods. Allow more time for travel, especially for peak-period appointments and longer-distance trips. Organize day around appointment (medical). Change routes if experienced travel time is high.	Missed appointment and possible missed or late fee. Wait for next available opening; this affects travel for rest of day. Several days elapse before next appointment. Pressure on the travelers.
Pick up and drop off children	High	Allow more time than ideal for the trip. Ask someone else to escort child. May affect residential location and school choices.	Child may miss a class. Anxiety over keeping child waiting. School or day care may charge fee for late pick-up or even call police if lateness is consistent.
Leisure (e.g., movies, sports events)	Medium–low	Schedule during off-peak periods.	Experiencing stress for a trip meant for leisure. Missed event (for one-time events such as sports). Forfeit of money paid for tickets. More difficulty in finding parking.
Leisure (e.g., visit friends)	Low	Call and reschedule or meet somewhere else. Shorten planned visit to meet the start time for next scheduled event.	Guilt for wasting someone else's time.
Shopping	Low	None (especially if unplanned or short trip). Choose off-peak times. Abandon trip or go to a different store. Shorten shopping time and possibly limit number of items shopped for.	None (as long as groceries are not immediately needed). Affects the subsequent trips planned for the day. May miss the sale.
Return home	High–medium	Stop and take a break. Problematic as one may not be able to leave earlier to allow for unreliability in return-home trip. Choose travel time for trip *to* activity so that travel *from* the activity to home is reliable.	Fatigue and stress (especially if kids are traveling). Children at home needing attention. Pets at home needing attention. Ice cream bought at the grocery store can melt!
Work	High	Allow more time than ideal for travel (especially if work schedule is fixed). Prepare for day in advance and wake early. Affects the residential-location choice.	Loss in pay and other types of penalties. Poor reflection. A particular cause of concern in current economy.

Table A-2 Classification of Freight Movers by Characteristics [29].

Group	Level of Schedule Flexibility	Level of Operational Adaptability	Cost of Variability	Example Company
1	Flexible	Complete	High	Refrigerated carrier; carrier that operates in a very congested arterial network (e.g., grocery store deliveries by large company)
2	Flexible	None	High	Carrier that pays drivers by the hour
3	Inflexible	Complete	High	Carrier that must meet tight time windows for delivery (e.g., delivery companies such as FedEx, or residential moving company)
4	Inflexible	None	High	Carrier that moves air freight or fresh seafood and must deliver within tight time window
5	Flexible	Complete	Low	Carrier that moves natural resources
6	Flexible	None	Low	Carrier that has no delivery time windows
7	Inflexible	Complete	Low	Oversize or overweight specialty movers
8	Inflexible	None	Low	Drayage trucking company

Table A-3 Actions of Unreliability for Freight Movers [29].

Group	Level of Schedule Flexibility	Level of Operational Adaptability	Cost of Variability	Suggestions for Action
1	Flexible	Complete	Large	Move to times and routes when reliable travel is available; widen time windows.
2	Flexible	None	Large	Move to times and routes when reliable travel is available; widen time windows.
3	Inflexible	Complete	Large	Spread particularly congested deliveries across vehicles so that deliveries do not compound throughout the day.
4	Inflexible	None	Large	Increase price for services (because carrier has limited choices).
5	Flexible	Complete	Low	Undertake only cost-effective changes (because cost of variability is low).
6	Flexible	None	Low	Undertake only cost-effective changes (because cost of variability is low).
7	Inflexible	Complete	Low	Undertake only cost-effective changes (because cost of variability is low).
8	Inflexible	None	Low	Undertake only cost-effective changes (because cost of variability is low).

A.5 Incorporation of Travel Time Reliability into the HCM [30]

The objectives of SHRP-2 Project L08 were: 1) incorporate non-recurring congestion impacts into the Highway Capacity Manual (HCM) procedure, and 2) expand the analysis horizon from a single study period (typically an a.m. or p.m. peak period) to an extended time horizon of several weeks or months to assess the variability and the quality of service the facility provides to its users.

A deterministic approach to scenario generation was proposed for freeway facilities. This approach enumerated different operational conditions of a freeway facility based on different realization of factors which affect the travel time.

The scenario generation for urban streets consisted of four sequential procedures; each procedure processes the set of analysis periods in chronologic order:

- The first procedure predicts weather event date, time, type (i.e., rain or snow), and duration.

- The second procedure identifies the appropriate traffic volume adjustment factors for each date and time during the reliability reporting period.

- The third procedure predicts incident event date, time, and duration. It also determines incident event type (i.e., crash or non-crash), severity level, and location on the facility.

- The fourth procedure uses the results from the preceding three procedures to develop one urban streets engine input file for each scenario in the reliability reporting period.

The research team recommended that travel time reliability be used as a performance measure to describe travel characteristics on freeways and urban streets. Subsequently, consideration can be given to using travel time reliability to define level of service (LOS).

A.6 Methodology for Estimating the Value of Travel Time Reliability for Truck Freight System Users [31]

The goal of NCHRP Project 08-99 was to develop and demonstrate a methodology for estimating the value of travel time reliability for truck freight system users. The research and modeling were comprised of four major activities:

1. An in-depth program of survey research to help fill the gaps in the body of knowledge regarding how truck service providers and shippers view unreliability, what thresholds of unreliability are significant and require actions to mitigate, and how supply chain participants respond in terms of strategies and behaviors to mitigate unreliability. This phase of the research comprised three different efforts: (1) an *initial* online survey of shippers and truck transportation service providers; (2) in depth interviews of shippers and transportation service providers (interviewees are not specifically drawn from the online survey roster); and (3) a shorter but more focused follow-up online survey, narrowing in on the most common response to unreliable conditions--adding buffer time to truck schedules.

2. A framework for assessing the economic valuation of travel time unreliability was prepared based on knowledge gained from the survey and interview research. In addition, an Excel-based modeling tool labeled the "Truck Freight Reliability Valuation Model" was developed to help estimate the additional costs per trip for various trip parameters given varying levels of travel time unreliability. The Buffer Index was the primary metric of uncertainty in the model.

3. Two case studies to demonstrate the use of the model in real world planning situations: 1) a major truck freight corridor in Georgia and 2) a U.S.–Mexico truck border crossing. The demonstrations applied corridor level data from existing studies (Buffer Index values at chokepoints, AADT truck volumes, and median trip times and speeds) to estimate the additional annual economic costs of unreliability.

4. Recommendations for future research were presented to extend the results of the study including a more complete survey and modeling protocol for a next phase of economic valuation research beyond the completion of NCHRP 08-99 project.

Figure A-2 through Figure A-5 summarize the survey responses of shippers and truck transportation service providers.
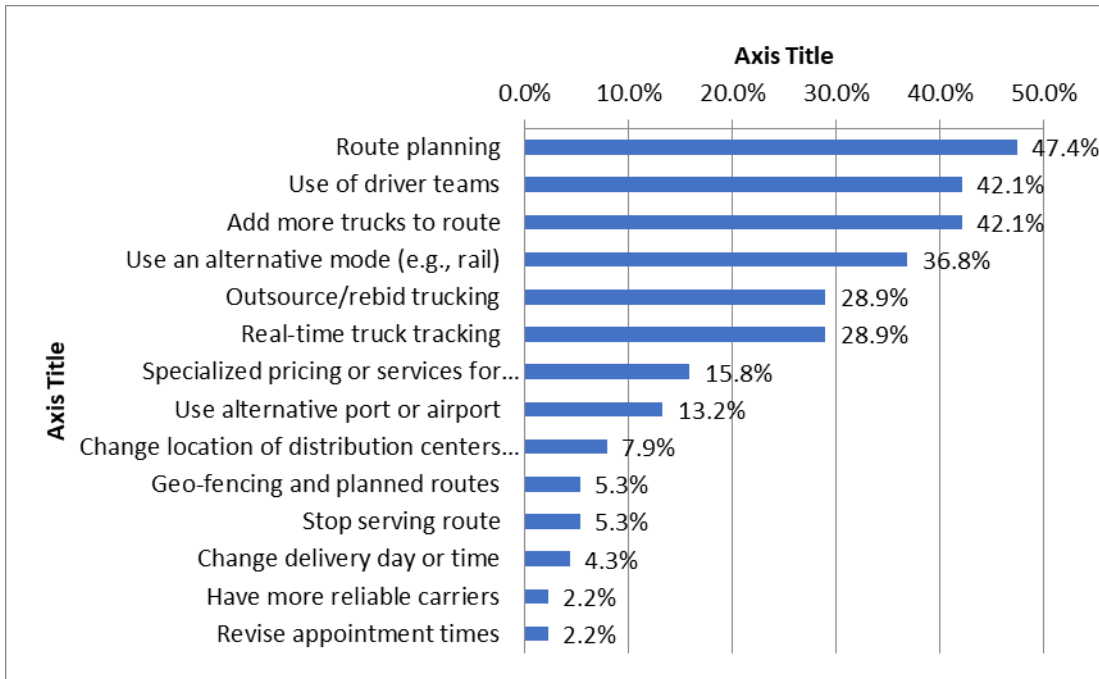
Figure A-2 Short-Term Immediate Responses—Shippers' Survey [31].
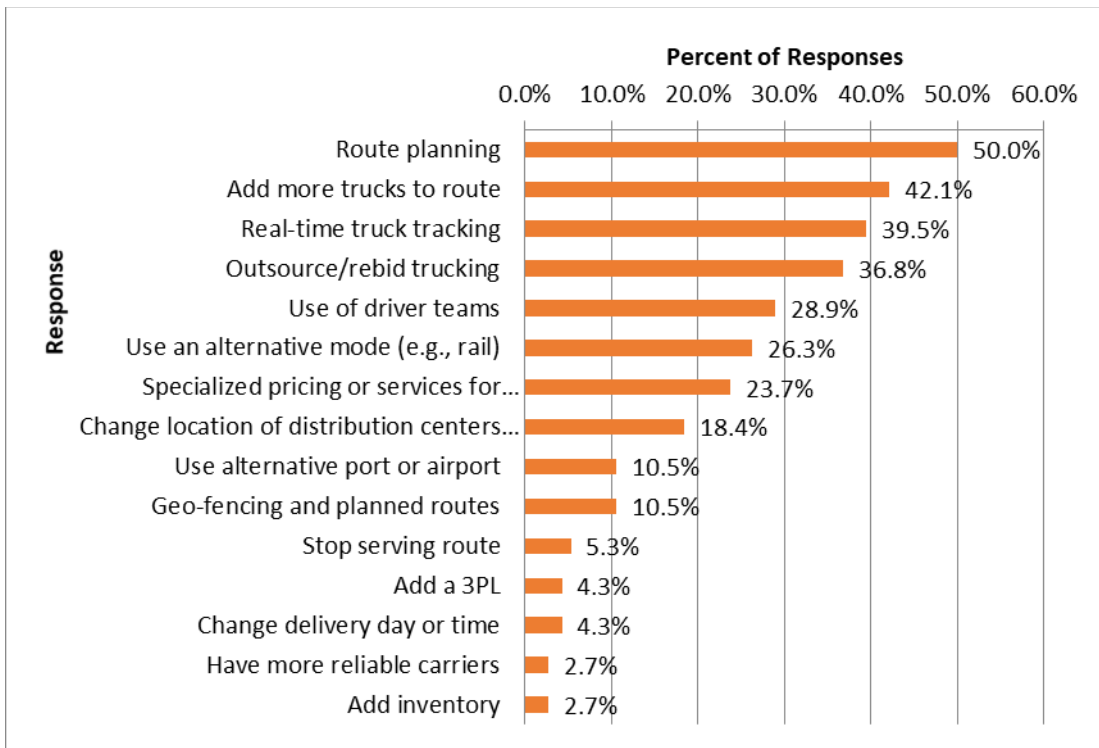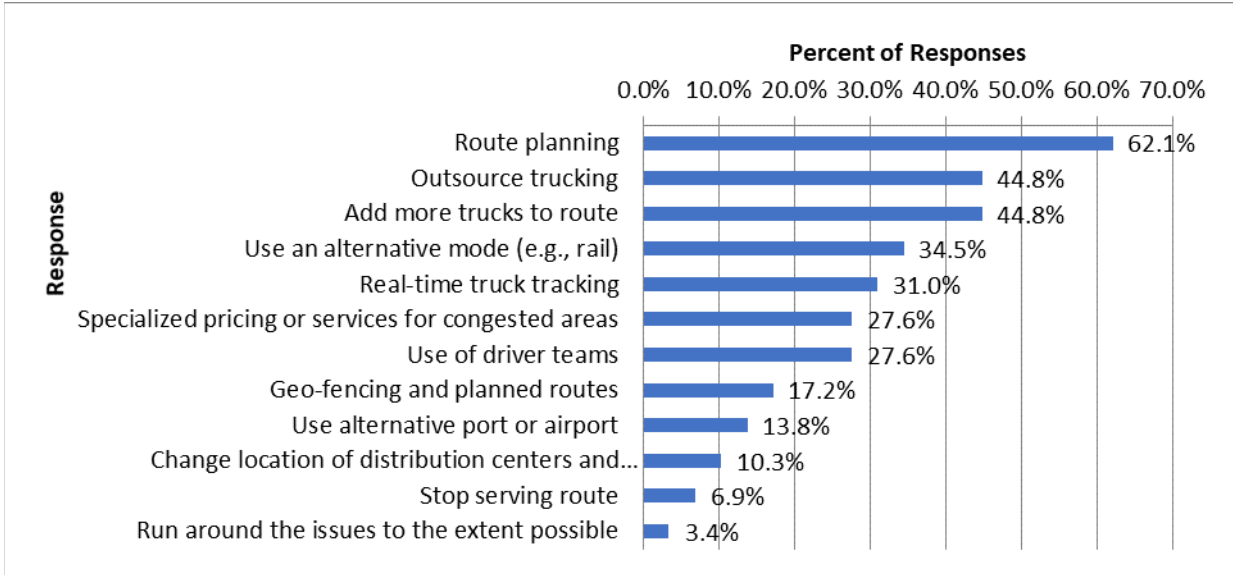

Figure A-3 Permanent Responses—Shippers' Survey [31].

143

Figure A-4 Short-Term Immediate Responses—Transportation Providers [31].
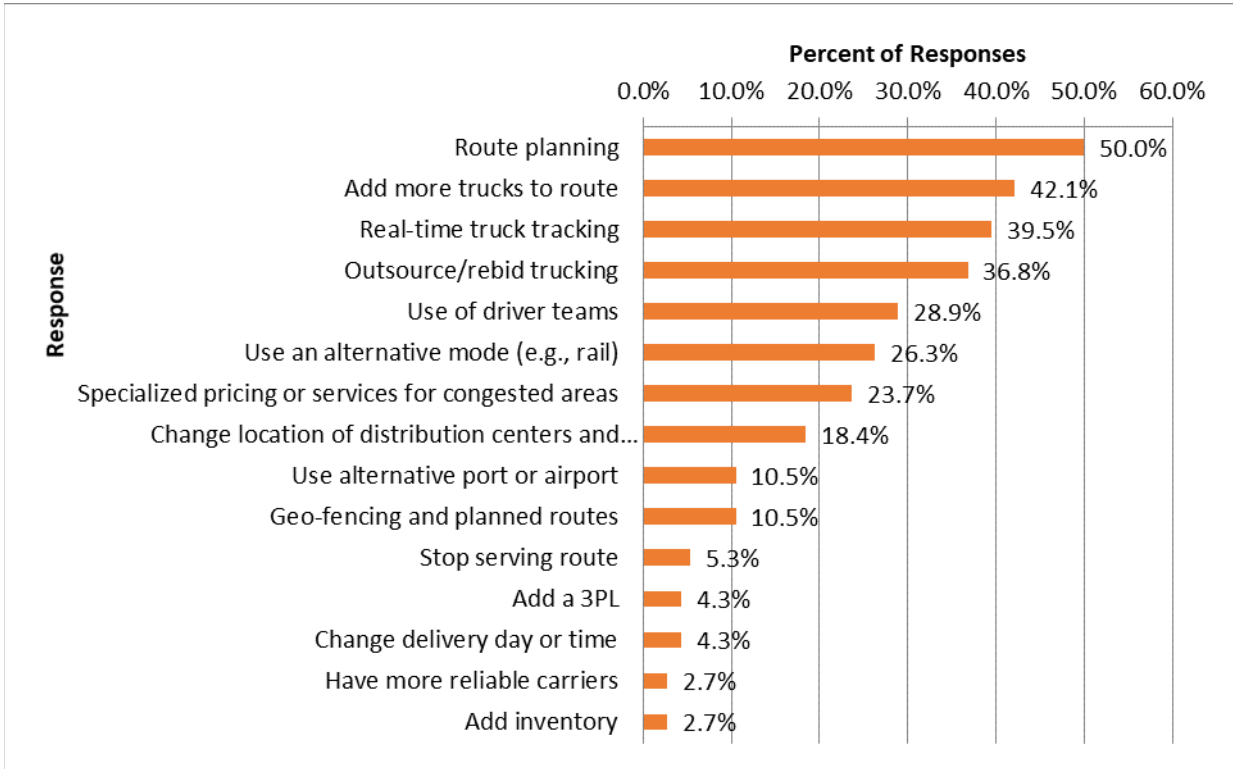

Figure A-5 Permanent Responses—Transportation Providers [31].

144

A.7 Predicting Travel Time Reliability using Mobile Phone GPS Data [32]

The authors present a method labeled "Travel Time Reliability Inference and Prediction (TRIP)" to predict the probability distribution of travel time on an arbitrary route in a road network at an arbitrary time, using GPS data from mobile phones or other probe vehicles. Each GPS observation consists of location, speed, and heading measurements, along with a time stamp. For mobile phones, a GPS measurement is recorded whenever phone applications access GPS information, not all of which are mapping or routing applications. Therefore, the frequency of GPS measurements varies, and the phone is not necessarily in a moving vehicle at the time when the measurements are taken. Motorized vehicle trips are isolated using a set of heuristics.

TRIP uses information from all the trips in the historical data to train a model for travel time on routes, learning the characteristics of individual roads and the effect of time of the week, road classification, and speed limit. We model travel time variability both at the trip level and at the level of the individual road network links included in the route. This decomposition is appropriate because some sources of variability affect the entire trip (such as driver habits, vehicle characteristics, or unexpected network-wide traffic conditions), while other sources of variability are localized (such as a delay due to a train crossing or construction). We define a network link to be a directed section of road that is not divided by an intersection, and on which the measured features of the road (road classification, speed limit, number of lanes, etc.) are constant.

The model captures weekly cycles in congestion levels, gives informed predictions for parts of the road network with little data. It utilizes a computational method for training and prediction based on maximum a posteriori estimation via Expectation Conditional Maximization. This yields an iterative training process with closed-form update equations that can be computed using parallelization across links and trips. As a result, it is computationally efficient even on large road networks and for large datasets.

The authors evaluated TRIP in a case study using large volumes of GPS data from Windows mobile phones in the Seattle metropolitan region. TRIP provided improved interval predictions (forecast ranges for travel time) relative to Microsoft's engine for travel time prediction as used in Bing Maps. It also provided deterministic predictions that are as accurate as Bing Maps predictions, despite using fewer explanatory variables, and differing from the observed travel times by only 10.1% on average over 35,190 test trips. The authors concluded that TRIP is the first method to provide accurate predictions of travel time reliability for complete, large-scale road networks.

Future work proposed by the authors included extending TRIP to incorporate additional variables, including those used in Clearflow learning and inference. For example, this would allow TRIP to take into account real-time information about traffic conditions, as measured using data from sensors installed in highways, or average

145

measured GPS speeds from mobile phones during the current time period. This extension has the potential to provide narrower distribution forecasts and predictive intervals, and even more accurate deterministic estimates.

A.8 Estimating Path Travel-Time Reliability [33]

This study involved collection and analysis of Automatic Vehicle Identification (AVI) data from a 10-mile segment of I-35 running through San Antonio, Texas. AVI technology enables spatial travel-time measurement using fixed-location equipment to identify and track a subset of vehicles in the traffic stream. By matching the unique vehicle identifications at different reader locations, spatial estimates of travel times can be computed. The study corridor was selected because its AVI stations provided the highest number of travel-time readings of all the TransGuide AVI stations. Five freeway segments were defined between the AVI stations. The resulting segments varied in length between 1.12 and 2.68 miles and all had the same speed limit.

Statistical tests were performed to determine the probability distributions of travel times along the study corridor during uncongested traffic (steady state conditions). The authors demonstrated through goodness-of-fit tests (the Kolmogorov-Smirnov K-S test, the Anderson-Darling A-D test, and the chi-square test) that the assumption of normality is, from a theoretical standpoint, inconsistent with field travel-time observations and that a lognormal distribution is more representative of roadway travel times. However, visual inspection of outlier observations at the tail of the distribution demonstrated that the normality assumption may be sufficient from a practical standpoint given its computational simplicity.

Path travel-time reliability was estimated as the probability that the trip travel time between an origin-destination pair (t_t) is less than some arbitrary travel time (t) assuming that travel times are normally distributed. Key parameters in estimating path travel-time reliability include not only estimating the path mean travel time but also estimating the travel-time variance. The authors addressed the assumption of segment travel-time independence which ignores any covariance across segments. They found that this assumption is not very accurate given that traffic congestion propagates both temporally and spatially, resulting in segment travel times that are typically highly correlated.

The authors proposed five methods for the estimation of path travel-time variance from its component segment travel-time variances. The analysis demonstrated that computing the trip travel-time coefficient of variation as the conditional expectation over all realizations of the various roadway segments that make up a trip (Method 3) provided estimates within 13% of field observations for both uncongested and congested conditions.

A.9 Travel Time Reliability as a Service Measure for Urban Freeways in Florida [34]

This paper summarizes the findings of a research project sponsored by the Florida Department of Transportation (FDOT) to develop travel time reliability (TTR) service measure for use in Florida and to serve as a basis for including a reliability service measure in the Highway Capacity Manual (HCM). A service measure defines the quality of service provided by a highway segment. The HCM defines six levels of service (LOS) for freeways based on traffic density (vehicles per mile per lane). LOS is a spatially localized measure. Because TTR is directly related to nonrecurring sources of congestion, a TTR-based service measure provides a way to identifying deficiencies, measure the performance of operations-related improvements and communicate performance to nontechnical audiences. SHRP-2 Project L08 examined the issue of a travel time reliability service measure and recommended the use of a Reliability Rating as the basis for a service measure. However, SHRP-2 Project L08 stopped short of defining actual LOS ranges.

The authors presented four options for defining reliability LOS for Florida:

1. Travel time reliability LOS based on the SHRP-2 Project L08 Reliability Rating;

2. Travel time reliability LOS based on the amount of Vehicle-Miles of Travel (VMT) that occurs in travel (space-mean) speed ranges;

3. Travel time reliability LOS based on a speed statistic from the distribution of travel speeds; and

4. Travel time reliability LOS based on a travel time reliability index for the mean, 80th, and 95th percentile Travel Time Index (TTI).

Two travel time reliability LOS measures based on the first and second options for urban freeways were recommended by the authors. Although the study did not recommend final LOS ranges, the two options are based on the same concept that urban freeway LOS degrades as a function of travel time, not density (current measure of effectiveness used in HCM). For freeway facilities that are routinely uncongested or for long distance trips, density is still the key factor determining the user experience. When non-recurring congestion occurs on these facilities, it is usually caused by disruptions such as incidents, inclement weather, and work zones.

The authors concluded that using travel time for facility-based LOS analysis on urban freeways is consistent with the HCM approach to urban streets. Achieving this consistency for urban facilities in the HCM requires deliberations within the Highway Capacity and Quality of Service Committee of the TRB to finalize the LOS ranges.

A.10 Impact of Data Source on Travel Time Reliability Assessment [35]

This study investigated the effects of travel-time/speed data sources on travel time reliability measures by utilizing two independent data sources, Bluetooth and INRIX, to derive different TTR performance metrics. Data were gathered from two freeway segments I-95 and I-270 in Maryland where I-270 contains one HOV lane. Travel time data were obtained from permanently deployed Bluetooth sensors and INRX for the entire 2012 year. Two primary issues regarding data quality are addressed: determining an equivalent INRIX path travel time and high-occupancy vehicle (HOV) lane travel time.

The Bluetooth technique provides direct measurement of segment travel time between two consecutive Bluetooth sensors as individual vehicles enter and exit the segment. INRIX reports data on roadway segments of different lengths using a common industry convention known as Traffic Message Channel (TMC) Location Codes. Because of the temporal and spatial changes in traffic conditions, adding up the INRIX travel time measured at the same instant for each TMC would be problematic. The authors developed a backtracking algorithm for estimating the equivalent path travel time based on INRIX data.

Although the Bluetooth technique is capable of detecting individual vehicle travel time for different lanes, it cannot automatically separate vehicle travel time for an HOV lane. To examine the impact of the I-270 HOV lane, the authors developed a classification technique to separate vehicle travel time on the HOV lane from that on mixed-traffic lanes. For INRIX, only one measure of aggregated traffic information at each time stamp is provided, and it does not specify traffic information for different types of lanes.

The researchers applied the Welch's t-test to examine the statistical differences between TTR performances measures derived from the two sources. The test results indicated that there was no significant evidence that reliability performance measures derived from the Bluetooth and INRIX data were different from each other on the I-95 segment. However, reliability measures obtained from these sources were statistically significantly different from each other on I-270, due to presence of HOV lanes.

Figure A-6 depicts the hourly Travel Time Index (TTI) and Planning Time Index (PTI) measures based on both Bluetooth and INRIX data obtained from I-270. Because INRIX data on I-270 segment does not differentiate between lanes, the reliability measures obtained from INRIX and Bluetooth are different from each other. To examine the effect of HOV operations on reliability index, Bluetooth data may be used. The authors found that among all the TTR performance measures, standard deviation and performance variation measures are more sensitive to the data source.
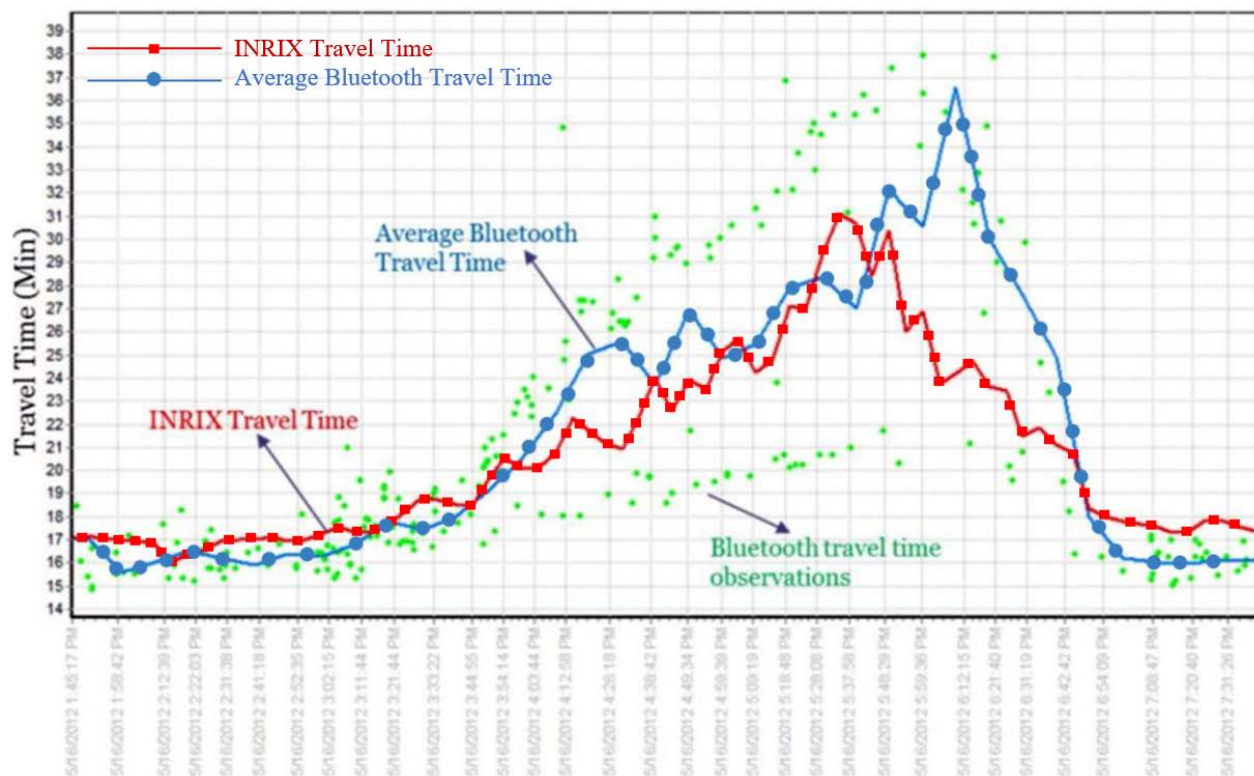
Figure A-6 Plot of INRIX and Bluetooth Data for I-270 Peak Hours of May 16, 2012 [35].

A.11 Travel Time Reliability in Indiana [36]

The objectives of this study were: 1) to assess the reliability of travel times on a number of different routes in Indiana, 2) to formulate a methodology to obtain travel time data using Bluetooth technology, and 3) to observe daily and inter-daily variations as well as those due to poor weather conditions and estimate econometric models to predict travel time and variability. To accomplish the first objective, travel time reliability was studied on 3 State Routes, 3 US Routes and 1 Interstate in the Indiana cities of Lafayette, Frankfort, Crawfordsville, Attica, Brownsburg, Avon, and Indianapolis. Travel time data were collected using a GPS-based floating car technique. The findings of this phase of the study showed that travel time variability on the roadway sections studied was generally not a problem. The standard deviation of travel time during peak periods ranged between 5% and 10% of the mean travel time. This implies that in order for travelers to arrive at their destinations with less than 15% probability of being late, they should incorporate an additional buffer of a bit more than 10% of the average travel time. However, the data indicated that on heavier traveled corridors, the standard deviation of travel time can rise above 10% and in rare cases above 15%, requiring higher buffers.

The second phase of the study involved collecting travel time data using Bluetooth technology on a segment of I-69 freeway in Northeast Indianapolis. Bluetooth technology had a high sampling rate of up to 10% of the traffic flow. The authors found that Bluetooth technology was relatively inexpensive to implement and it eliminated the need for complex algorithms to calculate travel time from point speed data.

The third phase of the study was to analyze travel time data obtained using Bluetooth technology along two segments of I-69 in Indianapolis for a period of two weeks to observe daily and inter-daily variations as well as those due to poor weather conditions and estimate econometric models to predict travel time and variability. The data showed that at any point during the day, the travel time may vary by up to 100% of the average travel time. The authors speculated that this was due to individual driver behavior. In addition, the average travel time was observed to increase by up to 300% during the peak hours. The standard deviation of individual travel times also increased during peak periods. Travel times during the same day of the week were found to vary significantly particularly during the peak hours.

To study the variability in travel time due to adverse weather, travel time data collected during a snow event were compared to travel time data obtained during good weather conditions. As expected, the analysis indicated that both the mean travel time and standard deviation of travel time were significantly different under adverse and normal weather conditions.

A.12 The Impact of Adverse Weather on Travel Time Variability of Freeway Corridor [37]

The authors examined the effect of adverse weather such as rain, snow, ice, fog, and storm on the travel time reliability of freeway corridors. Travel times were obtained from the Regiolab-Delft which stores real-time traffic data collected from a network of freeways, provincial roads, and an urban network in the southwest of the Netherlands. Weather data for one year were collected from the weather stations of the Dutch Meteorological Institute KNMI. The study revealed that adverse weather events had a significant effect on the 90th percent travel time and resulted in 4-fold increases compared to that associated with normal weather condition. In general, adverse weather conditions make travel time less reliable. Average travel time variability doubled in adverse weather condition, compared to normal conditions. The study found that rain has little or no effect on travel time variability below a certain critical threshold, but progressively impacts travel time variability above it. Statistical analysis also showed that ice had greater effect than other conditions examined (such as fog and snow) on travel time reliability.

A.13 Analytical Procedures for Determining the Impacts of Reliability Mitigation

Strategies [38]

The primary objective of SHRP-2 Project L03 was to develop predictive models that relate highway improvements (such as capacity improvement) to travel time reliability. In other words, how can reliability be related to highway, traffic, and operating conditions? Because of cost considerations, the research team undertook an empirical approach based on data collected by other transportation agencies to characterize congestion and reliability. Sources of traffic data were the traffic management centers (TMCs) at a number of cities including Atlanta, Houston, Seattle, and Jacksonville. Incident and event data were provided by *Traffic.com* from their Traveler Information Management System (TIMS). Weather data were collected from the National Climatic Data Center (NCDC) of the National Oceanic and Atmospheric Administration (NOAA). Satellite imagery (lane configurations) and the 2007 Highway Performance Monitoring data were the sources for highway geometric data.

The project had four distinct analytical steps i.e. 1) Exploratory analysis to understand the concept of reliability and various related parameters 2) Before-and-after case studies 3) Cross-sectional statistical modeling and 4) Congestion-by-source analysis. Based on the exploratory analyses, the research team decided to add the 80th percentile travel time to the list of reliability performance metrics since the 95th percentile travel time was too extreme a value to be influenced significantly by operations strategies. They also found that the Buffer Time Index (BTI) was too erratic for use as primary reliability metric.

The second step of the project was to perform before-and-after analysis to predict the change in reliability due to improvements. The term *before* refers to the time period prior to implementing the improvement, and the term *after* refers to the time period after implementing the improvement. Ideally, a control group is included in the before-and-after analysis to help account for the influence of background factors. In this project, the same highway section or network was studied with and without the improvement. Results of the before-and-after studies indicated that the average congestion is reduced and reliability is improved from all forms of improvements considered, including capacity expansion. However, the research team recognized early in the research that it would be impossible to study all the possible improvement types in the field due to data limitations. Therefore, cross sectional analysis (step 3) was utilized for reliability prediction.

In the cross-sectional statistical modeling step of the project, simple as well as complex models were developed to predict the overall travel time characteristics of a highway section in terms of both mean TT and TTR performance.

153

Micro-level congestion-by-source analysis was carried out in step-4 of the project to determine the factors that cause congestion. For example, Figure A-7 shows that incidents, high demand, and weather were the main causes of congestion based on an analysis of the 50 worst congested peak periods of the Atlanta study sections. The research team also conducted a detailed study of the causes of congestion by source for the Seattle area. They investigated all seven causes of congestion (traffic incidents, weather, work- zones, fluctuations in demand, special events, traffic control devices, and bottlenecks). The study revealed that a majority of travel delays and thus congestion in the region was the direct result of traffic demand exceeding roadway capacity.
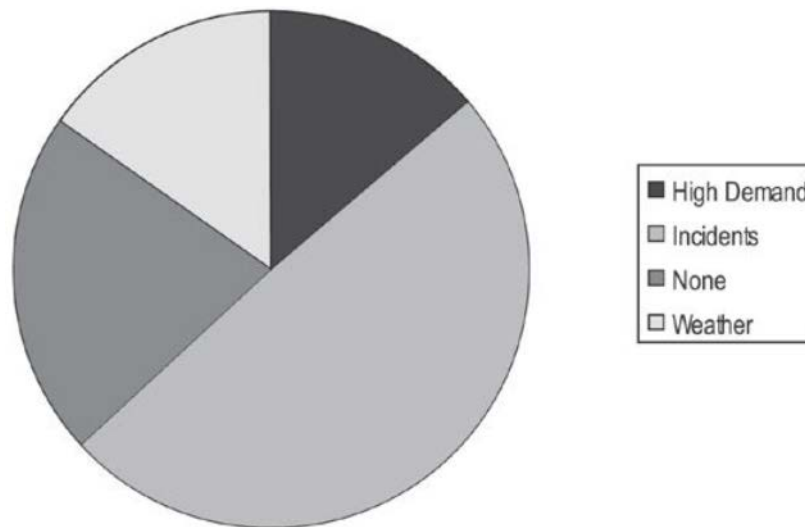

Figure A-7 Congestion Causes for the 50 Worst Congested Peak Periods in Atlanta (2008) [38].